UNIVERSITY OF TURKU

CALCIUM SIGNALLING IN THE FILAMENTOUS AND NITROGEN-FIXING CYANOBACTERIUM *ANABAENA* SP. PCC 7120

Julia Walter

TURUN YLIOPISTON JULKAISUJA – ANNALES UNIVERSITATIS TURKUENSIS
SARJA - SER. AI OSA - TOM. 612 | ASTRONOMICA - CHEMICA - PHYSICA - MATHEMATICA | TURKU 2019

UNIVERSITY OF TURKU

CALCIUM SIGNALLING IN THE FILAMENTOUS AND NITROGEN-FIXING CYANOBACTERIUM *ANABAENA* SP. PCC 7120

Julia Walter

TURUN YLIOPISTON JULKAISUJA – ANNALES UNIVERSITATIS TURKUENSIS
SARJA - SER. AI OSA - TOM. 612 | ASTRONOMICA - CHEMICA - PHYSICA - MATHEMATICA | TURKU 2019

University of Turku

Faculty of Science and Engineering
Department of Biochemistry
Laboratory of Molecular Plant Biology
FI-20520 Turku, Finland

Supervised by

Prof. Eva-Mari Aro
Laboratory of Molecular Plant Biology
Department of Biochemistry
University of Turku
FI-20520 Turku, Finland

Dr. Peter Gollan
Laboratory of Molecular Plant Biology
Department of Biochemistry
University of Turku
FI-20520 Turku, Finland

Reviewed by

Prof. Anthony Larkum
Laboratory of Climate Change Cluster
University of Technology Sydney
Broadway NSW 2007, Australia

Dr. David Fewer
Laboratory of Microbiology
Department of Food and Environmental Sciences
University of Helsinki
FI-00014 Helsinki, Finland

Opponent

Prof. Rakefet Schwarz
Laboratory of Molecular Microbiology
The Mina and Everard Goodman Faculty of Life Sciences
Bar-Ilan University
Ramat-Gan 5290002, Israel

The originality of this publication has been checked in accordance with the University of Turku quality assurance system using the Turnitin OriginalityCheck service.

ISBN 978-951-29-7740-6 (PRINT)
ISBN 978-951-29-7741-3 (PDF)
ISSN 0082-7002 (Print)
ISSN 2343-3175 (Online)
Grano Oy - Turku, Finland 2019

LIST OF ORIGINAL PUBLICATIONS

This thesis is composed of the following scientific articles, referred to in the text by their Roman numerals.

I. Walter, J., Lynch, F., Battchikova, N., Aro, E.M., and Gollan, P.J. (2016) Calcium impacts carbon and nitrogen balance in the filamentous cyanobacterium *Anabaena* sp. PCC 7120. *J Exp Bot* 67(13): 3997-4008. doi: 10.1093/jxb/erw112

II. Walter, J., Selim, K.A., Leganés, F., Fernández-Piñas, F., Vothknecht, U.C., Forchhammer, K., Aro, E.M., and Gollan, P.J. (2019) A novel Ca^{2+}-binding protein influences photosynthetic electron transport in *Anabaena* sp. PCC 7120. *Biochim Biophys Acta Bioenerg* 1860(6): 519-532. doi: 10.1016/j.bbabio.2019.04.007

III. Walter, J., Leganés, F., Aro, E.M., and Gollan, P.J. (2019) The small Ca^{2+}-binding protein CSE links Ca^{2+} signalling with nitrogen metabolism and filament integrity in *Anabaena* sp. PCC 7120. (Manuscript).

TABLE OF CONTENTS

LIST OF ORIGINAL PUBLICATIONS 3
TABLE OF CONTENTS 4
ABBREVIATIONS 7
ABSTRACT 11
TIIVISTELMÄ 12
1. INTRODUCTION 14
1.1. Cyanobacteria 14
1.1.1 Classification of cyanobacteria 15
1.1.2 Cell physiology of filamentous cyanobacteria 16
1.2 Cyanobacterial photosynthesis 17
1.2.1 Linear electron transport across the thylakoid membrane 18
1.2.2 Regulation and photoprotection of the photosynthetic apparatus 20
1.2.3 Cyanobacterial light-harvesting – the phycobilisome complex 21
1.3 *Anabaena* as a model for the development of multicellularity 24
1.3.1 Heterocysts 24
1.3.2 Akinetes 25
1.3.3 Hormogonia 26
1.4 C and N balance in cyanobacteria 26
1.4.1 Heterocyst formation and N_2 fixation 28
1.4.2 Carbon concentrating mechanisms 30
1.5 Ca^{2+} as a signalling molecule and second messenger in biological systems 31
1.5.1 Effect of Ca^{2+} on plant photosynthesis 32
1.5.2 Involvement of Ca^{2+} on cellular and metabolic processes in cyanobacteria 33
2. AIMS OF THE STUDY 34
3. METHODOLOGY 35
3.1. Cyanobacterial strains and growth conditions 35
3.1.1 Generation of modified *Anabaena* strains 35

3.1.2 Culture conditions 35
3.1.3 Ca^{2+} shift experiments 36
3.1.4 N and C_i limitation experiments 37
3.2. Microscopy 37
3.2.1 Bright-field and fluorescence microscopy for the determination of heterocyst frequencies and filament lengths 37
3.2.2 Transmission and Scanning electron microscopy 37
3.3. Biophysical methods 38
3.4. Transcript analyses 38
3.4.1 Total RNA isolation and next generation sequencing 38
3.4.2 Reverse transcription-quantitative polymerase chain reaction 38
3.5. Protein analyses 39
3.5.1 Overexpression and purification of recombinant CSE protein 39
3.5.2 $^{45}Ca^{2+}$ autoradiography 39
3.5.3 Protein analyses of thylakoid membrane protein complexes 40
3.6. Bioinformatics methods 40
4. MAIN RESULTS 41
4.1. Ca^{2+} regulates primary metabolic pathways 41
4.1.1 Gene expression is adjusted by $[Ca^{2+}]_e$ 41
4.1.2 Physiological parameters respond to changes in $[Ca^{2+}]_e$ 43
4.2. CSE is a small Ca^{2+}-binding protein newly described in heterocystous cyanobacteria 43
4.2.1 CSE overexpression affects PBS assembly and photosynthetic ETC 45
4.2.1.1 Differentially expressed genes in *cse*-oex include downregulated PBS rod subunits 46
4.2.1.2 Characterisation of PET in the *cse*-oex strain 46
4.2.1.3 Distribution of photosynthetic protein complexes in the thylakoid membrane of *cse*-oex 48

4.2.2 CSE is required for maintaining heterocyst differentiation and filament integrity 49
4.2.2.1 Cell morphology is further affected by *cse* knockout 49
4.2.2.2 Expression of genes involved in heterocyst differentiation is altered by *cse* knockout 50
4.2.2.3 Expression patterns of heterocyst differentiation genes during N step-down in *Δcse* 51
5. DISCUSSION 52
5.1. Ca^{2+} influences the C/N ratio through regulation of uptake transporter gene expression 52
5.2. CSE – a novel player in the complex network of maintaining the metabolic equilibrium? 54
5.2.1 Disturbed PBS-PSII connectivity and PQ pool overreduction lead to decreased photosynthetic capacity in the *cse* overexpressor 56
5.2.2 Deletion of the *cse* gene in *Anabaena* induces filament fragmentation and downregulates N_2 fixation abilities 58
5.2.3 Hypothetical scheme describing the role of Ca^{2+} and CSE in *Anabaena* metabolism 60
6. CONCLUDING REMARKS 64
7. ACKNOWLEDGEMENTS 66
8. REFERENCES 67
ORIGINAL PUBLICATIONS 81

ABBREVIATIONS

2D	two dimensional
2-OG	2-oxoglutarate
2-PG	2-phosphoglycolate
3-PGA	3-phosphoglycerate
AET	alternative electron transport
ANOVA	analysis of variance
APC	allophycocyanin
ATP	adenosine triphosphate
BLAST	Basic local alignment search tool
BN	blue native
C	carbon
C_i	inorganic carbon
Ca^{2+}	calcium ion
$^{45}Ca^{2+}$	radiolabelled calcium ion
$[Ca^{2+}]_e$	external calcium ion concentration
$[Ca^{2+}]_i$	intracellular calcium ion concentration
CBB	Calvin-Benson-Bassham
CcbP	cyanobacterial calcium-binding protein
CCM	carbon concentrating mechanism
cDNA	complementary deoxyribonucleic acid
CET	cyclic electron transport
ChIP	chromatin immunoprecipitation
chl	chlorophyll
CO_2	carbon dioxide
Cox	cytochrome *c* oxidase
CSE	Calcium Sensor EF-hand
Cyd	cytochrome *bd* quinol oxidase
$cytb_6f$	cytochrome b_6f
DM	*n*-dodecyl-β-D-maltoside
DNA	deoxyribonucleic acid

Em	erythromycin
EPS	extracellular polymeric substances
ETC	electron transport chain
F_0	minimum chlorophyll fluorescence under measuring light
$FADH_2$	flavin adenine dinucleotide hydroquinone
FC	fold change
Fd	ferredoxin
FDR	false discovery rate
Fe-S	iron-sulfur
Fld	flavodoxin
Flv	flavodiiron protein
F_m'/F_m^D	maximum chlorophyll fluorescence in light/dark
FNR	ferredoxin-$NADP^+$-reductase
FR	far-red
F_s	steady-state chlorophyll fluorescence
F_v/F_m	maximum quantum yield of Photosystem II
GFP	green fluorescent protein
GOE	Great Oxygenation Event
GOGAT	glutamine oxoglutarate aminotransferase
GS	glutamine synthetase
H^+	proton
H_2	hydrogen
HCO_3^-	bicarbonate
HEP	heterocyst envelope polysaccharides
HGL	heterocyst glycolipid layer
His	histidine
Hox	bidirectional hydrogenase
IPTG	isopropyl β-D-1-thiogalactopyranoside
ITC	isothermal titration calorimetry
K_d	dissociation constant
L_C	phycobilisome core linker protein
L_{CM}	phycobilisome core-membrane linker protein

LET	linear electron transport
lp	large pore
L_R	phycobilisome rod linker protein
L_{RC}	phycobilisome rod-core linker protein
L_{RT}	phycobilisome terminal rod-capping linker protein
Mn_4O_5Ca	manganese-calcium cluster
MS	mass spectrometry
n	number of bound ligands
N	combined nitrogen
N_2	atmospheric dinitrogen
Na^+	sodium ion
$NAD(P)^+$/NAD(P)H	nicotinamide adenine dinucleotide (phosphate)
Nm	neomycin
NPQ	non-photochemical quenching
O_2	molecular oxygen
O_2^-	superoxide
$^1O_2$	singlet oxygen
OCP	orange carotenoid protein
OD	optical density
OEC	oxygen-evolving complex
ORF	open reading frame
P680	photosystem II reaction centre
P700	photosystem I reaction centre
PAGE	polyacrylamide gel electrophoresis
PAM	pulse-amplitude modulation
PBP	phycobiliprotein
PBS	phycobilisome
PC	phycocyanin
PCR	polymerase chain reaction
PEC	phycoerythrocyanin
PET	photosynthetic electron transport
P_i	inorganic phosphate

pmf	proton-motive force
PQ/PQH_2	plastoquinone/plastoquinol
PSI	photosystem I
PSII	photosystem II
PVDF	polyvinylidene difluoride
Q_A/Q_B	plastoquinone A/plastoquinone B
RNA	ribonucleic acid
ROS	reactive oxygen species
RT	room temperature
RTO	respiratory terminal oxidase
RTX	repeats-in-toxin
RuBisCO	ribulose-1,5-bisphosphate carboxylase/oxygenase
RuBP	ribulose-1,5-bisphosphate
SDS	sodium dodecyl sulfate
SEM	scanning electron microscopy
sRNA	small ribonucleic acid
TCA	tricarboxylic acid
TEM	transmission electron microscopy
TF	transcription factor, transcriptional regulator
WT	wild-type
Y(I)	photosystem I maximum effective yield
Y(II)	photosystem II maximum effective yield
Y(NA)	photosystem I acceptor side limitation
Y(ND)	photosystem I donor side limitation

ABSTRACT

Cyanobacteria fix atmospheric CO_2 into sugars using water and sunlight in a process called photosynthesis, generating O_2 as a by-product. Cyanobacteria not only contribute substantially to global primary production, but also to the global nitrogen cycle. Nitrogen fixation is a particular feature of a wide range of bacteria and archaea. Filamentous cyanobacterial strains spatially separate oxygenic photosynthesis and anoxic nitrogen fixation in two different cell types - the vegetative cells and specialised cells called heterocysts, respectively. As a model organism for cyanobacterial photosynthesis and nitrogen fixation, *Anabaena* (*Nostoc*) sp. PCC 7120 was used in this thesis to study the effects of Ca^{2+} on regulation mechanisms of the metabolic equilibrium between the two most abundant elements - carbon and nitrogen - whose ratio is an indicator of the metabolic performance.

Ca^{2+} is a ubiquitous second messenger, enzyme co-factor and component of membranes in eukaryotic cells and organisms, such as mammals and plants. However, the importance of Ca^{2+} in cellular processes in prokaryotes, particularly in cyanobacteria, is not as well understood. High amounts of Ca^{2+} are known to be toxic, therefore, the concentration of free intracellular Ca^{2+} is tightly regulated by Ca^{2+} channels and pumps, and Ca^{2+}-binding proteins, respectively. Results in this thesis have demonstrated that Ca^{2+} is a key regulator of the intracellular carbon and nitrogen balance, through regulation of gene expression of the respective carbon and nitrogen uptake transporters, which is vital for metabolic homeostasis of the cells. A novel Ca^{2+}-binding protein (CSE) in *Anabaena* sp. PCC 7120 was described and connected to the maintenance of the metabolic balance between photosynthetic light reactions and nitrogen fixation, based on the characterisation of the *cse* gene and protein. The CSE protein shows many features of a Ca^{2+} sensor and regulator protein and thus is likely to interact with a protein partner upon sensing changes of intracellular Ca^{2+} levels. Overexpression of CSE impaired photosynthetic electron transport across the thylakoid membrane, possibly through defects in the proper assembly of the light-harvesting complexes, called phycobilisomes in cyanobacteria, and damage of photosystem II dimers. Deletion of CSE, in contrast, severely disturbed heterocyst development and filament integrity, possibly through the lack of functional Ca^{2+} signalling during early heterocyst differentiation or the release of Ca^{2+} ions due to the knockout of this Ca^{2+}-binding protein. These results indicate a possible dual function of CSE as a Ca^{2+} buffer as well as a Ca^{2+} sensor protein.

TIIVISTELMÄ

Syanobakteerit sitovat ilmakehän hiilidioksidia sokereiksi käyttämällä vettä ja auringonvaloa yhteyttämiseksi kutsutussa prosessissa. Sen lisäksi, että syanobakteerit yhteyttävinä primärituottajina osallistuvat merkittävästi globaaliin biomassan tuotantoon, niillä on myös iso rooli maapallon typpikierrossa. Typen sitominen on rihmamaisten syanobakteerikantojen erityisominaisuus. Nämä syanobakteerit erottavat happea tuottavan yhteyttämisen ja hapettomat olosuhteet vaativan typen sitomisen tilallisesti käyttämällä vegetatiivisen kasvun soluja yhteyttämiseen ja heterokysteiksi kutsuttuja erikoistuneita soluja typen sitomiseen. Solunsisäistä hiilen ja typen välistä suhdelukua käytetään kuvaamaan syanobakteerisolujen yleistä kelpoisuutta, ja väitöskirjassani tutkin Ca^{2+}-ionien vaikutusta näiden kahden alkuaineen aineenvaihduntatasapainon säätelymekanismeihin käyttämällä syanobakteerien yhteyttämisen ja typensidonnan mallieliöitä *Anabaena* (*Nostoc*) sp. PCC 7120 –syanobakteeria tutkimuskohteena.

Ca^{2+}-ionien rooli toissijaisina lähetteinä, entsyymien kofaktoreina ja kalvorakenteiden osina on hyvin tunnettu aitotumaisissa eliöissä ja soluissa, mutta esitumaisissa eliöissä, etenkin syanobakteereissa, Ca^{2+}-ionien merkitystä on tutkittu verrattain vähän. Suuret Ca^{2+}-pitoisuudet ovat tiettävästi haitallisia soluille, minkä takia vapaiden Ca^{2+}-ionien konsentraatio on tarkasti säädelty Ca^{2+}-kanavien ja -pumppujen, sekä Ca^{2+}-ioneja sitovien proteiinien avulla. Tutkimuksessani havaitsin Ca^{2+}-ionien vaikuttavan hiilen ja typen sisäänotosta vastaavien proteiinien geenien ekspressioon, minkä takia Ca^{2+} on tärkeä säätelytekijä solunsisäisen hiili-typpi -tasapainon säilyttämisessä. Löysin tutkimuksessani *Anabaena* -syanobakteerissa esiintyvän uudentyyppisen Ca^{2+}-ioneja sitovan proteiinin (CSE). Kyseisen proteiinin toiminta on yhteydessä solun aineenvaihduntatasapainon ylläpitämiseen yhteyttämisen valoreaktioiden ja typen sitomisen välillä. CSE-proteiinissa on monia Ca^{2+}-sensori-/säätelyproteiinin piirteitä, minkä takia CSE on todennäköisesti vuorovaikutuksessa toisten proteiinien kanssa solunsisäisen Ca^{2+}-signaalin läsnä ollessa. CSE-proteiinin ylituotto haittasi yhteyttämisen elektroninsiirtoreaktiota, mahdollisesti vioittamalla fykobilisomien, syanobakteereille ominaisten valohaavien, kokoamisketjua tylakoidikalvostolla, sekä vaurioittamalla valoreaktio II:n dimeerimuotoisia proteiinikomplekseja. Sen sijaan *Anabaena* -kannat joista CSE-proteiinin geeni oli poistettu, ilmensivät vakavasti häiriintynyttä heterokystien kehitystä ja rihmojen eheyttä. Nämä viat johtuivat mahdollisesti Ca^{2+}-signaloinnin toiminnan häiriöistä heterokystien aikaisten kehitysvaiheiden aikana. Tulokseni osoittavat, että CSE-proteiinilla on kaksoisrooli Ca^{2+}-puskurina ja Ca^{2+}-sensoriproteiinina.

„Nothing in life is to be feared, it is only to be understood. Now is the time to understand more, so that we may fear less."

- Marie Skłodowska Curie -

1. INTRODUCTION

1.1. Cyanobacteria

Cyanobacteria, formerly known as blue-green algae, encompass a distinctive group of prokaryotes in the clade of Bacteria, capable of performing oxygenic photosynthesis. With their exceptional ability of converting sunlight energy into chemical energy from water and carbon (C) dioxide (CO_2), cyanobacteria were responsible for changing a reduced, high CO_2 atmosphere into an oxidised, low CO_2 atmosphere about 2.5 billion years ago, by releasing molecular oxygen (O_2) as a photosynthetic by-product. The "Great Oxygenation Event" (GOE) eventually led to the evolution of organisms with oxygenic respiration and life as we know it today on the planet Earth (Shestakov and Karbysheva, 2017). Furthermore, oxygenic photosynthesis of green plants and algae can be traced back to an ancient endosymbiotic event, in which a cyanobacterium was engulfed by a eukaryotic cell. Therefore, cyanobacteria are considered the evolutionary progenitors of photosynthetic chloroplasts (Gould *et al*., 2008; Lee and Hwang, 2018).

Cyanobacteria contribute about 30% to global CO_2 fixation and are considered among the most important primary producers of organic biomass on Earth (Bryant, 2003). Additionally, they contribute substantially to the global nitrogen (N) cycle (Montoya *et al*., 2004), because cyanobacteria are capable of atmospheric dinitrogen (N_2) fixation and conversion into vital amino acids (Thomas *et al.*, 1977), next to several strains of eubacteria and archaea (Klipp *et al*., 2005).

Because of their short generation times and small modifiable genome sizes, some cyanobacterial species are implemented as suitable and promising model organisms for biotechnological platforms for the production of biofuels and chemicals, such as bio-hydrogen (H_2) (Kosourov *et al*., 2014), butanol (Lan and Liao, 2011), sunscreens (Derikvand *et al*., 2016), and additives for cosmetics (Morone *et al*., 2019) and food (Panjiar *et al*., 2017). Therefore, genetic tools have been under strong investigation, of which promoters, riboswitches, CRISPR/Cas, small ribonucleic acid (sRNA) tools and genome modelling tools are the most promising to investigate cyanobacterial metabolism (Al-Haj *et al*., 2016; Sengupta *et al*., 2018; Sun *et al*., 2018).

1.1.1 Classification of cyanobacteria

Cyanobacteria inhabit both aquatic and terrestrial ecosystems, including environments with extremely harsh conditions, such as hot springs, deserts, ice or hypersaline and alkaline lakes (Rampelotto, 2013). Due to the pleiomorphic nature of their morphological features, it is rather difficult to determine taxonomic relations between species. Based on the type of carboxysomes (intracellular compartment for CO_2 fixation) and the phylogeny of the enzyme ribulose-1,5-bisphosphate carboxylase/oxygenase (RuBisCO), cyanobacteria can be grouped into α- and β-cyanobacteria (Price *et al*., 1998). The two types of carboxysomes differ in their assembly, as well as in the components they enclose. While α-carboxysomes contain RuBisCO in the 1A form, β-carboxysomes enclose 1B RuBisCO and are generally larger than the α-form (Kerfeld and Melnicki, 2016).

Another morphological taxonomy was determined by Rippka *et al*. (1979), in which 178 strains of cyanobacteria were categorised into five sections. While Sections I and II consist of unicellular cyanobacteria, which divide through binary fission (Section I) or multiple fission (Section II), Sections III to V comprise multicellular, filamentous strains, which are further subdivided into groups based on their ability to differentiate vegetative cells into N_2-fixing heterocysts. Section III cyanobacteria have filaments that only comprise photosynthetic vegetative cells, whereas strains from Sections IV and V are heterocystous. Among the heterocyst-forming cyanobacteria, Section IV strains grow unbranched filaments in one plane, but Section V strains grow branched filaments in multiple planes (Rippka *et al*., 1979).

With technological advances, cyanobacterial genome sequencing has become available in the past two decades, allowing the phylogenetic comparison of ribosomal RNA and protein sequences. In a study by Shih *et al*. (2013), 126 sequenced cyanobacterial strains were classified into seven subclades (A-G), with subclade A being highly evolved and subclade G including basal lineages, according to sequence similarities of 31 conserved proteins and 16S ribosomal RNA. Their phylogeny demonstrated that no unique protein for the morphology of a subclade was present and that the phenotypical filamentous trait has evolved several times independently within the phylum of cyanobacteria (Shih *et al*., 2013).

Attempts to determine the most recent common ancestor between cyanobacteria and plastids have yielded controversial results in the origin of the cyanobacterial endosymbiont (Shih *et al*., 2013; Ochoa de Alda *et al*., 2014). While Shih *et al*. (2013) claimed that the plastid ancestor belonged to a basal lineage from the subclade F of their phylogenetic tree, Ochoa de Alda *et al*. (2014) showed that plastids are rather more closely related to evolved extant cyanobacterial species than to descendants from extinct basal lineages. According to their study, plastids evolved during the diversification of the subclades A (non-heterocystous) and B1 (heterocystous) of filamentous cyanobacteria, which are more highly developed than unicellular species and only arose 0.5 – 1 billion years after the GOE (Schirrmeister *et al*., 2013). Several other studies have also stated that a heterocystous cyanobacterium was involved in the endosymbiotic event, giving rise to photosynthetic plastids in extant Archaeplastida (Deusch *et al*., 2008; Criscuolo and Gribaldo, 2011).

1.1.2 Cell physiology of filamentous cyanobacteria

Cyanobacteria are gram-negative bacteria due to the composition of the cell envelope (Hoiczyk and Hansel, 2000). In filamentous strains, a filament comprises individual vegetative cells (Figure 1) that contain two plasma membranes, of which the outer is continuous along the filament. Many cyanobacteria species secrete extracellular polymeric substances (EPS), mostly consisting of polysaccharides, through the membranes (Pereira *et al*., 2015). The space between both membranes is called the periplasm and contains several peptidoglycan layers. Between two consecutive cells the peptidoglycan layer is called the septum and contains pores and protein complexes for cell-cell communication through the exchange of nutrients and signalling molecules (Flores *et al*., 2006). Inside the cells, a complex thylakoid membrane system containing the photosynthetic and respiratory machinery (Mullineaux, 2014) fills most of the cytoplasm apart from the middle of the cell where ribosomes, lipid droplets, polyphosphate or cyanophycin granules and carboxysomes, for instance, are located (Gonzalez-Esquer *et al*., 2016). Carboxysomes are special compartments consisting of a polyhedral protein shell for CO_2 fixation by the enzyme RuBisCO (Kerfeld and Melnicki, 2016). Under N limiting conditions, vegetative cells in some filamentous strains can differentiate into N_2-fixing heterocyst cells (Figure 1), whose physiology is described in Section 1.3.1.

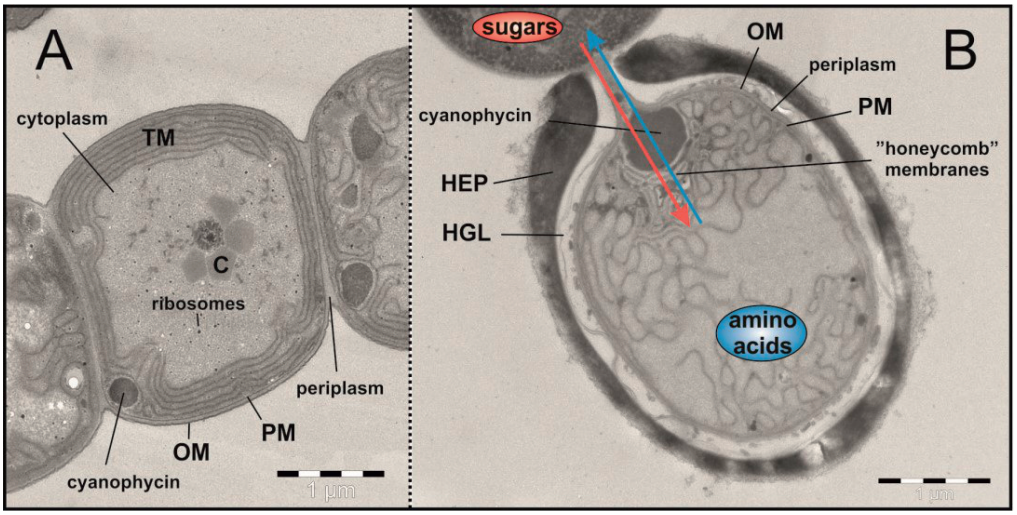

Figure 1: Structure of a cyanobacterial vegetative cell (**A**) and a nitrogen-fixing heterocyst (**B**) from the filamentous cyanobacterium *Anabaena* sp. PCC 7120. Abbreviations: carboxysome (C), heterocyst envelope polysaccharides (HEP), heterocyst glycolipid layer (HGL), outer plasma membrane (OM), inner plasma membrane (PM), thylakoid membranes (TM). Image **B** exhibits nutrient exchange between a heterocyst and the adjacent vegetative cell as indicated by arrows. The scale bar shows 1 µm. Images by J. Walter (2018).

1.2 Cyanobacterial photosynthesis

Oxygenic photosynthesis provides organic matter and releases O_2 as a by-product by converting sunlight energy into chemical energy in two processes – the photosynthetic light reactions in the thylakoid membranes and CO_2 fixation in the Calvin-Benson-Bassham (CBB) cycle. In the photosynthetic light reactions, absorption of photons and transfer of excitation energy drive the extraction of electrons from water. Subsequent electron transfer towards electron acceptors and relocation of protons (H^+) across the thylakoid membrane produce the reducing agent nicotinamide adenine dinucleotide phosphate (NADPH) and energy carrier adenosine triphosphate (ATP), respectively, which are required in the CBB cycle.

The CBB cycle (for reviews see Price *et al.*, 1998; Raines, 2003) comprises three stages, of which the first one – CO_2 fixation - takes place within the carboxysome in cyanobacteria. CO_2 and its soluble derivative bicarbonate (HCO_3^-) diffuse across the proteinaceous shell into the carboxysome, where the enzyme carbonic anhydrase converts HCO_3^- into CO_2, and CO_2 accumulates around the enzyme RuBisCO, which catalyses the carboxylation of ribulose-1,5-bisphosphate (RuBP) into 3-phosphoglycerate (3-PGA). This triose phosphate is then transferred into the

cytoplasm and reduced to glyceraldehyde-3-phosphate in the second stage of the CBB cycle, being the precursor for the hexose sugar glucose. During the third stage, the RuBisCO substrate RuBP is regenerated from glyceraldehyde-3-phosphate through several energy-consuming reactions.

1.2.1 Linear electron transport across the thylakoid membrane

Light reactions and linear electron transport (LET) of oxygenic photosynthesis in cyanobacteria occur in the thylakoid membrane system with the help of membrane-embedded protein complexes, namely the two photosystems PSI and PSII, the cytochrome b_6f ($cytb_6f$) complex and the ATP synthase complex (see a review by Nagarajan and Pakrasi, 2016) (Figure 2). Cyanobacteria harvest light energy through a pigment-protein complex called phycobilisome (PBS) (further described below) that is attached to the outer surface of the photosystems and channels absorbed energy to the chlorophyll (chl) *a*-containing reaction centres of PSI and PSII (P700 and P680, respectively) (MacColl, 1998). Thus, electrons reach a higher energy level and are transferred to respective electron acceptors in a process referred to as charge separation (Cardona *et al*., 2012). In PSII, P680 becomes oxidised ($P680^+$) by reducing the first electron acceptor pheophytin (Klimov *et al*., 1977), which immediately transfers the electron to the first stable plastoquinone (PQ), Q_A (Diner *et al*., 1991). The electron gap in $P680^+$ is filled by an electron deriving from the splitting of water into H^+ and O_2 at the manganese-calcium cluster (Mn_4O_5Ca) in the O_2-evolving complex (OEC) of PSII (Barber, 2012). Q_A passes on the electron to a second PQ, Q_B, which accepts two electrons and two H^+ from the stroma. The protonated PQH_2 (plastoquinol) is a mobile electron carrier transmitting both electrons to $cytb_6f$, one of which is re-directed to the PQ pool, in what is known as the Q cycle (Mitchell, 1975), and the other one is transferred to another lumenal mobile electron carrier, plastocyanin (or cyt c_6). $Cytb_6f$ also accepts the two H^+ and releases them into the thylakoid lumen (Kurisu *et al*., 2003). The electron in plastocyanin is then passed on to the PSI reaction centre, filling the electron gap of $P700^+$ that is generated through charge separation in P700 induced by light-harvesting. Further in PSI, the excited electron from P700 is transferred via phylloquinone and three iron-sulfur (Fe-S) clusters towards ferredoxin (Fd) (Nelson and Yocum, 2006), and flavodoxin (Fld) (Nogués *et al*., 2005) and the ferredoxin-$NADP^+$-reductase (FNR), reducing nicotinamide adenine dinucleotide phosphate ($NADP^+$) to NADPH and providing reducing power needed in the CBB cycle for the production of sugars. The H^+ derived from the water splitting in PSII and also those

released from cytb$_6$f trigger a H^+ gradient across the thylakoid membrane, which contributes to the electrochemical membrane H^+-motive force (pmf) that is used as driving force for the production of ATP from adenosine diphosphate (ADP) and inorganic phosphate (P_i) via the ATP synthase complex (Allen, 2002). ATP is the ultimate energy carrier needed in many metabolic processes including the CBB cycle.

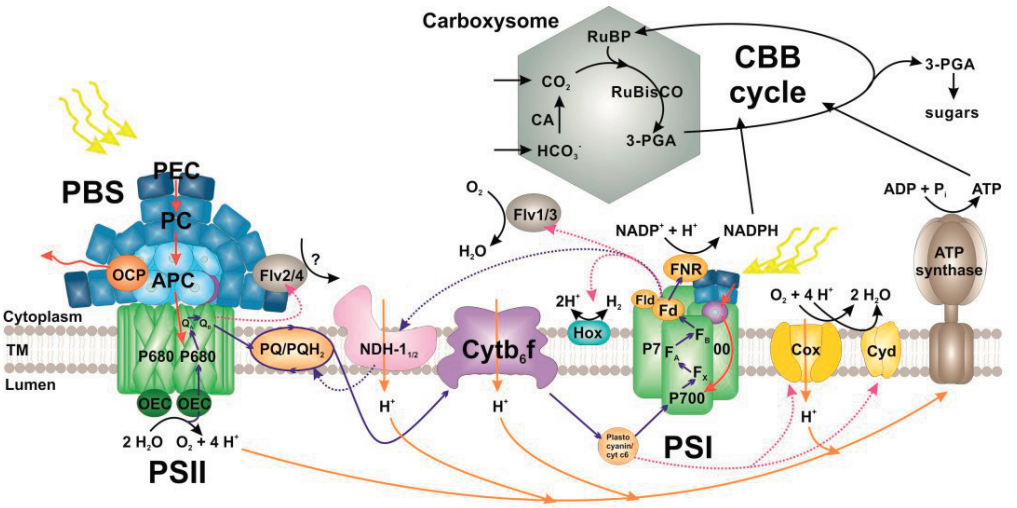

Figure 2: Schematic overview of electron transfer routes across the thylakoid membrane in vegetative cells of *Anabaena* sp. PCC 7120. Blue arrows indicate linear electron transport (full lines) and cyclic electron transport (dashed lines), whereas pink dashed arrows show alternative electron transport. Red arrows in the photosystems (PS) demonstrate the transfer of excitation energy. The purple allophycocyanin (APC) disc in the phycobilisome (PBS) (also the modified PBS at PSI) represents the terminal emitter. Orange arrows display proton translocation. See the text for further details (Sections 1.2.1 and 1.2.2). Abbreviations: adenosine diphosphate (ADP), adenosine triphosphate (ATP), carbonic anhydrase (CA), Calvin-Benson-Bassham (CBB), carbon dioxide (CO_2), cytochrome *c* oxidase (Cox), cytochrome *bd* quinol oxidase (Cyd), cytochrome (Cyt), iron cluster (F), ferredoxin (Fd), flavodoxin (Fld), flavodiiron protein (Flv), ferredoxin-$NADP^+$-reductase (FNR), proton (H^+), water (H_2O), bicarbonate (HCO_3^-), bidirectional hydrogenase (Hox), nicotinamide adenine dinucleotide phosphate ($NADP^{(+)}H$), nicotinamide adenine dinucleotide dehydrogenase (NDH), molecular oxygen (O_2), orange carotenoid protein (OCP), oxygen-evolving complex (OEC), photosystem II reaction centre (P680), photosystem I reaction centre (P700), phycocyanin (PC), phycoerythrocyanin (PEC), 3-phosphoglycerate (3-PGA), inorganic phosphate (P_i), plastoquinone (PQ), plastoquinol (PQH_2), ribulose-1,5-bisphosphate carboxylase/oxygenase (RuBisCO), ribulose-1,5-bisphosphate (RuBP), thylakoid membrane (TM).

1.2.2 Regulation and photoprotection of the photosynthetic apparatus

The redox potential of the PQ pool under stress conditions is tightly controlled by several photoprotective mechanisms, including 1) state transitions, 2) extra electron valves defined as alternative electron transport (AET) routes, namely flavodiiron proteins Flvs, respiratory terminal oxidases (RTO) and the bidirectional hydrogenase (Hox), 3) non-photochemical quenching (NPQ) by the orange carotenoid protein (OCP), and 4) cyclic electron transport (CET) around PSI (see Figure 2). As far as state transitions are concerned, several theories exist. In the mobile PBS model, PBS diffuse across the stromal side of the thylakoid membrane between the photosystems, which is induced by excitation with light of different wavelengths and changes in the redox state of the PQ pool (Joshua and Mullineaux, 2004). Blue or far-red (FR) light preferentially excite electrons in chl of the photosystems, of which about 90% are located in PSI, leading to a PBS shift from PSI towards PSII, thus inducing State 1. Light that is predominantly absorbed by PBS, or incubation in darkness, however, initiate the even distribution of PBS between both photosystems, known as State 2 (reviewed in Calzadilla *et al*., 2019). In the spillover model, however, it is proposed that PBS are constantly attached to PSII in both states, but transfer excess excitation energy to PSI in State 2 upon membrane rearrangement and movement of the photosystems rather than movement of the PBS (Federman *et al*., 2000). Under stress conditions, such as low CO_2 and high light, electrons accumulate in the electron transport chain (ETC) due to the lack of terminal electron acceptors (CO_2) or enhanced charge separation, both of which lead to damage of the D1 protein in the PSII core. To prevent costly damage, cyanobacteria employ different mechanisms acting as extra electron valves. RTOs, namely cytochrome *bd* quinol oxidase (Cyd) and cytochrome *c* oxidase (Cox), accept electrons for the reduction of O_2 into water mainly in darkness, but also to a small extent in light (Ermakova *et al*., 2016; for a review see Lea-Smith *et al*., 2016). The main electron valves in cyanobacteria, however, are the Flv proteins (see Allahverdiyeva *et al*., 2015 for a review). In cyanobacteria, Flv1/3 and Flv2/4 form dimers and are involved in photoprotection of the photosystems. Flv1/3 is associated with the photoprotection of PSI under fluctuating light conditions by accepting electrons after PSI and reducing O_2 into water in a process referred to as "Mehler-like" reaction (Allahverdiyeva *et al*., 2013). Hence, the production of the harmful reactive oxygen species (ROS) superoxide O_2^- and subsequent photoinhibition of PSI is prevented by Flv1/3 activity, and excess electrons,

stemming from the water-splitting in PSII, are re-directed towards the production of water downstream of PSI (water-water cycle). For Flv2/4, however, the exact function and mechanism are still unclear, but it is known that they work in photoprotection of PSII by accepting excess electrons, preventing the overreduction of the PQ pool (Zhang *et al*., 2009, 2012; Bersanini *et al*., 2014). Besides Flv2/4, the OCP protein is connected to the PBS core, quenching excess excitation energy absorbed by the PBS and releasing it as heat, known as NPQ (Wilson *et al*., 2006; see Kirilovsky, 2015 for a review). A last photoprotective mechanism involves CET through the NADPH dehydrogenase complex-1 (NDH-1), which accepts electrons after PSI via Fd and recycles it back to the PQ pool, thus increasing pmf and stimulating the production of ATP (Mi *et al*., 1995; see a review by Battchikova *et al*., 2011).

1.2.3 Cyanobacterial light-harvesting – the phycobilisome complex

Cyanobacteria are considered the plant chloroplast ancestors, and many of the main components of photosynthesis have remained highly conserved in plants throughout evolution (Nelson and Yocum, 2006). The key difference, however, lies in the development of a different type of light-harvesting antennae. In plants, light-harvesting complexes are embedded in the thylakoid membrane in close proximity to the photosystems, whereas in cyanobacteria, light-harvesting PBS are connected to the photosystems on the stromal surface of the thylakoid membrane. Collected light energy is transferred to chl of the photosystems' reaction centres, initiating photosynthetic electron transport (PET) as described above (for a review see Stadnichuk *et al*., 2015). PBS are pigment-protein complexes, about 3000 – 7000 kDa in size, and are composed of phycobiliproteins (PBP), which bind 200 – 500 phycobilin pigments (linear tetrapyrroles: phycocyanobilin, phycoerythrobilin, phycourobilin and phycoviolobilin), and colourless linker proteins (Figure 3). These PBS components can vary in number and type between cyanobacterial species and growth conditions, however, the basic PBS structure comprises a core consisting of PBP allophycocyanin (APC) cylinders from which PBS rods radiate. Core cylinders and the rods consist of discs of trimeric α- and β-polypeptides of the respective PBPs, which are stacked into hexamers forming a hollow cylinder (for a review see Stadnichuk *et al*., 2015). In *Anabaena* (*Nostoc*) sp. PCC 7120 (hereafter referred to as *Anabaena*), the APC core comprises three complete cylinders made of two hexamers (A1, A2 and B) and two half-cylinders made of one hexamer (C1 and C2) (Chang *et*

al., 2015). Attached to the cylinders are eight rods normally consisting of one to four stacked hexamers of the PBP phycocyanin (PC) and one hexamer of phycoerythrocyanin (PEC) (or phycoerythrin in some other cyanobacteria). All three PBPs bind the chromophore phycocyanobilin, which absorbs light energy of different wavelengths depending on the PBP it is connected to. PEC is located at the distal part of the rod structure and absorbs short wavelengths first (absorption maximum at 570 nm). The captured energy is then transferred via PC discs in the rods towards the APC core cylinders, which absorb light of long wavelengths (absorption maximum at 650 nm) (Bryant, 1982). The PBS core is connected to PSII in close vicinity to the CP43 protein via the terminal emitter ApcE, which is a pigmented core-membrane linker protein (L_{CM}) that channels excitation energy to the PSII reaction centre P680 (Liu *et al*., 2013; Chang *et al*., 2015; Tang *et al*., 2015).

PBS are assembled via different types of linker proteins that connect the discs within the rods (L_R, CpcC), the terminal rod caps with the rod (L_{RT}, CpcD), the rods with the core (L_{RC}, CpcG), the discs within the core cylinders (L_C, ApcC) and the core with the membrane (L_{CM}, terminal emitter ApcE) (Liu *et al*., 2005). L_{CM} is a large polypeptide that occurs in two copies per PBS and contains repetitions of the conserved protein domain PFAM00427, of which the number of repetitions determines the type of PBS (bicylindrical, tricylindrical or pentacylindrical) in different cyanobacterial species. In *Anabaena*, the L_{CM} protein has four PFAM00427 domains and, therefore, the APC core is pentacylindrical. Furthermore, *Anabaena* has four genes (*cpcG1/2/3/4*) encoding L_{RC} in contrast to the unicellular cyanobacterium *Synechocystis* sp. PCC 6803 (*Synechocystis*), which has tricylindrical PBS and two L_{RC} genes. *Anabaena* CpcG1/G2 L_{RC} connect two pairs of side rods (Rs) to the core, while CpcG4 is the main L_{RC}, linking top and bottom rods (Rt and Rb) to the core. CpcG3 is a specific L_{RC} for PSI (named CpcL), attaching one to three rods to a PSI-specific core cylinder consisting of ApcD, which is connected to PSI at the interface of two monomers via hydrophobic interactions (Bryant *et al*., 1991; Dong *et al*., 2009; Watanabe *et al*., 2014; Chang *et al*., 2015).

Light-harvesting by PBS is regulated by three processes: 1) NPQ through excess energy dissipation as heat by OCP (described above in Section 1.2.2), 2) re-adjustment of the rod length/composition according to the prevailing light conditions, known as chromatic acclimation, which involves cyanobacteriochromes, two-component systems and transcriptional regulation of PBS rod genes (Gutu and

Kehoe, 2011; Wiltbank and Kehoe, 2018), and 3) degradation mediated by the NblA protein, which intercalates into the PBS discs, causes disassembly and marks proteins for degradation by the Clp protease complex (see Forchhammer and Schwarz, 2018 for a recent review).

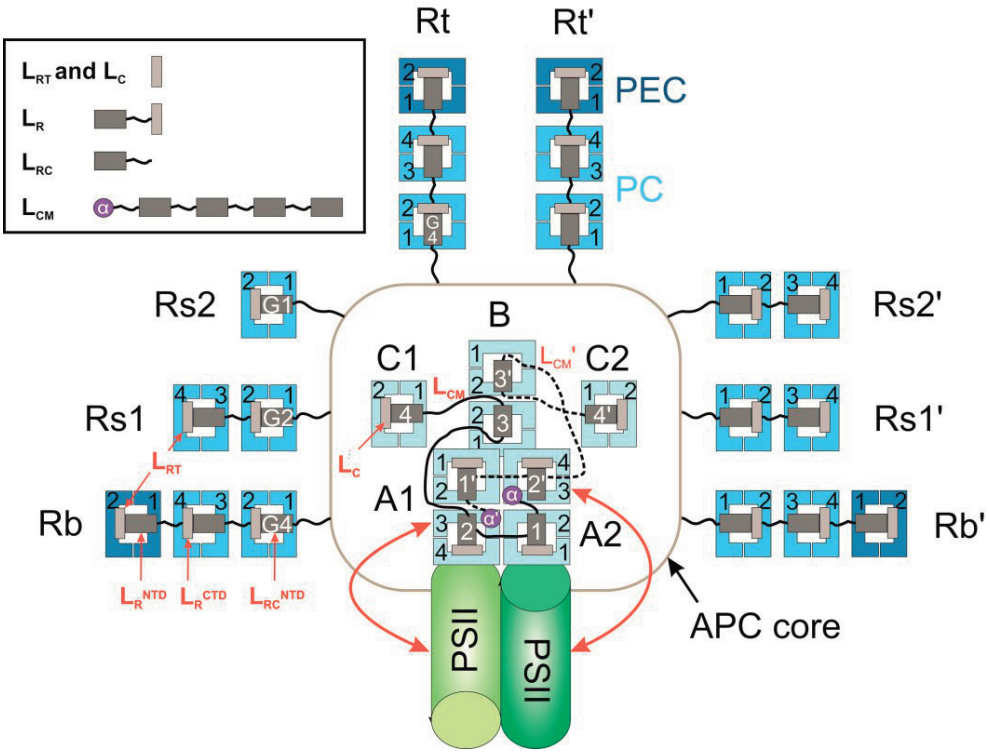

Figure 3: Structure of an *Anabaena* sp. PCC 7120 phycobilisome (PBS) complex connected to a photosystem II (PSII) dimer. From the pentacylindrical allophycocyanin (APC) core, eight PBS rods radiate, with two bottom rods (Rb and Rb'), shorter side rods (Rs1, Rs1', Rs2 and Rs2') connected to the half-cylinders, and two top rods (Rt and Rt'). The rods typically comprise one to four phycocyanin (PC) discs and one terminal phycoerythrocyanin (PEC) disc as rod caps. PBS subunits are connected by non-pigmented linker proteins (rod terminating linkers L_{RT}, rod linkers L_R, rod-core linkers L_{RC}, core linkers L_C and core-membrane linkers L_{CM}) which contain either, or both, the conserved protein domains Pfam00427 (dark grey box) and Pfam01383 (light grey box) (see Figure inset). L_{CM} is the terminal emitter ApcE, which is present in two copies, connecting the core cylinders to the PSII core (red arrows) via the α-subunit in the third trimer of A1 and A2. Figure modified from Chang *et al*. (2015) with adjustments according to Ducret *et al*. (1996). See the text for further details (Section 1.2.3). Abbreviations: carboxy-terminal domain (CTD), amino-terminal domain (NTD).

1.3 *Anabaena* as a model for the development of multicellularity

Anabaena is a filamentous, heterocystous cyanobacterium representing *β*-cyanobacteria and Section IV cyanobacteria with unbranched filaments, and its genome sequence has been available since 2001 (Kaneko *et al*., 2001). Under optimal growth conditions, the filaments mostly consist of photosynthetic vegetative cells, which can undergo morphological and physiological changes under nutrient-limiting conditions in order to cope with drastic changes in the environment. In many filamentous cyanobacteria, three cell differentiation processes are known to lead to the formation of N_2-fixing heterocysts, resting akinetes or motile hormogonia in some species (Herrero *et al*., 2016).

1.3.1 Heterocysts

The best-studied cell differentiation process in *Anabaena* is the irreversible formation of N_2-fixing heterocysts (Figure 1) (see reviews by Kumar *et al*., 2010 and Herrero *et al*., 2016). They are easily distinguishable from vegetative cells by their increased cell size due to a thick cell wall, an oval cell shape and a pale green colour, and they are unable to undergo cell division (Mitchison and Wilcox, 1972). Fully developed heterocysts contain the nitrogenase complex for the fixation of N_2 under N limitation. This complex is highly O_2-sensitive and therefore heterocysts comprise a variety of mechanisms to maintain intracellular anaerobiosis. As a protection barrier against O_2 diffusion through the cell membranes, the heterocyst cell envelope is composed of two additional outer layers in contrast to vegetative cells. During the first steps of cell differentiation, an O_2-impermeable heterocyst-specific glycolipid layer (HGL) develops on top of the outer vegetative cell membrane which is protected by a thick outer layer of heterocyst envelope polysaccharides (HEP). At this stage, the developing heterocyst is referred to as pro-heterocyst. For the determination of the heterocyst frequency as a physiological parameter, Alcian Blue dye, that stains polysaccharides blue, is used to detect pro-heterocysts and heterocysts. Furthermore, during heterocyst differentiation, the cell reorganises inner photosynthetic thylakoid membranes and complexes to provide anoxic conditions. Thus, the OEC in PSII is inactivated and heterocyst-specific respiratory complexes, such as Flv proteins and RTOs are employed to consume O_2 (Valladares *et al*., 2007; Ermakova *et al*., 2013, 2014; reviewed in Magnuson and Cardona, 2016). The PSI complex, in contrast, is still fully active for CET in heterocysts and provides

ATP for N_2 fixation. Furthermore, PBS amounts are significantly decreased in heterocysts compared to vegetative cells, but are still detectable (Magnuson and Cardona, 2016). In particular, the presence of the PBS rod-core linker protein CpcL, which is specific for PBS connected to PSI, indicates the presence of active PBS at PSI in heterocysts (Watanabe *et al*., 2014). Membrane reorganisation also leads to the formation of a special membrane system called the "honeycomb", with respiratory function in close proximity to the heterocyst poles, where heterocysts are connected to adjacent vegetative cells for the exchange of nutrients. Diffusion of O_2 into the heterocysts through these channels is prevented by a plug consisting of cyanophycin granules, a N storage material. However, if O_2 still manages to enter via the heterocyst poles, the surrounding honeycomb reduces it by oxidation of diaminobenzidine (Murry *et al*., 1981). All of these mechanisms help to keep O_2 at a very low level inside the heterocyst to support full activity of the nitrogenase complex in light and darkness (Bothe *et al*., 2010), which is in contrast to some non-heterocystous diazotrophs that separate photosynthesis and N_2 fixation temporally (Bergman *et al*., 1997). The nitrogenase complex is assembled from amino acids provided through degradation of PBS proteins during cell differentiation. As forementioned, nutrient exchange occurs between vegetative cells and heterocysts, making them highly dependent on each other. While photosynthetic vegetative cells provide C-based energy storage compounds (sugars), such as sucrose, the heterocysts supply N compounds, such as the amino acids glutamate and alanine (Thomas *et al*., 1977; Curatti *et al*., 2002; Pernil *et al*., 2010).

1.3.2 Akinetes

Akinetes are enlarged spore-like resting cells that are particularly resistant against long-term exposure to unfavourable conditions (Zhou and Wolk, 2002; Flores and Herrero, 2010), such as cold, drought and nutrient deficiencies (Adams and Duggan, 1999, Singh and Montgomery, 2011). Akinetes have previously been reported to share common regulation mechanisms of cell differentiation with heterocysts, and therefore might be evolutionary related through a common ancestor (Wolk *et al*., 1994). Indeed, both cell types possess the same type of outer envelope (Cardemil and Wolk, 1979; Leganés, 1994), and their differentiation is dependent on the expression of the heterocyst differentiation genes *hepA* and *hetR* (Leganés *et al*., 1994; Leganés, 1994; Campbell *et al*., 2007). In addition, earlier research has shown that akinete differentiation is further regulated by the availability of Ca^{2+} (Wolk,

1965). Nonetheless, akinete formation has mostly been studied in other filamentous heterocystous cyanobacteria strains (Cardemil and Wolk, 1979; Leganés, 1994; Adams and Duggan, 1999; Zhou and Wolk, 2002; Argueta *et al.*, 2006), but is reported to be absent in the strain *Anabaena*. Although a marker gene for akinete differentiation (*all4050* - *anaK*) is present in *Anabaena*, the gene might be inactive due to a spontaneous mutation (Zhou and Wolk, 2002, Argueta *et al*., 2006). In contrast, Prasanna and co-workers analysed 20 *Anabaena* species according to their morphology (and other factors) in 2006, presenting an akinete frequency of 4.8% in *Anabaena* sp. PCC 7120.

1.3.3 Hormogonia

Hormogonia are short motile filaments consisting of small vegetative cells with gas vesicles and are well-known to occur in some filamentous cyanobacterial species, such as *Nostoc* sp., *Scytonema* sp. and *Calothrix* sp. (Rippka *et al*., 1979). Vegetative filaments differentiate into hormogonia during nutrient limitations or symbiotic plant infection, in order to inhabit new environments, or to move towards the plant roots, respectively. After receiving the environmental stimulus, cell division is induced simultaneously in all cells of the filament, whereas deoxyribonucleic acid (DNA) replication and protein biosynthesis are ceased to a great extent. Therefore, the cells of the hormogonia remain small in size, but still photosynthetically active and can accumulate gas vacuoles for buoyancy (for a review see Meeks and Elhai, 2002). In 1962, Lazaroff and Vishniac described the developmental cycles of *Nostoc muscorum* (former description of *Anabaena*, Rippka *et al*., 1979) in dark-to-light transitions. In continuous light, heterocystous filaments break at the heterocysts, forming gliding hormogonia and releasing free heterocysts. Thus, hormogonia are non-heterocystous and unable to survive in N-deprived conditions.

1.4 C and N balance in cyanobacteria

Cyanobacteria constantly encounter changes in the environment, i.e. in nutrient availability, light intensity, temperature or pH, which have an effect on metabolic processes (Agostoni and Montgomery, 2014). To cope with these alterations, the balance in nutrient distribution between the primary metabolic pathways needs to be tightly regulated. In this regard, C and N are the most vital chemical elements which account for the survival of the cell. Their ratio (C/N) is an important indicator

of the metabolic status of the cell, which regulates the performance of primary metabolic processes (see a recent review by Zhang, C.C. *et al.*, 2018) (Figure 4).

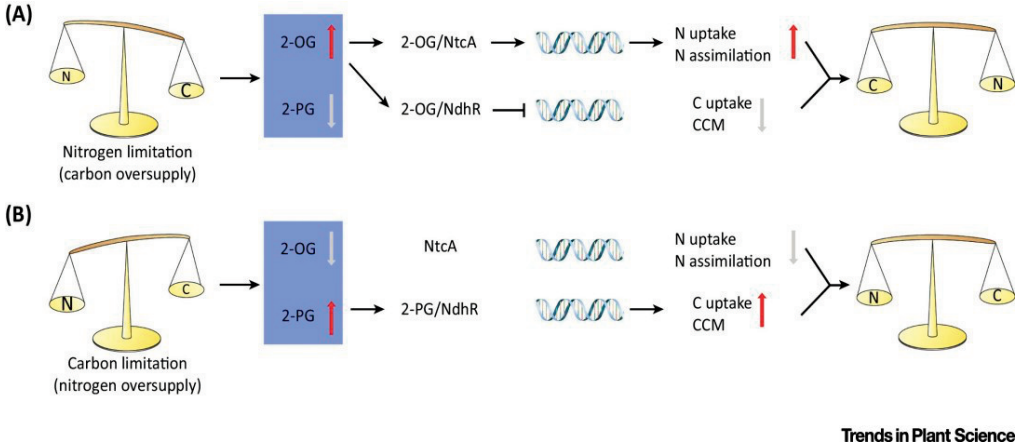

Figure 4: Schematic overview of the metabolic and transcriptional regulation of the carbon (C) and nitrogen (N) balance in cyanobacteria during N limitation (**A**) and C limitation (**B**) (Zhang, C.C. *et al.*, 2018). Abbreviations: C-concentrating mechanisms (CCM), 2-oxoglutarate (2-OG), 2-phosphoglycolate (2-PG).

Inorganic C (C_i) is present in the form of CO_2 and its soluble derivative HCO_3^- (both referred to as C_i) and is an essential building block for all organic compounds, such as sugars, lipids, amino acids and pigments. The latter two compounds additionally require N as a main structural component, which is also crucial for the synthesis of the energy carrier ATP and the nucleic acids DNA and RNA. The ultimate regulator for the C/N balance is 2-oxoglutarate (2-OG), which is the intermediate molecule that connects C metabolism with N metabolism (Muro-Pastor *et al.*, 2001). In the CBB cycle, C_i is fixed into glucose, which is catabolised to pyruvate in a process called glycolysis. Pyruvate then enters the tricarboxylic acid cycle (TCA; also known as citric acid cycle or Krebs cycle) as its derivative acetyl-CoA to produce the reducing agents nicotinamide adenine dinucleotide (NADH) and flavin adenine dinucleotide hydroquinone ($FADH_2$), and the key intermediate compound 2-OG. Therefore, the 2-OG level is directly correlated to the rate of C_i uptake and fixation. 2-OG then undergoes transamination by accepting an amino group from the α-amino acid glutamine derived from N metabolism, resulting in the formation of the α-amino acid glutamate in the glutamine synthetase-glutamine oxoglutarate aminotransferase (GS-GOGAT) cycle. Hence, relatively low levels of 2-OG indicate a balanced C/N ratio in non-stressed conditions (Figure 4), which is perceived by another signalling

molecule, the P_{II} protein, a sensor for the metabolic status of the cell (Espinosa *et al*., 2006). Trimeric P_{II} protein binds three monomers of the co-activator PipX, thus inhibiting and regulating nitrate and nitrite uptake in N-sufficient conditions. In N-depleted conditions, however, 2-OG is not transaminated and instead accumulates in the cell. Higher levels of 2-OG induce the release of the PipX proteins from P_{II}, two of which are transferred to the N control protein NtcA (Vega-Palas *et al*., 1992; Valladares *et al*., 2008). This transcription factor (TF) is the master regulator of N metabolism, activating or inhibiting the transcription of many N metabolism-related genes, and initiating fixation of N_2 to maintain the C/N balance (further described below).

1.4.1 Heterocyst formation and N_2 fixation

As described above, N starvation triggers a series of events to cope with this stress condition. In non-diazotrophic (non-N_2-fixing) cyanobacteria, N step-down induces the degradation of PBS subunits mediated by the NblA protein to release N-rich phycobilin pigments, which results in bleaching of the cells known as chlorosis (Baier *et al*., 2004; Forchhammer and Schwarz, 2018). Diazotrophic strains, however, are capable of synthesising the nitrogenase complex for fixing N_2. They can be divided into heterocystous and non-heterocystous N_2 fixers, of which the latter can usually only fix N_2 under micro- or anoxic conditions because the nitrogenase complex is highly O_2-sensitive (see Bergman *et al*., 1997 for a review). In the case of heterocystous cyanobacteria, the nitrogenase complex is spatially separated from O_2-evolving photosynthetic processes by the formation of heterocysts, as described in the previous section.

Heterocyst differentiation is initiated in vegetative cells by the activity of the master TF NtcA upon N step-down. NtcA stimulates the expression of the second master regulator of heterocyst formation, HetR, as one of the first targets. HetR is reported to have a dual function as TF as well as a Ca^{2+}-dependent protease, that supposedly degrades the only cyanobacterial Ca^{2+}-binding protein (CcbP) characterised so far, even though the location of the active site of the protease domain is still controversial (Zhou *et al*., 1998; Dong *et al*., 2000; Risser and Callahan, 2007). Nevertheless, it is proposed that CcbP degradation releases a Ca^{2+} signal in the differentiating vegetative cell about four hours after N step-down that, in turn, upregulates HetR protein levels and is required for heterocyst development (Zhao

et al., 2005; Shi *et al*., 2006). The HetR protein also contains a DNA-binding domain and binds *in vitro* to the promoters of several heterocyst differentiation genes, such as *hetR* itself, *hetZ*, *hetP*, *hetC*, *patS*, *hepA* and *pknE* (Flaherty *et al*., 2014). While HetP is important for the commitment of a vegetative cell to differentiation into a pro-heterocyst about nine hours after N step-down (Videau *et al*., 2016), HetC then induces the inhibition of cell division and the expression of genes for the biosynthesis of the heterocyst envelope, composed of an inner gas-impermeable HGL layer and an outer HEP layer (Wang and Xu, 2005). Interaction of HetC with PatB (the TF of the nitrogenase complex), CoxBII, NblA, RbcL and others further leads to cytoplasmic maturation of the heterocyst by downregulating photosynthesis (degradation of PBS) and expressing N_2 fixation-related protein complexes, such as the nitrogenase or RTO complexes (Tsujimoto *et al*., 2014). This developmental process occurs in about every 10^{th} cell in a filament under N-deprived conditions, due to the action of heterocyst pattern formation proteins. The best studied inhibition protein is the small peptide PatS (Yoon and Golden, 1998), which is mainly expressed in heterocysts (Yoon and Golden, 2001). PatS diffuses in a processed form along adjacent cells, in which it inhibits the activity of HetR, leading to the regression of heterocyst differentiation before commitment (Corrales-Guerrero *et al*., 2013).

With heterocyst maturation, the major protein complex for the fixation of N_2 is synthesised from the main *nif* operon, the *nifHDK* operon. The nitrogenase complex is composed of two protein components, namely the dinitrogenase (MoFe protein) and the dinitrogenase reductase (Fe protein). The dinitrogenase reductase accepts electrons from an electron donor, Fd or Fld, deriving from CET around PSI in heterocysts, and transfers this electron (e^-) to the dinitrogenase subunit, where N_2 is thus reduced to nitrate. Concomitantly, H^+ are reduced to H_2, which is subsequently consumed by two different hydrogenases in *Anabaena*, the uptake hydrogenase and Hox (Tamagnini *et al*., 2007). The overall equation for the reduction of N_2 is (Saeki, 2004):

$$N_2 + 8\,H^+ + 8\,e^- + 16\,ATP = 2NH_3 + H_2 + 16\,ADP + 16\,P_i$$

It is visible from the equation that the N_2 fixation process is highly costly for the cell, as it requires energy in the form of 16 ATP, whose production relies on LET between the photosystems, CET around PSI, and respiration. Reductants such as NADPH are

generated in the oxidative pentose phosphate pathway by metabolising carbohydrates supplied from vegetative cells (Böhme, 1998).

In contrast to *Anabaena*, some cyanobacterial species, such as *Anabaena variabilis*, contain two additional sets of nitrogenases. In case of molybdate limitation, a vanadium (V)-type nitrogenase compensates the lack of the Mo-type nitrogenase inside the heterocysts. In addition, a second Mo-type nitrogenase is present in vegetative cells, but is only active under strict anaerobiosis (Thiel, 2004).

1.4.2 Carbon concentrating mechanisms

Over the course of evolution, cyanobacteria have developed specific mechanisms to improve their photosynthetic capacity when the GOE led to an oxidised atmosphere with low levels of available CO_2. The so-called C_i concentrating mechanisms (CCMs) raise the level of CO_2 within the cells and concentrate it around the enzyme RuBisCO (see Price *et al*., 2008 for a review), which, in cyanobacteria, has lower specificity for CO_2 over O_2 but higher CO_2-fixation rates per active site compared to plant-type RuBisCO (Whitney *et al*., 2011). Without CCMs, this would result in higher rates of energy-consuming photorespiration and lower rates of CO_2 fixation in cyanobacteria. Therefore, cyanobacterial RuBisCO is encapsulated in specialised cell compartments, called the carboxysomes, which consist of a proteinaceous shell that is only permeable to small polar molecules, such as the predominant water-soluble C_i species HCO_3^-. In addition to RuBisCO, carboxysomes also contain the enzyme carbonic anhydrase, which catalyses the conversion of HCO_3^- into CO_2 in close proximity to the active site of RuBisCO. The carboxysome protein shell constitutes a gas-impermeable barrier, thus preventing O_2 influx into the carboxysome to a great extent, as well as preventing CO_2 leakage from the carboxysome (Kerfeld and Melnicki, 2016). The substrate for the carboxylation process, RuBP and the resulting fixed three-C-sugar 3-PGA enter and leave the carboxysome, respectively, through small pores in the protein shell, and are further processed into bigger sugar molecules in the CBB cycle in the cytoplasm. Recently, carboxysomes have been intensively studied for their great potential for biotechnological applications and improving CO_2 fixation in plants (Hanson *et al*., 2016; Long *et al*., 2018; Plegaria and Kerfeld, 2018).

Furthermore, CCMs actively take up C_i into the cell via several HCO_3^- and CO_2 uptake transporter systems both in the plasma membrane and thylakoid membrane (Badger and Price, 2003). BCT1 (encoded by *cmpABCD*), SbtAB and BicA are high, medium and low affinity HCO_3^- transporters in the plasma membrane, respectively, requiring the binding of ATP (BCT1) or sodium (Na^+) (SbtAB and BicA). In the thylakoid and plasma membranes, special NDH-1 complexes (NDH-1MS containing NdhD3/F3 and NDH-1MS' containing NdhD4/F4; Battchikova *et al*., 2011), summarised as NDH-$1_{3/4}$, are involved in CO_2 uptake and its subsequent conversion into HCO_3^-. The expression of all C_i uptake transporters is highly induced under C_i-limiting conditions as a consequence of the regulation by the TFs CmpR (promoting expression of the *cmp* operon; Takahashi *et al*., 2004) and NhdR (also known as CcmR; repressing expression of *sbt*, *bic* and *ndh-1₃* genes; Wang *et al*., 2004) and the signalling molecules 2-OG from the TCA cycle and 2-phosphoglycolate (2-PG) from oxygenation of RuBP by RuBisCO. As described above, under high C_i conditions, the imbalanced C/N ratio represents N starvation. In this condition, 2-OG accumulates in the cell and stimulates alternative N uptake and assimilation systems through binding to NtcA and P_{II} (Muro-Pastor *et al*., 2001). Simultaneously, 2-OG binds to the repressor NdhR and promotes its interaction with DNA, thus inhibiting the expression of the C_i transporters and re-balancing the C/N ratio (Jiang *et al*., 2018). Under low C_i conditions, RuBisCO is more likely to catalyse the oxygenation reaction of RuBP into the toxic compound 2-PG, which also binds to NdhR, however, preventing its interaction with DNA (Haimovich-Dayan *et al*., 2015). Hence, the expression of C_i transporters is not inhibited, promoting active C_i uptake in order to maintain the C/N balance (summarised in Zhang, C.C. *et al*., 2018; Figure 4).

1.5 Ca^{2+} as a signalling molecule and second messenger in biological systems

The calcium ion (Ca^{2+}) plays a pivotal role in a variety of cellular processes, due to its low solubility in water, its binding capacity to 4-12 oxygen atoms of carboxyl and carbonyl groups and its capability to change the function of proteins by altering their shape and charge as well as precipitating phosphate ions (Clapham, 2007). In the latter case, a high intracellular Ca^{2+} concentration ($[Ca^{2+}]_i$) is toxic because free phosphate ions are required for metabolic processes, such as RNA and DNA biosynthesis. Therefore, $[Ca^{2+}]_i$ has to be tightly regulated by Ca^{2+} channels and pumps and Ca^{2+}-binding proteins (Bagur and Hajnóczky, 2017). A typical Ca^{2+}-binding protein binds Ca^{2+} via a highly conserved domain called the EF-hand, which

is a helix-loop-helix structure with at least four conserved acidic amino acid residues. The 12 amino acid loop has the consensus sequence D-x-D-x-D-G-x-V/I-T/S-x-x-E and is flanked by nine amino acids forming α-helices (Michiels *et al*., 2002).

The basic Ca^{2+} signalling cascade constitutes four steps. Firstly, an external stimulus, such as changes in temperature, light, pH or nutrient starvation, induces a Ca^{2+} signal with a distinct signature, usually a transient or oscillation with specific spatiotemporal features (duration, amplitude, period, frequency) (McAinsh and Pittman, 2009). Ca^{2+} is either taken up externally through ion channels or released from internal storages such as Ca^{2+}-binding proteins or cellular compartments. The wave of free Ca^{2+} is then perceived by Ca^{2+} sensors, or binds directly to DNA, RNA or protein complexes, triggering a stress response, such as ion homeostasis, hormone signalling, cell division, ROS scavenging and pathogen defence (DeFalco *et al*., 2009). Therefore, $[Ca^{2+}]_i$ is kept at very low levels, making this system highly sensitive and effective (Agostoni and Montgomery, 2014).

1.5.1 Effect of Ca^{2+} on plant photosynthesis

In the past few decades, investigation of Ca^{2+} signalling events in plants has gained attention with the discovery of a complex network of Ca^{2+}-binding proteins, such as calmodulins and Ca^{2+}-dependent protein kinases, as well as the development of highly sensitive Ca^{2+} detection systems, including the bioluminescent Ca^{2+} sensors aequorin and a vast range of green fluorescent protein (GFP)-based "cameleon" proteins. $[Ca^{2+}]_i$ is maintained at around 100 nM, but transiently increases during a wide range of responses to environmental stimuli, such as temperature shock, wind, drought, salinity and touch (summarised in White and Broadley, 2003). More recent attention has been focussed on the contribution of plant chloroplasts in Ca^{2+} sequestration and signalling events. The negatively charged surface of the thylakoid membrane can sequester up to 15 mM Ca^{2+}, whereas the stromal $[Ca^{2+}]$ is kept at 150 nm in non-stressed conditions (Rocha and Vothknecht, 2012; Stael *et al*., 2012a; Nomura and Shiina, 2014; Sello *et al*., 2018). Chloroplasts are of particular interest in Ca^{2+} signalling as they accommodate the machinery for photosynthesis, which is also subject to Ca^{2+} regulation (Hochmal *et al*., 2015). Ca^{2+} is a structural component of the photosystems in the thylakoid membranes, with one Ca^{2+} in the OEC and Ca^{2+}-binding PsbO in PSII and two identified Ca^{2+} in monomeric plant PSI (Heredia and

De Las Rivas, 2003; Caspy and Nelson, 2018). Additionally, Ca^{2+} transients measured in chloroplasts have implicated Ca^{2+} signalling in light-to-dark transitions within the chloroplast. Ca^{2+} is taken up into the chloroplast and bound to the negatively charged thylakoid membrane during illumination, leaving a free Ca^{2+} level of about 150 nM, while shortly after the offset of light (~ 30 min), a strong increase in free Ca^{2+} levels from internal storages was detected that led to the inactivation of CBB cycle enzymes for CO_2 fixation, such as fructose-1,6-bisphosphatase (Sai and Johnson, 2002).

1.5.2 Involvement of Ca^{2+} on cellular and metabolic processes in cyanobacteria

In cyanobacteria, Ca^{2+} is involved in phototactic orientation and gliding motility via Ca^{2+}-binding surface proteins (oscillins), heterocyst and hormogonia differentiation (see above), PBS degradation via NblA (Agostoni and Montgomery, 2014) and in the composition of the photosynthetic photosystems. In trimeric PSI crystal structures of *Synechocystis*, six Ca^{2+} were found, two of which were detected in the structures of the PSI subunits PsaL and PsaB, which are possibly involved in the formation of oligomeric PSI or of a docking site for a yet unidentified Ca^{2+}-binding protein (Malavath *et al*., 2018). Additionally, monomeric PSII crystal structures of *Thermosynechococcus elongatus* and *T. vulgaris* included four Ca^{2+}, one of which was located to the OEC and others to the subunits CP43 and PsbK (Müh *et al*., 2008; Umena *et al*., 2011).

For a long time, Ca^{2+} signalling was not considered to exist in cyanobacteria due to the lack of molecular evidence for Ca^{2+} channels and Ca^{2+}-binding proteins. In the past 20 years, the role of Ca^{2+} in abiotic stress response in *Anabaena*, specifically, has been identified by the recombinant expression of bioluminescent Ca^{2+} sensors that showed a transient increase in $[Ca^{2+}]_i$ from a resting level of about 0.2 µM up to 4 µM free Ca^{2+} (Torrecilla *et al*., 2000, 2001, 2004a). It has been reported that Ca^{2+} plays a role in growth behaviour (Singh and Mishra, 2014), the regulation of ROS (Singh and Mishra, 2016), acclimation to heat stress (Tiwari *et al*., 2016), the production of exopolysaccharides (Singh *et al*., 2016) and the composition of fatty acids and hydrocarbons (Singh *et al*., 2017). The most prominent role of Ca^{2+} in *Anabaena* is the regulation of heterocyst formation early after N deprivation (Torrecilla *et al*., 2004b) through the activity of CcbP, which binds Ca^{2+} via negative surface charges (Zhao *et al*., 2005; Hu *et al*., 2011).

2. AIMS OF THE STUDY

Cyanobacteria inhabit different terrestrial and marine environments and constantly encounter changes in their growth conditions, which requires tight metabolic regulation in order to acclimate to and cope with abiotic stresses. Such abiotic stresses include variations in temperature, light, pH and nutrient availability. One of the important macronutrients is Ca^{2+}, which is known to be an essential secondary messenger molecule in eukaryotes. In prokaryotes, particularly in cyanobacteria, Ca^{2+} signalling was long thought not to exist, and related research was scarce. However, with increasing knowledge about Ca^{2+} signalling components in plants and especially in the chloroplast, the effect of Ca^{2+} on cyanobacterial metabolism has begun to gain attention during the past 40 years (Piccioni and Mauzerall, 1978), because cyanobacteria are considered the progenitors of photosynthetic chloroplasts and are promising platforms for future biotechnological applications. Therefore, it has been crucial to understand basic metabolic pathways, such as photosynthesis and N_2 fixation, and to identify their regulators and key players.

In this thesis, the four main objectives are the following:

1. Investigation of Ca^{2+}-dependent transcription regulation and the effect of Ca^{2+} on the C/N balance and cell physiology in *Anabaena*

2. Identification of novel Ca^{2+}-binding proteins in *Anabaena*

3. *In vitro* characterisation of the *Anabaena* gene *asr11311* encoding a novel Ca^{2+}-binding protein (CSE)

4. Study the crosstalk between Ca^{2+} signalling and primary metabolic pathways involving the CSE protein in *Anabaena*

3. METHODOLOGY

3.1 Cyanobacterial strains and growth conditions

3.1.1 Generation of modified Anabaena strains

Genetically modified *Anabaena* strains (Table 1) were obtained through triparental conjugation (Elhai and Wolk, 1988) of *Anabaena* wild-type (WT) with respective vectors. An *asr1131* overexpression (*cse*-oex) construct (*pBG2089*) was generated by inserting the gene and its native promoter and terminator sequences into the *RSF1010*-based low-copy number plasmid *pRL1342*, which contained an erythromycin (Em) resistance cassette for selection of transformants (Paper II). Knockout of the *asr1131* gene (*Δcse*) was achieved through homologous recombination of *asr1131* flanking regions, replacing the whole gene with a neomycin (Nm) resistance cassette. To select double recombinants, the *Δcse* vector contained the *pRL448*-derived *sacB* gene. The resulting *Δcse* mutant was complemented by introduction of the overexpression vector *pBG2089* (Paper III).

Table 1: *Anabaena* sp. PCC 7120 strains used in this thesis

Strain	Modified/introduced genes	Paper	Reference
WT (sp. PCC 7120)		I, II, III	
cse-oex	*asr1131*::Em^R (*pBG2089*)	II	This study
Δcse	*asr1131*::Nm^R	III	This study
Δcse::*pBG2089*	*asr1131*::Nm^R *asr1131*::Em^R (*pBG2089*)	III	This study

3.1.2 Culture conditions

In Papers I and III, *Anabaena* strains were grown in BG11 medium, which contains 0.25 mM $CaCl_2$ and was designated as "low Ca^{2+} BG11 medium" in Paper I (Rippka *et al.*, 1979). Additionally, in Paper I, cells were grown in "high Ca^{2+} BG11 medium" with 4-fold higher $CaCl_2$ concentration (1 mM $CaCl_2$), and in Paper III, cells were also grown in $BG11_0$ medium lacking any source of N. In Paper II, $BG11_0$ medium was supplemented with 10 mM $NaHCO_3$ ($BG11_0C$), to which 6 mM NH_4Cl ($BG11_AC$) was added when indicated. As a pH buffer, 10 mM TES-KOH (pH 8.0) was added to all

media. Liquid cultures were cultivated at 30°C with gentle agitation (120 rpm) in ambient air (low CO_2: 0.04% CO_2) or in air enriched with 3% CO_2 (high CO_2; standard growth condition). Continuous illumination of 35 - 50 µmol photons m^{-2} s^{-1} was provided by cool-white fluorescent lamps (L 30W/865 Osram). For the selection of transformants, pre-experimental cultures were supplemented with the respective antibiotics (see Table 1), which were omitted from cultures used for physiological/biophysical/gene expression experiments.

For physiological measurements, cells were collected during the logarithmic growth phase (optical density at 750 nm: OD_{750} = 0.6-1.0). Chl concentrations were measured and calculated through absorbance at 665 nm (OD_{665}) in 90% methanol, applying the extinction coefficient 78.74 L g^{-1} cm^{-1} (Meeks and Castenholz, 1971). Room temperature (RT) pigment absorption spectra and optical densities were determined with a Shimadzu UV-1800 UV spectrophotometer (Berner) and a Thermo Scientific Genesys 10S UV-Vis spectrophotometer. The dry biomass of cultures was determined according to Huokko *et al*. (2017). Total hexoses were measured by the colorimetric method described by DuBois *et al*. (1956). Total proteins were detected according to a modified Lowry procedure (Markwell *et al*., 1978). Nitrogenase activity was measured as described by Kosourov *et al*. (2014).

3.1.3 Ca^{2+} shift experiments

Anabaena WT cultures were grown in low and high Ca^{2+} BG11 medium (see Section 3.1.2). During the logarithmic growth phase, cells were resuspended to OD_{750} = 0.8 with the respective media (see Figure 5). After one-hour incubation, 2 ml samples were taken for RNA isolation. Furthermore, samples were taken for the determination of total proteins, carbohydrates and the dry biomass (methods mentioned above), over a time course of 24 hours after the shift. In addition, photosynthetic performance was determined through measurements of O_2 evolution (Clark-type O_2 electrode, Hansatech) and PSII maximum effective yield Y(II) (Dual-PAM-100, Walz). After three days of incubation in different Ca^{2+} media, bright-field and fluorescence micrographs were taken to calculate the heterocyst frequency in filaments.

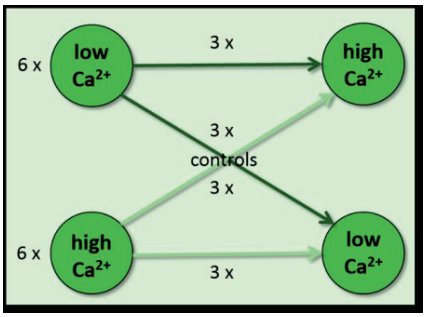

Figure 5: Schematic overview of the calcium (Ca^{2+}) shift experiment with *Anabaena* sp. PCC 7120. Six cultures were grown in low Ca^{2+} and six in high Ca^{2+} media to the exponential growth phase ("long-term" cultures). Three experimental cultures of each initial Ca^{2+} concentration were refreshed with medium containing the alternative Ca^{2+} concentration, and three control cultures were refreshed with medium containing the same Ca^{2+} concentration.

3.1.4 N and C_i limitation experiments

Anabaena WT and the mutant strain *Δcse* were pre-incubated in standard growth conditions (BG11 and high CO_2) for three days. During the logarithmic growth phase, 2 ml of samples were collected and stored at -20°C until RNA isolation (timepoint 0). The remaining cultures were refreshed and resuspended to OD_{750} = 0.6 with $BG11_0$ and BG11, respectively, and transferred to growth conditions reflecting N limitation ($BG11_0$ in high CO_2) or C_i limitation (BG11 in low CO_2). Samples of 2 ml were taken at the timepoints indicated and stored at -20°C until RNA isolation.

3.2 Microscopy

3.2.1 Bright-field and fluorescence microscopy for the determination of heterocyst frequencies and filament lengths

Bright-field and chl fluorescence images were taken with an AxioVert 200M inverted fluorescence microscope (Zeiss) to detect heterocysts with ×200 magnification (Paper I). In Paper II, proheterocysts and heterocysts were stained with 0.5% Alcian Blue dye. At least 1000 cells were counted from micrographs with ×400 magnification, obtained with a Wetzlar light microscope (Leitz), and the heterocyst frequency was estimated as the percentage of the total amount of counted cells. For filament length counts, a minimum of 300 filaments was counted (Paper III).

3.2.2 Transmission and Scanning electron microscopy

Anabaena cells were collected and pre-fixed in 0.2 M S-collidin-HCl buffer (pH 7.4) mixed with 25% glutaraldehyde in a ratio 4:1. The samples were then submitted to the Laboratory of Electron Microscopy (University of Turku, Finland) for Transmission and Scanning electron microscopy (TEM/SEM) specimen preparation.

TEM was carried out in the same facilities with a JEM-1400 Plus Transmission Electron Microscope, whereas SEM samples were further submitted to the Institute of Dentistry (University of Turku, Finland), where they were coated with gold particles, followed by SEM imaging.

3.3 Biophysical methods

Cultures were grown for two days and adjusted with fresh medium to a chl concentration of 7.5 µg ml^{-1} for all biophysical methods except P700 measurements with a pulse-amplitude modulated fluorometer/spectrometer (Dual-PAM-100; Walz, Effeltrich, Germany), which were recorded independently from chl fluorescence and for which the chl concentration was 15 µg ml^{-1}, and incubated in the growth chamber for at least 30 min. Experiments were performed with whole cell samples as described in Kämäräinen *et al.* (2016) and Huokko *et al*. (2017).

3.4 Transcript analyses

3.4.1 Total RNA isolation and next generation sequencing

Total RNA was isolated using a hot phenol method. Fresh or frozen cell pellets were resuspended in 0.56 ml RNA buffer (0.3 M saccharose, 10 mM sodium acetate, pH 4.5, 0.25 M EDTA and 2% SDS), and nucleic acids were extracted three times with an equal volume of hot phenol:chloroform:iso-amyl-alcohol (25:24:1) (5 min 95°C) and once with chloroform:iso-amyl-alcohol (24:1). Subsequently, RNA was precipitated overnight in 2 M LiCl and 70% ice-cold ethanol at -20°C. Genomic DNA was removed using the TURBO DNA-*free*™ kit (Invitrogen™) according to the manufacturer's manual. RNA concentration/purity and integrity were assessed with a NanoDrop spectrophotometer (Thermo Scientific) and agarose gel electrophoresis. RNA samples were submitted for RNA sequencing (RNAseq) to the Turku Centre for Biotechnology (Turku, Finland) using Illumina-HiSeq 2000 (Paper I) and the Beijing Genomics Institute (Shenzhen, China) using Illumina-HiSeq2500/4000 (Papers II and III).

3.4.2 Reverse transcription-quantitative polymerase chain reaction

Purified RNA (500 ng) was transcribed into first strand complementary DNA (cDNA) using the SuperScript® III First-Strand Synthesis System (Invitrogen™) according to

the manufacturer's protocol. Next, cDNA samples were diluted 5-fold and mixed with gene-specific primers (Paper III) and the iQ™ SYBR® Green Supermix (Bio-Rad) to amplify and detect transcripts with an iQ™5 Multicolor Real Time polymerase chain reaction (PCR) Detection System and the iQ™5 Optical System software 2.0 (Bio-Rad). Negative controls contained ultrapure water in place of the cDNA template. The constitutively expressed *rpoA* gene (Mella-Herrera *et al*., 2011) was used as a reference gene, and normalised expression ratios between target and reference genes were calculated with the Pfaffl method (Pfaffl, 2001). Equal primer amplification efficiencies were determined in template dilution series.

3.5 Protein analyses

3.5.1 Overexpression and purification of recombinant CSE protein

CSE protein was fused to a poly-histidine (His) affinity tag by cloning the PCR-amplified *asr1131* gene into the pET-28a(+) vector (Novagen). Expression of the CSE protein in *Escherichia coli* BL21 cells was induced with 100 mM isopropyl β-D-1-thiogalactopyranoside (IPTG). CSE protein was purified by affinity chromatography using a non-commercial Ni-NTA column and gradually increasing concentrations of imidazole in the elution buffer (40-300 mM).

3.5.2 $^{45}Ca^{2+}$ autoradiography

A $^{45}Ca^{2+}$ overlay assay was performed as described in Stael *et al*. (2011). Purified CSE and control proteins were transferred onto a methanol-activated polyvinylidene difluoride (PVDF) membrane in 10 µl drops. The membrane was washed three times in one hour with a Ca^{2+}-removing buffer (5 mM $MgCl_2$, 60 mM KCl and 60 mM imidazole-HCl, pH 6.8) and subsequently incubated in the same buffer with addition of 0.1 µM $^{45}CaCl_2$ (13.90 mCi/mg; Perkin Elmer). Then, the membrane was rinsed with 50% ethanol. After drying the membrane, it was exposed on a phospho-imaging screen. The screen was then scanned for radioactive signals with a FUJI FLA-3000 (FUJIFILM), while the proteins on the membrane were stained with Coomassie Brilliant Blue.

3.5.3 Protein analyses of thylakoid membrane protein complexes

Thylakoid membrane protein complexes were extracted according to Zhang *et al*. (2009) and analysed in blue native polyacrylamide gel electrophoresis (BN-PAGE) as described by Zhang *et al*. (2004) with minor modifications. After solubilisation with 1.5% *n*-dodecyl-β-D-maltoside (DM), the membrane fraction was loaded onto a large pore (lp)-BN gel with an acrylamide concentration gradient of 3.5-12.5%. Protein complexes were further separated in two dimensional (2D)-sodium dodecyl sulfate (SDS)-PAGE as described in Zhang *et al*. (2004) using a 12%-SDS gel (6 M urea). Next, protein spots were visualised with SYPRO™ Ruby Protein Gel Stain (Invitrogen™) for imaging and silver staining for mass spectrometry (MS) analysis, according to the manufacturers' instructions. MS analysis of selected protein spots was performed as in Trotta *et al*. (2016).

3.6 Bioinformatics methods

RNAseq reads were aligned in the open source software Chipster (CSC Finland) (Paper I) and in Strand NGS (Papers II and III). Significantly differentially expressed genes were identified using a false discovery rate (FDR) cutoff of 0.05 and testing the means for variation (Analysis of variance - ANOVA). Gene descriptions were acquired from the following databases: Kyoto Encyclopedia of Genes and Genomes (KEGG), CyanoBase (Kazusa Genome Resources) and Joint Genome Institute Integrated Microbial Genomes & Microbiomes (JGI IMG/M).

For a prediction of the CSE tertiary structure, the Asr1131 amino acid sequence was submitted to I-TASSER (Yang *et al*., 2015). For a comparison, the predicted CSE structure was aligned in PyMOL (Schrödinger) to the crystal structure of troponin C (PDB: 2TN4). Furthermore, a search for Asr1131 homologs was performed using Basic local alignment search tool (BLAST) in CyanoBase and JGI IMG/M. The resulting hits from CyanoBase were aligned in MEGA6 using the multiple sequence alignment tool Muscle.

4. MAIN RESULTS

4.1 Ca^{2+} regulates primary metabolic pathways

Primary metabolic pathways are subject to environmental changes and need to be tightly regulated in all living organisms. In plants, it is well-known that Ca^{2+} acts as a second messenger and relays information via signals with specific signatures, i.e. frequency, duration, magnitude, and source (McAinsh and Pittman, 2009). In cyanobacteria, however, Ca^{2+} signalling has not been thoroughly investigated. Therefore, shifts in external Ca^{2+} concentrations ($[Ca^{2+}]_e$) were followed by analysis of changes in the transcriptome using RNAseq and changes in physiological parameters, such as dry weight, total proteins and total sugars. RNAseq is a powerful tool for detecting differential gene expression in a holistic systems biology approach. In Paper I, it was demonstrated that shifts from low Ca^{2+} (0.25 mM $CaCl_2$; comparable to freshwater; Rippka *et al*., 1979) to high Ca^{2+} (1 mM $CaCl_2$; promoting growth; Singh and Mishra, 2014), and *vice versa*, induced changes in gene expression relative to control cultures in which $[Ca^{2+}]_e$ remained unchanged (see Figure 5). Of the 6132 protein-encoding genes and 83 RNA-encoding genes in *Anabaena* (https://www.genome.jp/kegg-bin/show_organism?org=ana), 101 and 42 genes were statistically differentially expressed in the shift from low to high Ca^{2+} and in the shift from high to low Ca^{2+}, respectively. The most significantly differentially expressed genes included C_i and nitrate/nitrite uptake transporters, which are involved in maintaining the C/N balance in *Anabaena*, which was reflected in the accumulation of total biomass and total proteins, as detailed below.

4.1.1 Gene expression is adjusted by $[Ca^{2+}]_e$

In Paper I, Ca^{2+} shifts from either low to high Ca^{2+} or from high to low Ca^{2+} induced strong differential gene expression of the C_i and nitrate/nitrite uptake transporters one hour after the shift. During the shift to high Ca^{2+}, the entire *cmp* operon, as well as *bicA* and *sbtAB* genes, each encoding independent C_i uptake transporters, and the respective TF *cmpR* (also called *rbcR1*) were strongly upregulated. In addition, genes of several Na^+/H^+ antiporters, feeding Na^+ to BicA and SbtAB, were upregulated. In turn, in the shift to low Ca^{2+}, these same genes were strongly downregulated (Table 2; Paper I: Table 1 and Figure 1 **Cluster 1**). Uptake transporters and enzymes involved in N metabolism, on the other hand, were downregulated in response to high Ca^{2+} and upregulated in the shift to low Ca^{2+} (**Cluster 4**). Similar to Cluster 1

genes, **Cluster 2** genes included photosynthesis and C metabolism-related genes such as several photosystem core and reaction centre proteins, and stress-related genes, which were strongly increased in expression in the upward $[Ca^{2+}]_e$ shift and moderately decreased in the downward shift. **Cluster 3** genes, which comprised Hox subunits, however, were moderately downregulated in the shift to high Ca^{2+} and moderately upregulated in the shift to low Ca^{2+}.

Table 2: Summarising overview of the most significant transcriptomic changes from the calcium (Ca^{2+}) shift experiments in Paper I. Abbreviations: heterocyst glycolipid layer (HGL), dinitrogen (N_2).

Cluster	Genes	Shift to high Ca^{2+}	Shift to low Ca^{2+}
1	Inorganic carbon uptake transporters, Na^+:H^+ antiporter	strongly up	strongly down
2	Photosynthesis and carbon metabolism, stress-related genes	strongly up	moderately down
3	Bidirectional hydrogenase Hox	moderately down	moderately up
4	Nitrate uptake transporters and metabolism	strongly down	strongly up
		Long-term high Ca^{2+}	**Long-term low Ca^{2+}**
5	HGL and chlorophyll synthesis, N_2 fixation proteins	strongly up	strongly down
6	ribosomal proteins, sigma factors	strongly down	strongly up

The gene expression patterns described above were detected one hour after the Ca^{2+} shifts and referred to as "**short-term**" changes between Ca^{2+}-shifted cultures and their respective controls. In addition, differences in gene expression were detected in cultures originating from the same three-day pre-culture (see Figure 5 in the Methodology section), which were insensitive to one-hour shifts in $[Ca^{2+}]_e$. These so-called "**long-term**" changes were found in **Cluster 5** and **Cluster 6** genes. Cluster 5

genes showed high expression in the samples originating from the long-term high Ca^{2+} culture and low expression in the samples originating from the long-term low Ca^{2+} culture and included several N_2 fixation proteins and HGL and chl precursors. Cluster 6 genes comprised ribosomal proteins and sigma factors and were strongly downregulated in long-term high Ca^{2+} and strongly upregulated in long-term low Ca^{2+} conditions (Table 2; Paper I: Table 2 and Figure 1).

4.1.2 Physiological parameters respond to changes in $[Ca^{2+}]_e$

Alterations in $[Ca^{2+}]_e$ led to the inversed expression of C_i and nitrate uptake transporters, as described above. Whether or not this resulted in increased/decreased uptake of C_i and N and respective metabolic activity was assessed by measuring the accumulation of biomass as dry weight, total proteins and total sugars over a time course of 24 hours. In contrast to all other parameters, the biomass of cultures showed significant differences between high and low Ca^{2+} conditions four hours after a change in $[Ca^{2+}]_e$. The biomass of the culture shifted from high to low Ca^{2+} was clearly lower than its high Ca^{2+} control, whereas the culture shifted from low to high Ca^{2+} remained stable throughout the experiment compared to its low Ca^{2+} control (Paper I: Figure 2A). Conversely, total proteins accumulated slightly more in low Ca^{2+} conditions between two and eight hours after the shift, even though growth was compromised, and less in high Ca^{2+} 24 hours after the shift (Paper I: Figure 2B). Accumulation of total carbohydrates, however, was not affected by either Ca^{2+} shift (Paper I: Figure 2C).

4.2 CSE is a small Ca^{2+}-binding protein newly described in heterocystous cyanobacteria

After observing the drastic effects of Ca^{2+} on cyanobacterial metabolism, Ca^{2+} signalling intermediates containing the characteristic Ca^{2+}-binding motif called EF-hand were searched for in the sequenced genome of *Anabaena* sp. PCC 7120. Several proteins were identified having a single EF-hand domain (All2038, All3087, Alr3548 and All5017). However, only one small protein with two consecutive EF-hands and a molecular mass of about 8.5 kDa was discovered in *Anabaena*. This protein is annotated as a hypothetical protein and is encoded by the open reading frame (ORF) *asr1131* (Kaneko *et al*., 2001), which has not yet been assigned a function in published literature. Based on the characterisations (described below), it was designated as Ca^{2+} Sensor EF-hand (CSE). The predicted tertiary structure highly resembled the helix-loop-helix crystal structure of the Ca^{2+}-binding domain of the

well-known Ca^{2+} sensor troponin C. A BLAST search in the Integrated Microbial Genomes & Microbiomes (JGI IMG/M) database revealed 60 cyanobacterial homologs with more than 70% identity in 48 species, which were filamentous apart from four unicellular/colony-forming strains (Paper II: Table S2). Furthermore, only two of the filamentous species encoding CSE were non-heterocystous, one of which is able to perform anaerobic N_2 fixation. A multiple amino acid sequence alignment of selected CSE homologs demonstrated high conservation of the N-terminal EF-hand, whereas the C-terminal EF-hand displayed more variation in the first five positions of the conserved 12 amino acid loop sequence. In *Anabaena*, however, both domains possessed the conserved loop positions 1, 3 and 5 (three aspartate residues) required for binding Ca^{2+}, nevertheless, its C-terminal domain showed irregularities in the preceding nine amino acid flanking sequence (Paper II: Figure 1).

To evaluate the biochemical properties of Ca^{2+}-binding to CSE, recombinant His-tagged CSE protein was overexpressed in the bacterium *Escherichia coli* and purified with an outcome of 3-5 mg protein/ml. Size exclusion chromatography and multi angle light-scattering revealed the monomeric state of the protein in solution in the presence of Ca^{2+} as well as Mg^{2+} with a molecular mass of around 10 kDa (Paper II: Figures 2A and 2B). Circular dichroism spectra also showed that upon metal binding, both Ca^{2+} and Mg^{2+}, but not Na^{+}, induced conformational changes in CSE represented by shifts in the spectra characteristic for α-helices with specific minima at 207 nm and 222 nm (Paper II: Figure 2E). Competition assays demonstrated that CSE binds Ca^{2+} in preference to Mg^{2+}. In a $^{45}Ca^{2+}$ overlay assay, CSE bound radiolabelled $^{45}Ca^{2+}$ in the presence of Mg^{2+} in the buffer (Paper II: Figure 2C), and comprehensive isothermal titration calorimetry (ITC) metal-binding assays measured the binding kinetics in the presence or absence of both metal ions. The raw datasets were fitted to different binding site models to calculate binding stoichiometries (n = number of bound ligands) and dissociation constants (K_d). Binding of Ca^{2+} to CSE displayed an exothermic titration profile with K_d values of 5.9 ± 7.5 µM and 56.3 ± 50.1 µM when a two sequential-binding site model was used. These data suggested that only one EF-hand domain in CSE binds Ca^{2+} with high affinity. Therefore, further ITC raw data were only fitted to the one-binding site model, resulting in a K_d value of 1.4 ± 1.0 µM and n = 0.9, which indicated high-affinity binding of one Ca^{2+} per CSE protein molecule (Paper II: Table 1 and Figure 2D). Titration against Mg^{2+}, however, yielded an endothermic profile with n = 4.1 and a K_d value of 35.2 ± 2.1 µM, demonstrating

low binding capacity of CSE to Mg^{2+}. In ITC competition assays, CSE was 1) pre-incubated in Ca^{2+} and then titrated against Mg^{2+}, detecting no calorimetric changes; and 2) pre-incubated in Mg^{2+} and then titrated against Ca^{2+}, showing similar values to other Ca^{2+} titrations. Addition of NaCl, in contrast, impeded Ca^{2+}-binding and completely inhibited Mg^{2+}-binding to the CSE protein (Paper II: Table 1 and Figure S2). These data exemplified that CSE is able to bind Mg^{2+} but would always prefer Ca^{2+} if present.

On the genomic level, several potential TF-binding sites were identified in the promoter and terminator region of *cse*, encoded in *Anabaena* by ORF *asr1131* (Paper II: Figure S4). In a study by Picossi *et al*. (2015), gene targets of the global TF PacR (Photosynthetic assimilation of C_i Regulator) were isolated through chromatin immunoprecipitation followed by sequencing (ChIP-Seq) analysis, revealing many genes involved in photosynthesis and C_i assimilation as well as *asr1131*. A PacR-binding site perfectly matching the consensus sequence TNA-$N_{7/8}$-TNA is located 42 bp upstream of the *asr1131* transcriptional start site. In the same way, Videau and co-workers found putative binding sites of the HetR master regulator of heterocyst formation downstream of the *cse* coding sequence (Videau *et al*., 2014). In addition, a potential NtcA-binding site (GATACCTATTTCTAC) was detected 66 bp upstream from the *cse* transcription start point and closely resembles the NtcA-binding site of *alr0130* as identified in another ChIP-Seq study by Picossi *et al*. (2014). The presence of both PacR- and NtcA-binding sites suggested that CSE may be involved in maintaining the C/N balance in *Anabaena*. Therefore, *cse* gene expression during N and C_i step-down experiments was measured, unveiling opposing responses to each shift, i.e. rapid downregulation in the N step-down and upregulation in the C_i step-down experiment (Paper II: Figure 3).

4.2.1 CSE overexpression affects PBS assembly and photosynthetic ETC

For *in vivo* analysis of CSE function, *Anabaena* strains with 2-fold higher expression of *cse* than WT (*cse*-oex) (Paper II: Table 3) were generated and characterised in comparison to the WT. The *cse*-oex strain grew significantly slower than the WT in both N-rich and N-free growth media in 3% CO_2 and displayed a yellowish colouration due to a decreased PBS peak at 635 nm in RT absorption spectra (Paper II: Figure 4). Physiologically, *cse*-oex did not differ considerably from WT in protein and chl content in N-replete conditions but had lower amounts of chl in N_2-fixing conditions and slightly heavier cells (dry biomass) in both growth media. However,

under N limitation, heterocyst frequency and nitrogenase activity were similar in both strains (Paper II: Table 2).

4.2.1.1 Differentially expressed genes in *cse*-oex include downregulated PBS rod subunits

On the transcriptome level, gene expression in *cse*-oex mainly varied from the WT in the light-harvesting PBS subunits. Amongst the most downregulated genes in *cse*-oex was the entire *pec* cluster (*alr0524-alr0527*, log2 fold change (FC) = -2.8 to -2.4), followed by the *cpc* cluster (*alr0528-alr0536*, log2 FC = -2.2 to -0.9) and three genes of hypothetical proteins containing an OCP-like N-terminal domain. Furthermore, many genes involved in chl and porphyrin biosynthesis were significantly downregulated in *cse*-oex, for instance, *hemK*, *por*, *chlL* and *chlN*, in contrast to the gene *hemF2* whose gene expression was induced in the overexpressor. Surprisingly, genes related to photosynthetic processes had only minor changes in expression. Of all genes encoding photosynthetic subunit complexes, only *psaB* and *ndhD1* were about 2 - 3-fold downregulated in *cse*-oex compared to WT. With regards to N_2 fixation, the nitrogenase genes *nifH1/2* and *nifK* and cyanophycinase were downregulated, whereas a Mo-dependent nitrogenase-like protein was upregulated 3-fold. Other genes of interest included the Ca^{2+}-dependent protease *prcA* and the serine-threonine protein phosphatase *prpA*, which were upregulated 2-fold, and the hemerythrin DNase *alr3199* and the unknown proteins *alr0198/alr0199*, which were strongly downregulated (logFC = -3.1 and -2.4, respectively) (Paper II: Table 3).

4.2.1.2 Characterisation of PET in the *cse*-oex strain

Diminished gene expression of PBS subunits also suggested impairments of PET, corresponding to decreased growth rates in the *cse*-oex strain. Therefore, biophysical properties of the photosynthetic ETC were investigated. Energy transfer in the photosynthetic pigment-protein complexes was studied in low temperature (77K) as well as RT by exciting whole cell samples with monochromatic light filtered for specific wavelengths and recording the fluorescence emission spectra. While in 77K, excitation of chl with 440 nm resulted in curves with two emission peaks at 695 nm (PSII) and 730 nm (PSI) and a PSII:PSI ratio of 1:4 for both strains, excitation of PBS pigments with 580 nm demonstrated clear differences between *cse*-oex and the WT. In addition to unaffected PSII and PSI peaks, the PC peak at 646 nm was significantly lower in *cse*-oex compared to WT, whereas the APC peak at 663 nm was

significantly higher in the overexpressor, which was also observed in measurements of fluorescence spectra at RT with an APC peak at 660 nm (Paper II: Figure 5).

Further fluorescence parameters were calculated with a Dual-PAM-100 (Walz) from fluorescence induction curves, in which the *cse*-oex strain consistently showed higher fluorescence levels than the WT in both the absence and presence of actinic light (F_0 and F_s, respectively, in Paper II: Figures 6A and 6E). Despite higher overall fluorescence, application of saturating pulses showed that F_m' peaks relative to the F_s level were lower in *cse*-oex than in WT, thus PSII photochemical efficiency measured as F_v/F_m and Y(II) was significantly lower in the overexpressor in light intensities ranging from 0 to 220 µmol photons m^{-2} s^{-1} (Paper II: Figures 6B, 6C and 6F). Furthermore, transient rise in fluorescence during light-to-dark transitions, as a measure of NDH-1-mediated dark respiratory activity, was virtually absent in *cse*-oex (Paper II: Figure 6A inset). For a more detailed analysis of electron transfer features in PSII, chl fluorescence was induced by a single saturating flash and showed a considerably faster decay in *cse*-oex during the first three milliseconds, but a slower decay during the subsequent three seconds (Paper II: Figure 6D). Lastly, state transitions were evaluated by monitoring maximal fluorescence from saturating pulses during alternating actinic blue (State 1) and red (State 2) light illumination. Besides generally higher fluorescence levels and lower Y(II), the overexpressor displayed a gradual decline in Y(II) in State 1 in contrast to the WT (Paper II: Figures 6E and 6F).

In addition to PSII fluorescence measurements, P700 parameters were determined with a Dual-PAM-100 after 10 s of pre-illumination with FR light to induce PBS movement from PSI to PSII for complete PSI oxidation. While the PSI maximum effective yield Y(I) after FR light was considerably higher in *cse*-oex, subsequent illumination with actinic red light and saturating pulses did not increase Y(I) in *cse*-oex as much as in WT (Paper II: Figure 7A). The PSI donor side limitation Y(ND), in turn, was lower in the overexpressor after FR light treatment and remained low in *cse*-oex at WT level during the course of illumination (Paper II: Figure 7B). The PSI acceptor side limitation Y(NA), in contrast, was higher in the overexpressor compared to the WT throughout illumination with red light (Paper II: Figure 7C). Light curve measurements confirmed the lowered Y(I) data for a light regime from 0 to 220 µmol photons m^{-2} s^{-1} (Paper II: Figure 7D). Further analysis of the redox state of P700 during dark-FR light-dark transitions revealed faster P700 oxidation in *cse*-oex in the initial phase (1 s) of FR light illumination. After that, $P700^+$ was re-

reduced in FR light in *cse*-oex in contrast to the WT, wherein P700 remained oxidised in FR light. Re-reduction of $P700^+$ in darkness, however, showed no difference to the WT (Paper II: Figure 7E).

4.2.1.3 Distribution of photosynthetic protein complexes in the thylakoid membrane of *cse*-oex

To analyse the abundance of protein complexes in the thylakoid membrane, solubilised thylakoid membranes were separated with lpBN-PAGE. Major protein complexes consist of the chl-containing photosystems (PSI and PSII), thus appearing in green bands on the BN gel. Both photosystems occur as monomers, dimers and, in the case of PSI, tetramers in the thylakoid membrane. From the BN gel, it was visible that both photosystems were more abundant as monomers in the *cse*-oex strain, compared to the WT, including monomeric PSII lacking the CP43 protein. Photosystem dimers, however, were clearly less abundant in the overexpressor, particularly PSII dimers which were virtually absent. PSI tetramers, on the contrary, were more prominent in the overexpressor than in WT. Remarkably, a blue band at the top of the gel was substantially less pronounced in *cse*-oex (Paper II: Figure 8A).

Further separation of the protein complexes into subunits was performed in subsequent 2D-SDS-PAGE. As described above for *cse*-oex, PSII subunits CP43, CP47, D1 and D2 were more prominent in PSII monomers as well as CP43-less monomers and free CP43 than in WT, whereas these subunits were virtually absent from PSII dimers. Similarly, PSI subunits PsaA/B and PsaF were clearly more abundant in PSI monomers and tetramers in the overexpressor, but less abundant in PSI dimers. Notably in WT, PSI subunits were also present in the biggest complexes corresponding to the blue bands at the top of the BN gel, which were absent in *cse*-oex. In the same supercomplex, a prominent spot of around 100 kDa was detected, which was reduced in *cse*-oex compared to WT. This spot and a spot of about 20 kDa, that was also less abundant in *cse*-oex, were analysed by MS and contained peptides from the unknown proteins All3041 and Alr2489, which were also detected by Ladig *et al*. (2011) as putatively contaminating outer/plasma membrane proteins. In addition, several other proteins were present in PSI tetramers and supercomplexes with a molecular mass between 17 – 22 kDa and 25 – 32 kDa, which might correspond to PBS subunits (Bryant *et al*., 1991). While the protein spots around 22 kDa were mostly absent from *cse*-oex, the protein around 25 kDa was only present in the PSI tetramer and was more abundant in the overexpressor. In the

lower blue region of the BN gel, a few distinct spots were clearly less expressed in *cse*-oex, such as proteins of about 24 kDa or 50 kDa (Paper II: Figure 8B).

4.2.2 CSE is required for maintaining heterocyst differentiation and filament integrity

CSE knockout (*Δcse*) mutants were engineered by replacing the ORF *asr1131* with an antibiotic resistance cassette. Two fully segregated *Δcse* clones were obtained. Full segregation was confirmed at both DNA (both clones) and RNA (clone 1) level (Paper III: Figure 1). When grown in regular BG11 medium, *Δcse* displayed a phenotype with predominantly very short filaments in the presence of a low amount of normal long filaments, in contrast to primarily long filaments in the WT (Paper III: Figure 2). Filament length counts from four-day old cultures confirmed that more than 90% of filaments in *Δcse* were unicellular or had up to five cells per filament, besides a small number of slightly longer filaments (5-30 cells per filament) and normal length filaments (>80 cells). In contrast, the majority of the WT culture constituted long filaments (20- >80 cells) with >80 cells being the prevalent length (Paper III: Figure 3). Complementing the *Δcse* mutant with a vector overexpressing *cse* fully restored the long filament phenotype (Paper III: Figure 2G). When cells were grown in N-deficient medium, the abundance of short filaments in *Δcse* drastically decreased as observed from bright-field micrographs (Paper III: Figure 2D), because short filaments did not contain any heterocysts to support survival in N_2-fixing conditions as visible from the images. The long filaments, however, had a heterocyst frequency comparable to WT filaments. Therefore, growth of *Δcse* was severely compromised but still possible in $BG11_0$ medium lacking sources of N, also reflected in lower PBS and chl peaks at 635 nm and 680 nm, respectively, in RT absorption spectra and lower nitrogenase activities (Paper III: Figures 4H and 5).

4.2.2.1 Cell morphology is further affected by *cse* knockout

After observing the short-filament phenotype of *Δcse* with light microscopy, SEM and TEM provided further information about the cells' surface and intracellular constitution, respectively. Comparing *Anabaena* WT and *Δcse* SEM micrographs, the difference in filament length was clearly visible; WT cells formed long straight filaments while *Δcse* cells were less organised in short filaments and clumps. Another conspicuous feature was the rough cell surface of *Δcse* compared to the smooth cell surface of WT vegetative cells (Paper III: Figure 6). Total sugars, measured separately from cell pellets and the supernatant (growth medium),

revealed higher intra- and extracellular sugar contents in *Δcse*, indicating that the outer surface layer of *Δcse* may contain polysaccharides (Paper III: Figure 7).

The *Δcse* micrographs further revealed a structure that connected cells as a mutual envelope forming clumps of cells in addition to short filaments (Paper III: Figure 6E). Furthermore, abnormal cell features were observed that consisted of two dividing vegetative cells encapsulated in a HEP- or HGL-like layer, which was also evident in TEM micrographs (Paper III: Figure 6).

4.2.2.2 Expression of genes involved in heterocyst differentiation is altered by *cse* knockout

RNAseq was used to determine genes that were differentially expressed in the *Anabaena Δcse* strain compared to the WT in regular growth conditions (BG11 in CO_2-enriched air; 3% CO_2). The majority of differentially expressed genes belonged to the process of heterocyst differentiation. While two of the main regulators, *ntcA* and *hetC*, were only slightly downregulated, downstream targets of *hetC* for the biosynthesis of the heterocyst envelope, and cytoplasmic differentiation predominantly showed a more prominent decrease in expression. The gene cluster *alr2822-alr2841*, which is called HEP island, was downregulated by -2.5-fold on average, whereas the gene cluster *all5341-all5359*, encoding genes for HGL biosynthesis, was even more strongly downregulated (mean FC = -4.5). With regard to cytoplasmic differentiation, heterocyst-specific genes such as Flv proteins *flv1B/3B*, Fd, both cytochrome *c* oxidase operons (*cox2/3*), the *dev*-ABC transporter, and the uptake hydrogenase cluster were also strongly downregulated by -2.7 to -5.5-fold (average of each gene cluster). Furthermore, one important TF for the N_2-fixing abilities of heterocysts, *patB*, was identified with a FC of -4.7. Thus, expression of *nif* genes and other gene clusters associated with N_2 fixation, such as *all1424–all1427* and *all1431–all1440*, was mildly to strongly repressed (-1.1 to -6.4-fold).

Conversely, genes involved in heterocyst inhibition (*patU5/3*, *asr1734*, *patS*) were moderately upregulated (FC = 1.9 – 3.5), as were the heterocyst differentiation proteins *hetZ* (FC = 4.1; differentiation commitment, in an operon with *patU5/3*) and *hetP* (FC = 2.3; differentiation commitment), and the *patS* antagonist *patA* (FC = 2.6). The most upregulated genes, however, included enzymes of the biosynthesis pathways of the heterocyclic compounds chl and pyrimidine, which comprised the coproporphyrinogen III oxidase (FC = 17.9; *hemF2*), dihydroorotate dehydrogenase (FC = 6.5), and the Mg^{2+}-protoporphyrin IX monomethyl ester [oxidative] cyclase 1

(FC = 4.2). The third most upregulated gene was *hoxH* with FC = 5.9, belonging to the Hox complex, which is present in both vegetative cells and heterocysts (Paper III: Table 1).

4.2.2.3 Expression patterns of heterocyst differentiation genes during N step-down in *Δcse*

Closer inspection of the expression of the heterocyst differentiation regulators *ntcA* and *hetR* during the course of induced N limitation revealed different patterns between *Anabaena* WT and *Δcse* for both genes. In the WT, expression of these genes gradually increased during the first hours after the N step-down, peaking at eight hours after the shift. In *Δcse*, however, expression of *hetR* was strongly induced already one hour after N step-down, whereas expression of *ntcA* peaked after 24 hours (Paper III: Figure 8).

5. DISCUSSION

5.1 Ca^{2+} influences the C/N ratio through regulation of uptake transporter gene expression

Signalling molecules are essential in biological systems in order to adapt to changing environmental conditions (Agostoni and Montgomery, 2014). Torrecilla *et al*. (2000) showed that changes in $[Ca^{2+}]_e$ simulate $[Ca^{2+}]_i$ transients in *Anabaena*, but any effects these Ca^{2+} transients might have on cell metabolism have not been clarified. Therefore, in Paper I, the $[Ca^{2+}]$ of the growth media for liquid cultures was changed, which resulted in inversed trends in expression of C_i and N uptake transporter genes in *Anabaena*. After a shift from low to high Ca^{2+}, C_i pumps were upregulated, and nitrate transporters downregulated, whereas after a shift from high to low Ca^{2+} these expression patterns were reversed. These data indicate that Ca^{2+} might fine-tune the C/N balance through gene regulation of the corresponding uptake transporters. A possible Ca^{2+}-target might be the LysR-type TF CmpR (All0862; previously described as RbcR), which is an activator of the *cmp* operon, encoding the CCM component BCT1, a HCO_3^- transporter. Both CmpR and the *cmp* gene cluster were demonstrated to be upregulated under C_i-limiting conditions (López-Igual *et al*., 2012). The transcriptomic data discussed here, however, showed that *cmpR* and the *cmp* operon were upregulated in the shift to high Ca^{2+} and downregulated in the shift to low Ca^{2+}, even though cells were grown in high CO_2 in both cases. Therefore, expression of the BCT1 transporter might be dependent on Ca^{2+}, as suggested for the BCT1 subunit CmpA in *Synechocystis* which binds Ca^{2+} as a co-factor during HCO_3^- transport (Koropatkin *et al*., 2007). In addition to the *cmp* operon, genes of the Na^+-dependent HCO_3^- transporters BicA and SbtAB and the corresponding Na^+:H^+ antiporter, that supplies Na^+ to BicA and SbtAB for Na^+-dependent HCO_3^- uptake from the periplasm (Shibata *et al*., 2002; Price *et al*., 2004; Price, 2011), were similarly regulated to *cmp* genes in different Ca^{2+} regimes. Expression of these HCO_3^- transporters is controlled by the LysR-type transcriptional regulator NdhR (previously described as CcmR), which is a transcriptional repressor reversibly regulated by 2-OG and 2-PG (Wang *et al*., 2004; Jiang *et al.*, 2018). Both molecules derive from the activity of the enzyme RuBisCO, which was reported to be inactivated upon binding of Ca^{2+} (Karkehabadi *et al*., 2003). In summary, it is conceivable that a Ca^{2+} signal, which might occur through Ca^{2+} uptake by yet unidentified Ca^{2+} channels/pumps in the plasma membrane, may be involved in the adaptation to low CO_2 conditions by upregulating expression of the HCO_3^- transporters, simulated by the increase in $[Ca^{2+}]_e$. CmpR

might directly sense a Ca^{2+} signal initiating its activity and inducing *cmp* expression, whereas inactivation of RuBisCO by Ca^{2+} might reduce the amount of 2-OG and subsequently lower the activation of the repressor NdhR. Therefore, the transcription of the HCO_3^- transporters BicA and SbtAB are upregulated (summarised in Figure 6).

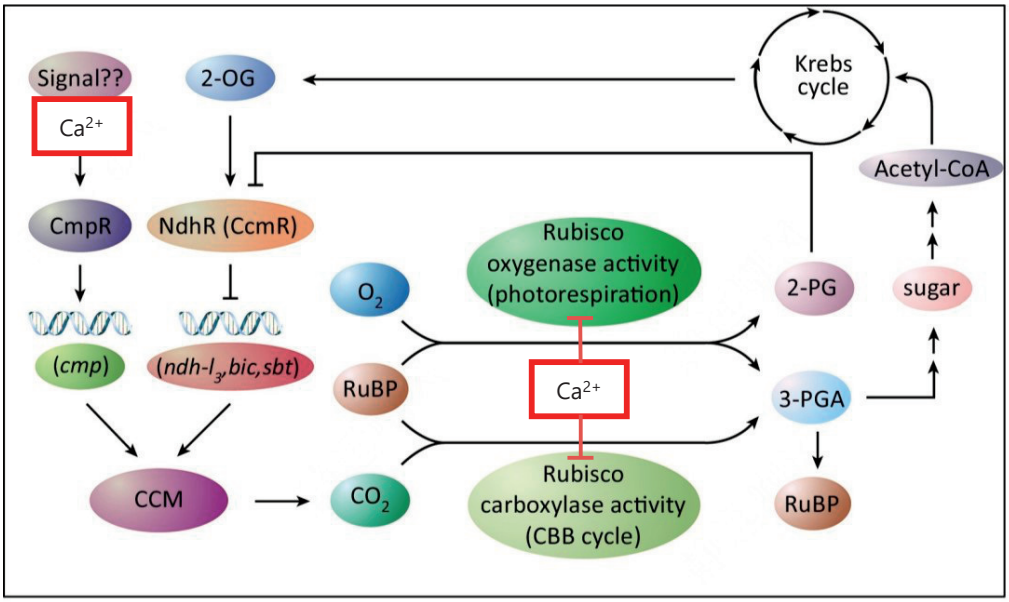

Figure 6: Transcriptional regulation of carbon-concentrating mechanisms (CCM) during low CO_2 conditions, involving 2-oxoglutarate (2-OG) and 2-phosphoglycolate (2-PG) as competing signalling molecules and calcium ions (Ca^{2+}) as a possible new key component of the signalling cascade. (Modified from Zhang, C.C. *et al.*, 2018). Abbreviations: acetyl-coenzyme A (acetyl-CoA), Calvin-Benson-Bassham (CBB), 3-phosphoglycerate (3-PGA), ribulose-1,5-bisphosphate carboxylase/oxygenase (Rubisco), ribulose-1,5-bisphosphate (RuBP).

According to gene expression data, the shift to high Ca^{2+} simulated low CO_2 conditions and thus a low C/N ratio that led to upregulation of the HCO_3^- transporters (Woodger *et al.*, 2007; López-Igual *et al.*, 2012) (described above) and concomitant downregulation of nitrate/nitrite uptake transporters, which is normally determined by the signalling molecule 2-OG and the proteins PII, PipX and NtcA (reviewed in Zhang *et al.*, 2018). Conversely, a shift to low Ca^{2+} induced the expression of nitrate/nitrite uptake transporters and downregulated HCO_3^- pumps, suggesting a high C/N ratio from published literature (Flores *et al.*, 2005). Due to the decrease in $[Ca^{2+}]_e$, it can be assumed that a modified Ca^{2+} signal or a subsequent

decrease in $[Ca^{2+}]_i$ occurred, which reversed the C/N ratio upon changing transporter expression levels. This would suggest the presence of a Ca^{2+} sensor mechanism, that perceives changes in $[Ca^{2+}]_i$ and orchestrates further downstream events through interaction with target proteins to fine-tune the C/N balance.

5.2 CSE – a novel player in the complex network of maintaining the metabolic equilibrium?

In a signalling network, a signal composed of messenger molecules is normally perceived by a sensor protein and translated into a response. In eukaryotic organisms, one of the most common protein motifs is the Ca^{2+}-binding EF-hand domain, which is present in many sensor proteins, inducing a conformational change in the protein structure upon binding of Ca^{2+} (Chazin, 2011). The EF-hand protein superfamily includes several classes of proteins with structural variations in the canonical EF-hand. Nevertheless, EF-hand proteins can be divided into two functional groups – Ca^{2+} sensors for signal translation and Ca^{2+} buffers for intracellular Ca^{2+} homeostasis (Denessiouk *et al*., 2014). Bacterial EF-hand proteins contain canonical domains, which hold the conserved 12-residue Ca^{2+}-binding loop and are more common in Ca^{2+} sensors, and non-canonical (disordered) EF-hand-like domains, which are modified in the length of the Ca^{2+}-binding loop or in the presence of the helices flanking this loop and occur more often in Ca^{2+} buffers (Grzybowska, 2018). However, pseudo EF-hands in S100 proteins, which display modifications in the conserved Ca^{2+}-binding residues, have not been detected in bacteria (Zhou *et al*., 2006), in contrast to Ca^{2+}-binding proteins that completely lack EF-hand domains. Such proteins contain β-rolls motifs (Baumann *et al*., 1993), Greek key motifs (Jobby and Sharma, 2005), bacterial immunoglobulin-like Ca^{2+} domains (Raman *et al*., 2010) and the Repeats-in-ToXin (RTX) exoproteins found in gram-negative bacteria. RTX proteins, for instance, bind Ca^{2+} ions via glycine- and aspartate-rich nonapeptide tandem repeats and have various biological functions, such as hemolysins, nodulation proteins and surface layer proteins for gliding motility (Hoiczyk and Baumeister, 1997; Sánchez-Magraner *et al*., 2007; Linhartová *et al*., 2010). Changes in $[Ca^{2+}]_i$ in bacteria also affect the cell cycle/division/differentiation, host-pathogen interactions, gene expression, pH homeostasis, chemotaxis, sporulation, protein phosphorylation, biofilm formation and stress resistance (summarised in Domínguez *et al*., 2015). Zhou *et al*. (2006) predicted the presence of 397 putative EF-hand proteins in prokaryotes, of which, however, only a few have been characterised (e.g., calerythrin in *Saccharopolyspora erythrea*,

calsymin in *Rhizobium etli* and several Cab-proteins in *Streptomyces coelicolor*). Ca^{2+} signals have been shown to occur in *Anabaena* in response to several stress conditions (Torrecilla *et al*., 2000, 2001, 2004a). However, the only reported Ca^{2+} signalling intermediate is CcbP, which is involved in the adaptation mechanism to N starvation, i.e. heterocyst differentiation (Zhao *et al*., 2005; Shi *et al*., 2006). CcbP, however, binds Ca^{2+} via negative surface charges and does not contain the features of a typical Ca^{2+}-dependent regulator protein and is, hence, more likely to operate as a Ca^{2+} buffer than a Ca^{2+} sensor (Hu *et al*., 2011). In contrast to CcbP, a previously undescribed protein encoded by the *asr1131* gene in *Anabaena* has been discovered during the studies presented here, and encodes a protein containing two Ca^{2+}-binding EF-hand domains, highly resembling the Ca^{2+}-binding domains of the well-known Ca^{2+} sensor and regulator proteins calmodulin and troponin C (Paper II: Figure 1B). Based on predicted homology, the protein encoded by *asr1131* was named "Ca^{2+} Sensor EF-hand" (CSE), which might represent the only protein in *Anabaena* sensing changes in the intracellular free Ca^{2+} status, because CcbP only acts as a Ca^{2+} buffer. Therefore, CSE might play an essential role in Ca^{2+} signalling events to happen in the cell. Biochemical analysis of recombinant CSE revealed that this protein specifically binds Ca^{2+} *in vitro* (Paper II: Figure 2 and Table 1), displaying a conformational change upon binding as visible in circular dichroism spectra (Paper II: Figure 2E), similar to the Ca^{2+} sensor calmodulin (Denessiouk *et al*., 2014), which also supports the hypothesis of CSE being a Ca^{2+} sensor. Furthermore, CSE binds only one Ca^{2+} ion with high affinity. This is in accordance with irregularities in the C-terminal EF-hand, which is also the case in CSE homologs from other cyanobacteria. Interestingly, CSE homologs are predominantly present in filamentous and heterocystous species, indicating its potential role in N metabolism, because these species are typical N_2 fixers and require tight regulation mechanisms to maintain the C/N balance. This hypothesis is supported by the occurrence of binding sites for the transcriptional regulators PacR, NtcA and HetR in the promoter and terminator regions of the *cse* gene. The presence of both PacR- and NtcA-binding sites was also reported for the promoter region of the RuBisCO RbcLXS operon (Picossi *et al*., 2015), whose expression is induced by PacR for CO_2 fixation and repressed by NtcA-binding upon N starvation and subsequent heterocyst formation. A similar transcriptional regulation may be possible for *cse* gene expression, which complies with the observation that *cse* gene expression was induced in a shift from high to low CO_2 conditions (low C/N ratio, induction by PacR) and downregulated in N step-down experiments (high C/N ratio, inhibition by NtcA) (Paper II: Figure 3).

For the studies presented here, a *cse* overexpression strain (*cse*-oex) with 2-fold upregulated *cse* expression, and a knockout strain (*Δcse*) of the *cse* gene in *Anabaena* were characterised. Strong but very different phenotypes were observed, which indicated the importance of the protein because even modest 2-fold overexpression in *cse* abundance (in *cse*-oex) resulted in phenotypes different from the WT.

5.2.1 Disturbed PBS-PSII connectivity and PQ pool overreduction lead to decreased photosynthetic capacity in the cse overexpressor

The *cse* gene was upregulated 2-fold, which triggered slower growth and pale green colouration resulting from lower amounts of phycobilin pigments in the *cse-oex* culture, compared to the WT, in both N-replete and N_2-fixing conditions (Paper II: Figure 4). Degradation of N-containing pigments such as chl and phycobilin is usually a sign of perturbed N-metabolism. Normally, the cells fix N_2 via the nitrogenase complex, but degrade these pigments as a source of N for the synthesis of essential amino acids in case N_2 fixation is hampered (Baier *et al*., 2004). However, when cells were grown in N-depleted media, heterocyst frequency and nitrogenase activity in *cse*-oex did not differ significantly from WT levels (Paper II: Table 2). Together with changes in pigments, this indicated that photosynthetic pigment-protein complexes and PET might have been compromised in their functionality in the *cse* overexpression strain instead. Transcriptomic analysis of *cse*-oex revealed strong downregulation of the PC and PEC genes for the light-harvesting PBS complexes in comparison to the WT (Paper II: Table 3). This was also apparent in fluorescence emission measurements when cells were excited with monochromatic light specific for PBS excitation and the PC-specific emission peak in *cse*-oex was almost absent compared to the WT (Paper II: Figure 5). Therefore, PBS in the overexpressor might have a modified shape or reduced number of rods. While an *Anabaena* mutant strain with PBS completely lacking the peripheral rods (Leganés *et al*., 2014) did not comply with the fluorescence emission spectra presented in this thesis (Paper II: Figure 5B), a *ΔcpcG1/2* mutant with PBS lacking only the side rods showed increased fluorescence emission from APC (Chang *et al*., 2015), similar to the data presented for *cse*-oex. Due to the absence of the side rods, the APC half core cylinders are freely accessible and might be destabilised and unable to transfer excitation energy efficiently, likely leading to a release of energy in the form of fluorescence deriving from the pigments (Chang *et al*., 2015).

Furthermore, analysis of thylakoid membrane protein complexes in the *cse*-oex strain revealed the predominant presence of PSII monomers instead of PSII dimers (Paper II: Figure 8), which is the only oligomeric PSII state that is able to bind PBS (Mörschel and Mühlethaler, 1983; Bald *et al*., 1996; Barber *et al*., 2003; Arteni *et al*., 2009; Chang *et al*., 2015). This indicates higher turnover of functional dimeric PSII (Aro *et al*., 2005; Nixon *et al*., 2010), explaining the observed lower PSII activity in *cse*-oex compared to the WT (Paper II: Figure 6). This result raises the question as to whether the overabundance of CSE causes improper PBS assembly and thus destabilised PSII dimers or if it instead hampers PSII dimerisation, leading to the uncoupling of PBS. Zhang *et al*. (2012) described a similar phenotype of their *Δflv4* mutant in *Synechocystis*, including PBS uncoupling and the lack of PSII dimers, probably due to simultaneous downregulation of the Sll0218 protein from the conserved *flv4-2* operon in the *Δflv4* mutant (Zhang *et al.*, 2012; Bersanini *et al.*, 2014, 2017; Chukhutsina *et al*., 2015). Indeed, Flv4 gene expression and its location to the thylakoid membrane, with concomitant PSII dimerisation, depend on Ca^{2+} (Paper I: Table 2; Zhang *et al*., 2012).

Besides the lack of PSII dimers, chl fluorescence kinetic measurements in *cse*-oex indicated overreduction of the PQ pool (Paper II: Figure 6D), which is a parameter of imbalanced electron transfer between the photosystems that impacts LET as well as CET and dark respiration (Schuurmans *et al*., 2014). The redox potential of the PQ pool under stress conditions is tightly controlled by photoprotective mechanisms, such as Flv proteins and OCP, which are highly dependent on the presence of intact PBS (Wilson *et al*., 2006; Bersanini *et al*., 2014). Three genes (*all1123*, *all3221*, *alr4783*) homologous to the PBS-binding N-terminus of OCP were significantly downregulated in *cse*-oex (Paper II: Table 3) and may be involved in the quenching of the harmful ROS singlet oxygen $^1O_2$ (Sedoud *et al*., 2014; López-Igual *et al*., 2016). To balance the distribution of excitation energy between the photosystems, PBS undergo so-called state transitions depending on the light wavelength. In *cse*-oex, Y(II) showed a decreasing trend during the course of blue light illumination, which induces “state 1”, in contrast to Y(II) in the WT (Paper II: Figure 6F). This might be a sign of either PBS uncoupling from PSII during “state 1” or damage of functional PSII due to PQ pool overreduction. In addition, in actinic red light (“state 2”), Y(I) was lower and Y(NA) was higher in *cse*-oex in comparison to the WT (Paper II: Figure 7), which indicated disturbed CET. Indeed, transcript levels of the NDH-1 complex subunit NdhD1, which is involved in CET as well as dark respiration (feeding of

electrons from the respiratory chain into the PQ pool; Mi *et al*., 1995; Battchikova *et al*., 2011), were downregulated in *cse*-oex compared to WT (Paper II: Table 3). Therefore, *cse*-oex only displayed a small and very short increase in chl fluorescence in light-to-dark shifts in contrast to the WT (F_0 rise, Paper II: Figure 6A inset). The respiratory pathway also involves the RTO Cox, whose subunit CoxA was reported to contain a conserved Ca^{2+}-binding site in eukaryotic and prokaryotic homologs (Vygodina *et al*., 2013), and thus might be a CSE-controlled Ca^{2+}-dependent process.

5.2.2 Deletion of the cse gene in Anabaena induces filament fragmentation and downregulates N_2 fixation abilities

The discovery of the novel Ca^{2+}-binding protein CSE, that is highly conserved in filamentous, heterocystous cyanobacteria and virtually absent from unicellular strains (Paper II: Figure 1A and Table S2), led to the assumption that this protein may be involved in the formation of cyanobacterial filaments and heterocyst differentiation. Indeed, *cse* gene knockout (*Δcse*) from *Anabaena* induced a short filament phenotype in two independent, fully segregated clones (Paper III: Figure 1). A similar phenotype has been reported previously to be induced by abiotic stresses, such as oxidative stress through ultraviolet light, and nutrient deficits (Singh and Montgomery, 2011). Furthermore, an excess of Ca^{2+} also induced filament fragmentation, with $[Ca^{2+}]_e$ higher than 10 mM $CaCl_2$ (Singh and Mishra, 2014).

In the *cse* knockout mutant, bright-field and electron microscopy micrographs revealed the predominance of highly fragmented *Anabaena* filaments next to a low frequency of long WT-like filaments (Paper III: Figures 2, 3 and 6). Isolation of the long filaments by selective harvesting unveiled that filament fragmentation was initiated after approximately one to two weeks in N-replete media in high CO_2. Hence, both types of filaments were genetically homogenous, and fragmentation was stress-induced. It was further observed that short filaments formed clumps of cells connected by a firm gelatinous envelope (previously described by Lazaroff and Vishniac, 1962). This cell anastomosis might be an attempt of the cells to compensate for unicellularity, which has been noted for several soil-isolated *Nostoc* and *Anabaena* species upon shift to N-limiting conditions (Foykar and Matavuly, 1998). Another feature depicted in the EM micrographs constituted pairs of dividing vegetative cells encapsulated in a single heterocyst-like outer envelope. This observation has been described in short filament mutants of *Anabaena* as “regressed heterocysts”, i.e. partially differentiated cells that entered the stage of heterocyst

formation but failed to fully complete this process (Bauer *et al*., 1995; Nayar *et al*., 2007; Flores *et al*., 2007; Merino-Puerto *et al*., 2011). As a result, cells with arrested heterocyst differentiation continued dividing, whereas mature heterocysts are known to be incapable of cell division (Mitchison and Wilcox, 1972).

Short filament phenotypes have been described in several heterocyst differentiation-deficient mutants (Buikema and Haselkorn, 1991a; Ernst *et al*., 1992; Bauer *et al*., 1995; Khudyakov and Golden, 2001; Merino-Puerto *et al*., 2010). Most of these mutants are impaired in proper morphogenesis of heterocysts, so that the heterocysts become the weak point of the filament, disconnect, and as a result disrupt filament integrity. In the studies presented here, transcriptomics analysis of *Anabaena* WT and *Δcse*, grown on nitrate, revealed the prominent downregulation of heterocyst-specific genes in *Δcse*. Even though the total amount of heterocysts was lower in *Δcse* because of the absence of heterocysts from fragmented filaments, several heterocyst differentiation and patterning genes were significantly upregulated (Paper III: Table 1), indicating transcriptomic downregulation of the heterocyst differentiation process in *Δcse*. Most importantly, neither of the two master regulators, *hetR* nor *ntcA*, showed significant differential expression in *Δcse* compared to the WT. Early gene targets of these regulators during heterocyst development include the gene neighbours *hetC* and *hetP*, whose protein products are assumed to be functionally linked (Corrales-Guerrero *et al.*, 2014). HetP and the functionally similar HetZ protein are responsible for the commitment of vegetative cells to differentiation into heterocysts (Videau *et al*., 2016; Zhang, H. *et al*., 2018), and these genes were significantly upregulated in *Δcse*. HetC, in contrast, was slightly downregulated in the *Δcse* mutant, whereas its downstream targets, responsible for the morphological heterocyst differentiation, were strongly repressed in their expression. At the same time, genes of heterocyst inhibitors were significantly upregulated. These results suggested that in *Δcse*, more cells attempted to commit to cell differentiation possibly to overcome the lack of heterocysts in the filaments, however, the differentiation process was prevented by the downregulation of respective differentiation genes and upregulation of heterocyst inhibitors (Figure 7). In fact, among the strongest upregulated transcripts in *Δcse* were genes from the chl and heme biosynthesis pathway, which might be an indication of higher requirements on N-storing pigments, such as chl and phycobilins, due to the inability of *Δcse* to fix N_2.

A Ca^{2+} signal has been described three times in the literature to occur during N step-down and heterocyst differentiation in the unicellular, non-diazotrophic cyanobacterium *Synechococcus elongatus* PCC 7942 and *Anabaena*, respectively. In the unicellular cyanobacterium, it was shown that the early Ca^{2+} transient upon N depletion was dependent on 2-OG and NtcA and affected gene expression of genes involved in the adaptation to N starvation, including the PBS-degrading *nblA*. Hence, it was suggested that a Ca^{2+} signal is involved in sensing an imbalance in the C/N ratio and is required during N step-down conditions (Leganés *et al*., 2009). Torrecilla *et al*. (2004b) also measured a short Ca^{2+} transient one to two hours after N step-down, whereas Shi *et al*. (2006) confirmed a very small increase in $[Ca^{2+}]_i$ within one hour after the shift but observed a much larger increase six hours after the shift. This major increase was ascribed to the degradation of CcbP, which has a Ca^{2+} buffering function in *Anabaena* (Zhao *et al*., 2005; Shi *et al*., 2006; Hu *et al*., 2011). The small transient in $[Ca^{2+}]_i$ about one hour after N depletion, however, correlated with the downregulation of *cse* expression one hour after N step-down (Paper II: Figure 3A). For that reason, it is conceivable that the early small transient in $[Ca^{2+}]_i$ is attributed to the downregulation of the *cse* gene, and might stimulate the Ca^{2+}-dependent protease activity of HetR for the degradation of CcbP (Zhou *et al*., 1998; Shi *et al*., 2006). In the *cse* knockout strain, unregulated Ca^{2+}-signalling clearly affected expression of *hetR* and *ntcA*, whose expression maxima were shifted from eight hours in the WT to one hour and 24 hours, respectively, in *Δcse* after the removal of N (Paper III: Figure 8). This dysregulation in *Δcse* could potentially lead to the formation of aberrant heterocysts and subsequent filament fragmentation.

5.2.3 Hypothetical scheme describing the role of Ca^{2+} and CSE in Anabaena metabolism

Speculations about the function of CSE need to be made with care because the protein might have two potential functions. As a Ca^{2+}-binding protein, it might buffer the free $[Ca^{2+}]_i$ depending on its expression level, i.e. a low amount of CSE might increase the $[Ca^{2+}]_i$, whereas a high amount of the protein might decrease the $[Ca^{2+}]_i$. This may affect many Ca^{2+}-regulated processes in the cell, such as the constitution of protein complexes and membranes, photosynthesis, heterocyst differentiation and stress signalling (described in Section 1.5.2), or the Ca^{2+}-dependent protease PrcA (Wood and Haselkorn, 1980; Maldener *et al.*, 1991). Then again, CSE is likely to be a regulator protein that might change the activity of a protein partner upon binding of Ca^{2+}. In fact, CSE (Asr1131) is annotated as “serine/threonine protein phosphatase

2B regulatory subunit" in the JGI IMG/M database, although experimental evidence is not provided, and the annotation probably derives from homology to mammalian Ca^{2+}-dependent regulatory phosphatase subunits. Interestingly, gene expression of the serine/threonine-protein phosphatase PrpA (Zhang *et al*., 1998) was upregulated in *cse*-oex (*prpA* log2 FC = 1.1) similar to the *cse* gene in *cse*-oex (*cse* log2 FC = 1.2) (Paper II: Table 3), indicating that PrpA might be an interaction partner of CSE. Even though PrpA is conserved throughout species, CSE may be a specific regulatory subunit in filamentous and heterocystous strains similar to calcineurin B, which binds to the calcineurin A phosphatase in eukaryotes (Rusnak and Mertz, 2000), as the combination of a few catalytic subunits with many regulatory subunits allows the broad spectrum of de-phosphorylation targets for protein phosphatases (Shi, 2009). In addition, calcineurin B contains four Ca^{2+}-binding EF-hand motifs, two of which bind Ca^{2+} with high affinity and two bind Ca^{2+} with low affinity (Kakalis *et al*., 1995; Gallagher *et al*., 2001). The high affinity EF-hands are specified as structural sites, which connect calcineurin B with calcineurin A under low $[Ca^{2+}]_i$, whereas the low affinity EF-hands are regulatory Ca^{2+} sensor domains, that activate the phosphatase under high $[Ca^{2+}]_i$ during Ca^{2+} signals (Yang and Klee, 2000; Li *et al*., 2011). The two EF-hand domains in CSE have similar features (high/ low affinity) as shown in ITC assays when a two sequential-binding site model was used (see Main Results, Section 4.2, page 44), and therefore, CSE might work in a similar way to calcineurin B.

Altogether, *cse* expression and function are dependent on the metabolic state of the cell (Figure 7). During N limitation, the C/N ratio increases, leading to the accumulation of 2-OG, which is fixed in the GS-GOGAT cycle together with ammonium (NH_4^+) to produce glutamate. High levels of 2-OG activate the NtcA master regulator of N_2 fixation, which might bind to a putative binding site in the *cse* promoter region (Paper II: Figure S4), possibly inhibiting *cse* expression (Paper II: Figure 3A). As a result, $[Ca^{2+}]_i$ might increase as evident in the minor transient one hour after the depletion of N (Torrecilla *et al*., 2004b; Shi *et al*., 2006). This Ca^{2+} signal might stimulate the Ca^{2+}-dependent protease activity of another master regulator, HetR, which has both TF and protease activity (Zhou *et al*., 1998). Upon HetR activation, the Ca^{2+} buffer protein CcbP is degraded, and its expression is downregulated by NtcA, thus releasing a second, higher Ca^{2+} signal about six hours after N step-down, that further stimulates HetR activity (Shi *et al*., 2006). As a TF, HetR initiates the differentiation of vegetative cells into N_2-fixing heterocysts, by

activating HetP and HetZ (the proteins responsible for the commitment of the cell to differentiation), and HetC, which instigates the morphological maturation of the developing heterocyst. HetR further activates the heterocyst inhibitor protein PatS, which in turn inhibits *hetR* expression.

In conditions with a low C/N ratio (low CO_2), *cse* expression is induced, probably by binding of the TF PacR to the binding site in the *cse* promoter (Paper II: Figures 3B and S4; Picossi *et al*., 2015). Upon sensing a Ca^{2+} signal that might occur during the acclimation to low CO_2 conditions (see Section 5.1 and Figure 6), CSE might interact with a hypothetical protein partner and downregulate photosynthetic processes. A possible CSE protein partner could be PrpA (described above), which upon CSE-binding might specifically de-phosphorylate the PBS L_{RC} proteins CpcG1/2, which are known to be phosphorylated when assembled (Piven *et al*., 2005; Angeleri *et al.*, 2016), thus impairing the proper assembly of PBS. These L_{RC} proteins are specific for pentacylindrical PBS because they connect the extra pair of side rods compared to bi- or tricylindrical PBS with six rods (Figure 2). Pentacylindrical PBS are exclusively present in filamentous cyanobacteria, as is CSE. Furthermore, it is possible that the upregulation of the Ca^{2+}-binding CSE protein in low CO_2 conditions decreased the availability of free Ca^{2+}, resulting in the release of Flv4 from the thylakoid membrane, thus destabilising PSII dimers through possible alterations of the All4445 protein from the *flv4-2* operon (Zhang *et al*., 2012; Bersanini *et al*., 2017). Consequently, PBS complexes disconnect from PSII monomers and the PQ pool becomes overreduced. Downregulation of both PBS assembly and PSII dimerisation upon *cse* expression induction might control light-harvesting under C_i stress conditions, when there is not enough CO_2 as terminal acceptor of electrons (see Figure 7).

These speculations about the role of CSE on photosynthesis have only been investigated in vegetative cells but not in heterocysts in this thesis. In heterocysts, the LET route of photosynthesis involving PSII ceases, but CET around PSI remains active, and PBS have been proven to be present (Magnuson and Cardona, 2016). After a strong decrease in *cse* gene expression in the initial stage of heterocyst differentiation (Paper II: Figure 3A), decreased *cse* expression fluctuated between basal levels at eight hours (normalised expression = 1.0) and minimal levels (normalised expression = 0.2) at 24 hours after N depletion. However, after 48 hours, *cse* gene expression returned to basal levels. Therefore, it is conceivable that CSE-dependent regulation of light-harvesting is also active in mature

heterocysts and might be employed to downregulate light-harvesting around PSII, in order to promote CET.

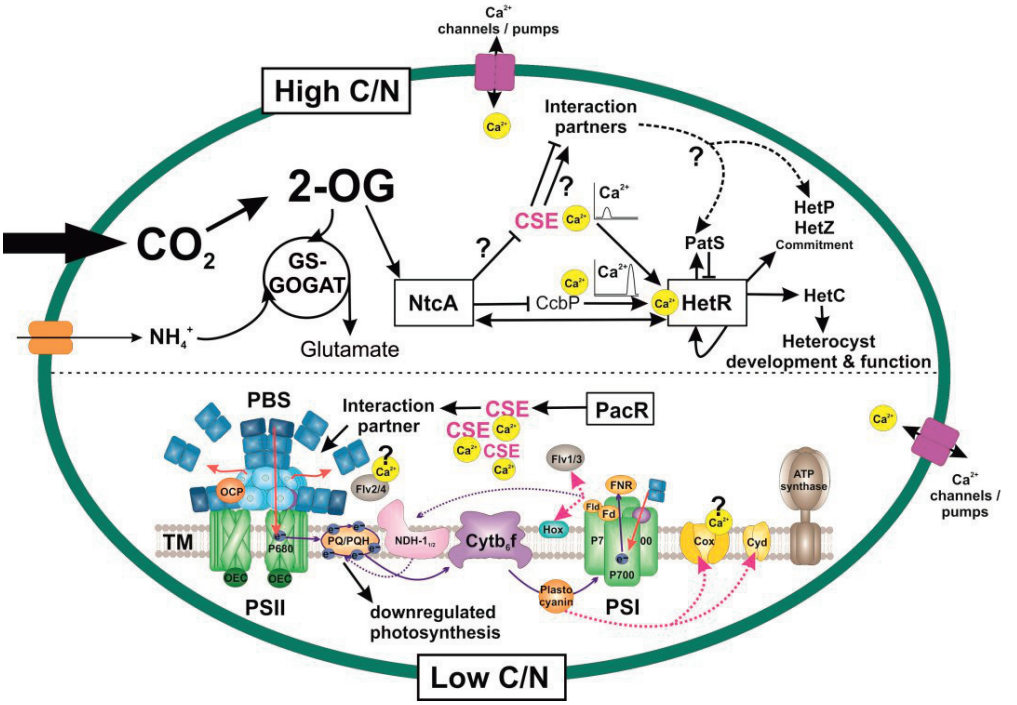

Figure 7: Schematic overview of dinitrogen fixation and photosynthetic processes in *Anabaena* sp. PCC 7120, involving the novel calcium (Ca^{2+})-binding protein CSE and Ca^{2+} signalling.

During nitrogen (N) starvation, the carbon (C) and N ratio increases, which activates a signalling cascade in order to adapt to this stress and activate N_2 fixation. Enhanced uptake of carbon dioxide (CO_2) leads to accumulation of 2-oxoglutarate (2-OG) because the glutamine synthetase-glutamine oxoglutarate aminotransferase (GS-GOGAT) cycle is downregulated due to the lack of ammonium (NH_4^+). High levels of 2-OG activate NtcA, possibly inhibiting the expression of the Ca^{2+}-binding protein CSE, which might lead to the accumulation of free Ca^{2+} ions. These might activate HetR and cause degradation of the cyanobacterial Ca^{2+}-binding protein CcbP, upon which a larger Ca^{2+} signal might be released for further stimulation of HetR activity, initiating heterocyst differentiation and N_2 fixation.

In low CO_2 conditions, the C/N ratio decreases, which activates the transcription factor PacR and induces expression of CSE. Upon binding Ca^{2+}, CSE undergoes a conformational change and might interact with a putative protein partner. Activated by CSE-binding, this protein partner might cause the disassembly of light-harvesting phycobilisome (PBS) side rods from the core, leading to downregulation of photosynthetic processes. Abbreviations: adenosine triphosphate (ATP), cytochrome *c* oxidase (Cox), cytochrome *bd* quinol oxidase (Cyd), cytochrome (Cyt), ferredoxin (Fd), flavodoxin (Fld), flavodiiron protein (Flv), Fd-$NADP^+$-reductase (FNR), bidirectional hydrogenase (Hox), nicotinamide adenine dinucleotide phosphate ($NADP^+(H)$), nicotinamide adenine dinucleotide dehydrogenase (NDH), orange carotenoid protein (OCP), oxygen-evolving complex (OEC), photosystem (PS), PSII reaction centre (P680), PSI reaction centre (P700), plastoquinone (PQ), plastoquinol (PQH_2), thylakoid membrane (TM).

Blue arrows indicate linear electron transport (full lines) and cyclic electron transport (dotted lines), whereas pink dotted arrows show alternative electron transport. Red arrows in the photosystems demonstrate the transfer of excitation energy. Yellow spheres correspond to Ca^{2+} ions and blue spheres display electrons. Framed proteins are transcriptional regulators. Bar-headed lines indicate inhibition.

6. CONCLUDING REMARKS

The work presented in this thesis sheds light on the important role of Ca^{2+} signalling on metabolic pathways in the filamentous and N_2-fixing cyanobacterium *Anabaena*. In summary:

1.) A Ca^{2+} signal has previously been connected to N_2 fixation in *Anabaena*, however, here, it has been shown for the first time that Ca^{2+} influences transcriptional regulation of transporters responsible for the metabolic balance between C_i and N (**Paper I**). This balance is crucial for the acclimation of the cells to stress conditions and thus needs to be tightly regulated. Because gene expression of the C_i uptake transporter BCT1, encoded in the *cmp* operon, and its transcriptional regulator *cmpR* correlated with the shifts in $[Ca^{2+}]_e$, a role for Ca^{2+} in the activation of CmpR expression (possibly involving a Ca^{2+} sensor protein) is proposed, which is necessary in conditions with a low C/N ratio, i.e. in low CO_2. This hypothesis requires further evidence, however, if proven correct this knowledge could have future applications for transferring cyanobacterial C_i transporters into plant chloroplasts (Rolland *et al*., 2016; Rae *et al*., 2017). Therefore, uptake of C_i into chloroplasts could be enhanced, increasing the rate of photosynthetic CO_2 fixation and biomass/food production.

2.) The small Asr1131 protein (CSE) was discovered, which, in *Anabaena*, is the only protein with more than one EF-hand domain and one of only a few described Ca^{2+}-binding proteins, including CcbP (Zhao *et al*., 2005), the oscillin-like glycoprotein Alr7304 for gliding motility (Hoiczyk and Baumeister, 1997) and the competence protein-like All3087 protein (Kumari and Chaurasia, 2015). In contrast to the Ca^{2+} buffering function of CcbP, CSE contains the features of a Ca^{2+} sensor and regulator protein. Upon binding of Ca^{2+}, it undergoes a conformational change and is very similar to a Ca^{2+}-binding subunit of the well-known Ca^{2+} sensors calmodulin and troponin C in eukaryotes. (**Paper II**). Therefore, it might be the only protein in *Anabaena* that senses changes in the $[Ca^{2+}]_i$ and relays this information to downstream targets. CSE contains two EF-hand domains, one of which has high affinity and the other one has low affinity to Ca^{2+} ions. This might indicate different functions of the EF-hands in CSE, potentially being involved in many Ca^{2+}-dependent processes.

3.) The expression of *cse* in *Anabaena* is responsive to changes in the C/N ratio, due to the presence of certain TF-binding sites in the *cse* promoter region. This makes it a novel intermediate of the C/N balance in *Anabaena* with implications for the regulation of both photosynthesis and heterocyst differentiation. It is proposed in this thesis that the CSE protein is a component of higher regulation mechanisms of light-harvesting, possibly involving Ca^{2+}-dependent (de)phosphorylation events, in multicellular cyanobacteria with pentacylindrical PBS (**Paper II**). In addition, CSE might be involved in Ca^{2+} signalling events required for cellular differentiation for stress-induced N_2 fixation (**Paper III**).

4.) The work in this thesis establishes that Ca^{2+} signalling plays versatile roles in adaptation mechanisms of the filamentous cyanobacterium *Anabaena* to changing environmental conditions. Re-adjustment of the C/N balance is achieved via Ca^{2+} acting as an effector molecule, controlling transcriptional regulation of C/N components/transporters, protein activities and cellular signal transduction cascades.

7. ACKNOWLEDGEMENTS

The work presented in this thesis was performed at the Laboratory of Molecular Plant Biology at the University of Turku. The Marie Curie Initial Training Network "Calipso" and the Academy of Finland are thankfully acknowledged for financial support.

I am forever grateful to Academician Prof. Eva-Mari Aro for the opportunity to work in such an excellent and unique research environment. I would like to thank my supervisor Dr. Peter Gollan for his support and guidance and for making my research project possible. I also highly appreciate the precious input of our collaborators from Spain and Germany and co-authors of the manuscripts. I am grateful to Prof. Eevi Rintamäki for her guidance through the chaotic world of university bureaucracy and paperwork. Prof. Anthony Larkum and Dr. David Fewer are acknowledged for their effort to improve the content of this thesis. I would also like to thank Prof. Rakefet Schwarz for agreeing to be my opponent during my doctoral disputation.

None of this would have been possible without the wonderful people working in our Molecular Plant Biology unit. Special thanks go to Eveliina, Anniina, Mika, Tapio, Hannele, Kurt and Mirja for keeping our labs running smoothly. Thanks to everyone for valuable scientific discussions, lessons and advice, particularly in the field of biophysics, photosynthesis and proteomics…I am especially grateful to Assoc. Prof. Yagut Allahverdiyeva-Rinne and all of her (past and present) group members, and Dr. Natalia Battchikova. Thanks a million, billion, trillion to Prof. em. Marjatta Raudaskoski for her moral support, friendship and inspiration. For his knowledge of the Finnish language and the impossible job of translating the tiivistelmä, I'm very grateful to Juh…uhm…Vesa. 😉

And of course, above all, I cannot thank the people enough who were not just colleagues or visitors but have become dear friends and made it worth not giving up: Martina A., Masha, Martina J,-T., Luca, Sara, Duncan and Katie, Dániel, Hari and Zsófi, Félix, Ilaria, Anita, Yugo, Magda, Caterina, Sema, Vali, Aksu, Tuomas, Ninni, Minna, Linda and the Shitty Movie Night gang Vesa, Heta, Juha and Janne…thank you from the bottom of my heart for the most amazing "nights out", all the crazy parties, awesome trips together, yummy dinners or Sunday brunches, and so on…and for standing my constant complaints about life, hahaha. 😊

The same goes without saying to my Turku friends Xu, Jesus and Ville, and my friends in Germany Caro, Sandra and Sarah. Furthermore, I would also like to acknowledge the "Calipsies" from the "Calipso" network. Our scientific meetings have always been a great pleasure, and it was so much fun to explore all these lovely places together all over Europe. Special thanks go to Bikram for being such a good friend and giving refuge to me in beautiful Vienna when Finnish summers or winters had been too cold and dark.

Most importantly, I have to thank my family, especially my mum, for supporting me in whatever I do, and for sending all the candy care packages to ensure my survival. Tausend Dank für alles, ich hab euch lieb! 🖤

8. REFERENCES

Adams, D.G., and Duggan, P.S. (1999) Tansley Review No. 107. Heterocyst and akinete differentiation in cyanobacteria. New Phytol 144: 3-33. doi: 10.1046/j.1469-8137.1999.00505.x

Agostoni, M., and Montgomery, B.L. (2014) Survival strategies in the aquatic and terrestrial world: the impact of second messengers on cyanobacterial processes. Life (Basel) 4(4): 745-769. doi: 10.3390/life4040745

Al-Haj, L., Lui, Y.T., Abed, R.M., Gomaa, M.A., and Purton, S. (2016) Cyanobacteria as chassis for industrial biotechnology: progress and prospects. Life (Basel) 6(4): 42. doi: 10.3390/life6040042

Allahverdiyeva, Y., Mustila, H., Ermakova, M., Bersanini, L., Richaud, P., Ajlani, G., Battchikova, N., *et al.* (2013) Flavodiiron proteins Flv1 and Flv3 enable cyanobacterial growth and photosynthesis under fluctuating light. Proc Natl Acad Sci U S A 110(10): 4111-4116.
doi: 10.1073/pnas.1221194110

Allahverdiyeva, Y., Isojärvi, J., Zhang, P., and Aro, E.M. (2015) Cyanobacterial oxygenic photosynthesis is protected by flavodiiron proteins. Life (Basel) 5(1): 716-743. doi: 10.3390/life5010716

Allen, J. (2002) Photosynthesis of ATP-electrons, proton pumps, rotors, and poise. Cell 110(3): 273-276. doi: 10.1016/s0092-8674(02)00870-x

Angeleri, M., Muth-Pawlak, D., Aro, E.M., and Battchikova, N. (2016) Study of O-phosphorylation sites in proteins involved in photosynthesis-related processes in *Synechocystis* sp. strain PCC 6803: Application of the SRM approach. J Proteome Res 15(12): 4638-4652.
doi: 10.1021/acs.jproteome.6b00732

Argueta, C., Yuksek, K., Patel, R., and Summers, M.L. (2006) Identification of *Nostoc punctiforme* akinete-expressed genes using differential display. Mol Microbiol 61(3): 748-757.
doi: 10.1111/j.1365-2958.2006.05263.x

Aro, E.M., Suorsa, M., Rokka, A., Allahverdiyeva, Y., Paakkarinen, V., Saleem, A., Battchikova, N., *et al.* (2005) Dynamics of photosystem II: a proteomic approach to thylakoid protein complexes. J Exp Bot 56(411): 347-356. doi: 10.1093/jxb/eri041

Arteni, A.A., Ajlani, G., and Boekema, E.J. (2009) Structural organisation of phycobilisomes from *Synechocystis* sp. strain PCC6803 and their interaction with the membrane. Biochim Biophys Acta 1787(4): 272-279.
doi: 10.1016/j.bbabio.2009.01.009

Badger, M.R., and Price, G.D. (2003) CO_2 concentrating mechanisms in cyanobacteria: molecular components, their diversity and evolution. J Exp Bot 54(383): 609-622.
doi: 10.1093/jxb/erg076

Bagur, R., and Hajnóczky, G. (2017) Intracellular Ca^{2+} sensing: its role in calcium homeostasis and signaling. Mol Cell 66(6): 780-788.
doi: 10.1016/j.molcel.2017.05.028

Baier, K., Lehmann, H., Stephan, D.P., and Lockau, W. (2004) NblA is essential for phycobilisome degradation in *Anabaena* sp. strain PCC 7120 but not for development of functional heterocysts. Microbiology 150(8): 2739-2749.
doi: 10.1099/mic.0.27153-0

Bald, D., Kruip, J., and Rögner, M. (1996) Supramolecular architecture of cyanobacterial thylakoid membranes: How is the phycobilisome connected with the photosystems? Photosynth Res 49(2): 103-118. doi: 10.1007/BF00117661

Barber, J., Morris, E.P., and da Fonseca, P.C. (2003) Interaction of the allophycocyanin core complex with photosystem II. Photochem Photobiol Sci 2(5): 536-541. doi: 10.1039/B300063J

Barber, J. (2012) Photosystem II: the water-splitting enzyme of photosynthesis. Cold Spring Harb Symp Quant Biol 77: 295-307.
doi: 10.1101/sqb.2012.77.014472

Battchikova, N., Eisenhut, M., and Aro, E.M. (2011) Cyanobacterial NDH-1 complexes: novel insights and remaining puzzles. Biochim Biophys Acta 1807(8): 935-944. doi: 10.1016/j.bbabio.2010.10.017

Bauer, C.C., Buikema, W.J., Black, K., and Haselkorn, R. (1995) A short-filament mutant of *Anabaena* sp. strain PCC 7120 that fragments in nitrogen-deficient medium. J Bacteriol 177(6): 1520-1526. doi: 0.1128/jb.177.6.1520-1526.1995

Baumann, U., Wu, S., Flaherty, K.M., and McKay, D.B. (1993) Three-dimensional structure of the alkaline protease of *Pseudomonas aeruginosa*: a two-domain protein with a calcium binding parallel beta roll motif. EMBO J 12(9): 3357-3364. doi: 10.1002/j.1460-2075.1993.tb06009.x

Bergman, B., Gallon, J.R., Rai, A.N., and Stal, L.J. (1997) N_2 fixation by non-heterocystous cyanobacteria. FEMS Microbiol Rev 19(3): 139-185. doi: 10.1111/j.1574-6976.1997.tb00296.x

Bersanini, L., Battchikova, N., Jokel, M., Rehman, A., Vass, I., Allahverdiyeva, Y., and Aro, E.M. (2014) Flavodiiron protein Flv2/Flv4-related photoprotective mechanism dissipates excitation pressure of PSII in cooperation with phycobilisomes in cyanobacteria. Plant Physiol 164(2): 805-818. doi: 10.1104/pp.113.231969

Bersanini, L., Allahverdiyeva, Y., Battchikova, N., Heinz, S., Lespinasse, M., Ruohisto, E., Mustila, H., *et al*. (2017) Dissecting the photoprotective mechanism encoded by the *flv4-2* operon: a distinct contribution of Sll0218 in Photosystem II stabilization. Plant Cell Environ 40(3): 378-389. doi: 10.1111/pce.12872

Böhme, H. (1998) Regulation of nitrogen fixation in heterocyst-forming cyanobacteria. Trends Plant Sci 3(9): 346-351. doi: 10.1016/S1360-1385(98)01290-4

Bothe, H., Schmitz, O., Yates, M.G., and Newton, W.E. (2010) Nitrogen fixation and hydrogen metabolism in cyanobacteria. Microbiol Mol Biol Rev 74(4): 529-551. doi: 10.1128/MMBR.00033-10

Bryant, D.A. (1982) Phycoerythrocyanin and phycoerythrin: Properties and occurrence in cyanobacteria. J Gen Microbiol 128: 835-844. doi: 10.1099/00221287-128-4-835

Bryant, D.A., Stirewalt, V.L., Glauser, M., Frank, G., Sidler, W., and Zuber, H. (1991) A small multigene family encodes the rod-core linker polypeptides of *Anabaena* sp. PCC7120 phycobilisomes. Gene 107(1): 91-99. doi: 10.1016/0378-1119(91)90301-Q

Bryant, D.A. (2003) The beauty in small things revealed. Proc Natl Acad Sci U S A 100(17): 9647-9649. doi: 10.1073/pnas.1834558100

Buikema, W.J., and Haselkorn, R. (1991a) Isolation and complementation of nitrogen fixation mutants of the cyanobacterium *Anabaena* sp. strain PCC 7120. J Bacteriol 173(6): 1879-1885. doi: 10.1128/jb.173.6.1879-1885.1991

Calzadilla, P.I., Zhan, J., Sétif, P., Lemaire, C., Solymosi, D., Battchikova, N., Wang, Q., and Kirilovsky, D. (2019) The cytochrome b_6f complex is not involved in cyanobacterial state transitions. Plant Cell 31(4): 911-931. doi: 10.1105/tpc.18.00916

Campbell, E.L., Summers, M.L., Christman, H., Martin, M.E., and Meeks, J.C. (2007) Global gene expression patterns of *Nostoc punctiforme* in steady-state dinitrogen-grown heterocyst-containing cultures and at single time points during the differentiation of akinetes and hormogonia. J Bacteriol 189(14): 5247-5256. doi: 10.1128/JB.00360-07

Cardemil, L., and Wolk, C.P. (1979) The polysaccharides from heterocyst and spore envelopes of a blue-green alga. Structure of the basic repeating unit. J Biol Chem 254(3): 736-741. Retrieved from http://www.jbc.org/content/254/3/736.long

Cardona, T., Sedoud, A., Cox, N., and Rutherford, A.W. (2012) Charge separation in photosystem II: a comparative and evolutionary overview. Biochim Biophys Acta 1817(1): 26-43. doi: 10.1016/j.bbabio.2011.07.012

Caspy, I., and Nelson, N. (2018) Structure of the plant photosystem I. Biochem Soc Trans 46(2): 285-294. doi: 10.1042/BST20170299

Chang, L., Liu, X., Li, Y., Liu, C.C., Yang, F., Zhao, J., and Sui, S.F. (2015) Structural organization of an intact phycobilisome and its association with photosystem II. Cell Res 25(6): 726-737. doi: 10.1038/cr.2015.59

Chazin, W.J. (2011) Relating form and function of EF-hand calcium binding proteins. Acc Chem Res 44(3): 171-179. doi: 10.1021/ar100110d

Chukhutsina, V., Bersanini, L., Aro, E.M., and van Amerongen, H. (2015) Cyanobacterial flv4-2 operon-encoded proteins optimize light harvesting and charge separation in Photosystem II. Mol Plant 8(5): 747-761. doi: 10.1016/j.molp.2014.12.016

Clapham, D.E. (2007) Calcium signaling. Cell 131(6): 1047-1058. doi: 10.1016/j.cell.2007.11.028

Corrales-Guerrero, L., Mariscal, V., Flores, E., and Herrero, A. (2013) Functional dissection and evidence for intercellular transfer of the heterocyst-differentiation PatS morphogen. Mol Microbiol 88(6): 1093-1105. doi: 10.1111/mmi.12244

Corrales-Guerrero, L., Mariscal, V., Nürnberg, D.J., Elhai, J., Mullineaux, C.W., Flores, E., and Herrero, A. (2014) Subcellular localization and clues for the function of the HetN factor influencing heterocyst distribution in *Anabaena* sp. strain PCC 7120. J Bacteriol 196(19): 3452-3460. doi: 10.1128/JB.01922-14

Criscuolo, A., and Gribaldo, S. (2011) Large-scale phylogenomic analyses indicate a deep origin of primary plastids within cyanobacteria. Mol Biol Evol 28(11): 3019-3032. doi: 10.1093/molbev/msr108

Curatti, L., Flores, E., and Salerno, G. (2002) Sucrose is involved in the diazotrophic metabolism of the heterocyst-forming cyanobacterium *Anabaena* sp. FEBS Lett 513(2-3): 175-178. doi: 10.1016/S0014-5793(02)02283-4

DeFalco, T.A., Bender, K.W., and Snedden, W.A. (2009) Breaking the code: Ca^{2+} sensors in plant signalling. Biochem J 425(1): 27-40. doi: 10.1042/BJ20091147

Denessiouk, K., Permyakov, S., Denesyuk, A., Permyakov, E., and Johnson, M.S. (2014) Two structural motifs within canonical EF-hand calcium-binding domains identify five different classes of calcium buffers and sensors. PLoS One 9(10): e109287. doi: 10.1371/journal.pone.0109287

Derikvand, P., Llewellyn, C.A., and Purton, S. (2017) Cyanobacterial metabolites as a source of sunscreens and moisturizers: a comparison with current synthetic compounds. Eur J Phycol 52(1): 43-56. doi: 10.1080/09670262.2016.1214882

Deusch, O., Landan, G., Roettger, M., Gruenheit, N., Kowallik, K.V., Allen, J.F., Martin, W., and Dagan, T. (2008) Genes of cyanobacterial origin in plant nuclear genomes point to a heterocyst-forming plastid ancestor. Mol Biol Evol 25(4): 748-761. doi: 10.1093/molbev/msn022

Diner, B.A., Petrouleas, V., and Wendoloski, J.J. (1991) The iron-quinone electron-acceptor complex of photosystem II. Physiol Plant 81(3): 423-436. doi: 10.1111/j.1399-3054.1991.tb08753.x

Domínguez, D.C., Guragain, M., and Patrauchan, M. (2015) Calcium binding proteins and calcium signaling in prokaryotes. Cell Calcium 57(3): 151-165. doi: 10.1016/j.ceca.2014.12.006

Dong, C., Tang, A., Zhao, J., Mullineaux, C.W., Shen, G., and Bryant, D.A. (2009) ApcD is necessary for efficient energy transfer from phycobilisomes to photosystem I and helps to prevent photoinhibition in the cyanobacterium *Synechococcus* sp. PCC 7002. Biochim Biophys Acta 1787(9): 1122-1128. doi: 10.1016/j.bbabio.2009.04.007

Dong, Y., Huang, X., Wu, X.Y., and Zhao, J. (2000) Identification of the active site of HetR protease and its requirement for heterocyst differentiation in the cyanobacterium *Anabaena* sp. strain PCC 7120. J Bacteriol 182(6): 1575-1579. doi: 10.1128/JB.182.6.1575-1579.2000

DuBois, M., Gilles, K.A., Hamilton, J.K., Rebers, P.A., and Smith, F. (1956) Colorimetric method for determination of sugars and related substances. Anal Chem 28(3): 350-356. doi: 10.1021/ac60111a017

Ducret, A., Sidler, W., Wehrli, E., Frank, G., and Zuber, H. (1996) Isolation, characterization and electron microscopy analysis of a hemidiscoidal phycobilisome type from the cyanobacterium *Anabaena* sp. PCC 7120. Eur J Biochem 236(3): 1010-1024. doi: 10.1111/j.1432-1033.1996.01010.x

Elhai, J., and Wolk, C.P. (1988) Conjugal transfer of DNA to cyanobacteria. Methods Enzymol 167: 747-754. doi: 10.1016/0076-6879(88)67086-8

Ermakova, M., Battchikova, N., Allahverdiyeva, Y., and Aro, E.M. (2013) Novel heterocyst-specific flavodiiron proteins in *Anabaena* sp. PCC 7120. FEBS Lett 587(1): 82-87. doi: 10.1016/j.febslet.2012.11.006

Ermakova, M., Battchikova, N., Richaud, P., Leino, H., Kosourov, S., Isojärvi, J., Peltier, G., *et al.* (2014) Heterocyst-specific flavodiiron protein Flv3B enables oxic diazotrophic growth of the filamentous cyanobacterium *Anabaena* sp. PCC 7120. Proc Natl Acad Sci U S A 111(30): 11205-11210. doi: 10.1073/pnas.1407327111

Ermakova, M., Huokko, T., Richaud, P., Bersanini, L., Howe, C.J., Lea-Smith, D.J., Peltier, G., and Allahverdiyeva, Y. (2016) Distinguishing the roles of thylakoid respiratory terminal oxidases in the

cyanobacterium *Synechocystis* sp. PCC 6803. Plant Phys 171: 1307-1319.
doi: https://doi.org/10.1104/pp.16.00479

Ernst, A., Black, T., Cai, Y., Panoff, J.M., Tiwari, D.N., and Wolk, C.P. (1992) Synthesis of nitrogenase in mutants of the cyanobacterium *Anabaena* sp. strain PCC 7120 affected in heterocyst development or metabolism. J Bacteriol 174(19): 6025-6032. doi: 10.1128/jb.174.19.6025-6032.1992

Espinosa, J., Forchhammer, K., Burillo, S., and Contreras, A. (2006) Interaction network in cyanobacterial nitrogen regulation: PipX, a protein that interacts in a 2-oxoglutarate dependent manner with PII and NtcA. Mol Microbiol 61(2): 457-469. doi: 10.1111/j.1365-2958.2006.05231.x

Federman, S., Malkin, S., and Scherz, A. (2000) Excitation energy transfer in aggregates of Photosystem I and Photosystem II of the cyanobacterium *Synechocystis* sp. PCC 6803: Can assembly of the pigment-protein complexes control the extent of spillover? Photosynth Res 64(2-3): 199-207. doi: 10.1023/A:1006485823403

Flaherty, B.L., Johnson, D.B.F., and Golden, J.W. (2014) Deep sequencing of HetR-bound DNA reveals novel HetR targets in *Anabaena* sp. strain PCC7120. BMC Microbiol 14: 255.
doi: 10.1186/s12866-014-0255-x

Flores, E., Frías, J.E., Rubio, L.M., and Herrero, A. (2005) Photosynthetic nitrate assimilation in cyanobacteria. Photosynth Res 83(2): 117-133. doi: 10.1007/s11120-004-5830-9

Flores, E., Herrero, A., Wolk, C.P., and Maldener, I. (2006) Is the periplasm continuous in filamentous multicellular cyanobacteria? Trends Microbiol 14(10): 439-443. doi: 10.1016/j.tim.2006.08.007

Flores, E., Pernil, R., Muro-Pastor, A.M., Mariscal, V., Maldener, I., Lechno-Yossef, S., Fan, Q., *et al.* (2007) Septum-localized protein required for filament integrity and diazotrophy in the heterocyst-forming cyanobacterium *Anabaena* sp. strain PCC 7120. J Bacteriol 189(10): 3884-3890.
doi: 10.1128/JB.00085-07

Flores, E., and Herrero, A. (2010) Compartmentalized function through cell differentiation in filamentous cyanobacteria. Nat Rev Microbiol 8(1): 39-50.
doi: 10.1038/nrmicro2242

Forchhammer, K., and Schwarz, R. (2018) Nitrogen chlorosis in unicellular cyanobacteria - a developmental program for surviving nitrogen deprivation. Environ Microbiol 21(4): 1173-1184.
doi: 10.1111/1462-2920.14447

Foykar, O., and Matavuly, M. (1998) The appearance of filament anastomosis in *Nostoc* and *Anabaena* strains. In: Elmerich, C., Kondorosi, A., Newton, W.E. (eds) Biological nitrogen fixation for the 21st century. Current Plant Science and Biotechnology in Agriculture, vol 31. Springer, Dordrecht. doi: 10.1007/978-94-011-5159-7_78

Gallagher, S.C., Gao, Z.H., Li, S., Dyer, R.B., Trewhella, J., and Klee, C.B. (2001) There is communication between all four Ca(2+)-bindings sites of calcineurin B. Biochemistry 40(40): 12094-12102. doi: 10.1021/bi0025060

Gonzalez-Esquer, C.R., Smarda, J., Rippka, R., Axen, S.D., Guglielmi, G., Gugger, M., and Kerfeld, C.A. (2016) Cyanobacterial ultrastructure in light of genomic sequence data. Photosynth Res 129(2): 147-157. doi: 10.1007/s11120-016-0286-2

Gould, S.B., Waller, R.F., and McFadden, G.I. (2008) Plastid evolution. Annu Rev Plant Biol 59: 491-517.
doi: 10.1146/annurev.arplant.59.032607.092915

Grzybowska, E.A. (2018) Calcium-binding proteins with disordered structure and their role in secretion, storage, and cellular signaling. Biomolecules 8(2): E42. doi: 10.3390/biom8020042

Gutu, A., and Kehoe, D.M. (2011) Emerging perspectives on the mechanisms, regulation, and distribution of light color acclimation in cyanobacteria. Mol Plant 5(1): 1–13.
doi: 10.1093/mp/ssr054

Haimovich-Dayan, M., Lieman-Hurwitz, J., Orf, I., Hagemann, M., and Kaplan, A. (2015) Does 2-phosphoglycolate serve as an internal signal molecule of inorganic carbon deprivation in the cyanobacterium *Synechocystis* sp. PCC 6803? Environ Microbiol 17(5): 1794-1804.
doi: 10.1111/ 1462-2920.12638

Hanson, M.R., Lin, M.T., Carmo-Silva, A.E., and Parry, M.A. (2016) Towards engineering carboxysomes into C3 plants. Plant J 87(1): 38-50. doi: 10.1111/tpj.13139

Heredia, P., and De Las Rivas, J. (2003) Calcium-dependent conformational change and thermal stability of the isolated PsbO protein detected by FTIR spectroscopy. Biochemistry 42(40): 11831-11838. doi: 10.1021/bi034582j

Herrero, A., Stavans, J., and Flores, E. (2016) The multicellular nature of filamentous heterocyst-forming cyanobacteria. FEMS Microbiol Rev 40(6): 831-854. doi: 10.1093/femsre/fuw029

Hochmal, A.K., Schulze, S., Trompelt, K., and Hippler, M. (2015) Calcium-dependent regulation of photosynthesis. Biochim Biophys Acta 1847(9): 993-1003. doi: 10.1016/j.bbabio.2015.02.010

Hoiczyk, E., and Baumeister, W. (1997) Oscillin, an extracellular, Ca^{2+}-binding glycoprotein essential for the gliding motility of cyanobacteria. Mol Microbiol 26(4): 699-708.
doi: 10.1046/j.1365-2958.1997.5971972.x

Hoiczyk, E., and Hansel, A. (2000) Cyanobacterial cell walls: news from an unusual prokaryotic envelope. J Bacteriol 182(5): 1191-1199. doi: 10.1128/jb.182.5.1191-1199.2000

Hu, Y., Zhang, X., Shi, Y., Zhou, Y., Zhang, W., Su, X.D., Xia, B., *et al.* (2011) Structures of *Anabaena* calcium-binding protein CcbP: insights into Ca^{2+} signaling during heterocyst differentiation. J Biol Chem 286(14): 12381-12388.
doi: 10.1074/jbc.M110.201186

Huokko, T., Muth-Pawlak, D., Battchikova, N., Allahverdiyeva, Y., and Aro, E.M. (2017) Role of type 2 NAD(P)H dehydrogenase NdbC in redox regulation of carbon allocation in *Synechocystis*. Plant Physiol 174(3): 1863-1880.
doi: 10.1104/pp.17.00398

Jiang, Y.L., Wang, X.P., Sun, H., Han, S.J., Li, W.F., Cui, N., Lin, G.M., *et al.* (2018) Coordinating carbon and nitrogen metabolic signaling through the cyanobacterial global repressor NdhR. Proc Natl Acad Sci U S A 115(2): 403-408.
doi: 10.1073/pnas.1716062115

Jobby, M.K., and Sharma, Y. (2005) Calcium-binding crystallins from *Yersinia pestis*. Characterization of two single betagamma-crystallin domains of a putative exported protein. J Biol Chem 280(2): 1209-1216. doi: 10.1074/jbc.M409253200

Joshua, S., and Mullineaux, C.W. (2004) Phycobilisome diffusion is required for light-state transitions in cyanobacteria. Plant Physiol 135(4): 2112-2119. doi: 10.1104/pp.104.046110

Kakalis, L.T., Kennedy, M., Sikkink, R., Rusnak, F., and Armitage, I.M. (1995) Characterization of the calcium-binding sites of calcineurin B. FEBS Lett 362(1): 55-58.
doi: 10.1016/0014-5793(95)00207-p

Kämäräinen, J., Huokko, T., Kreula, S., Jones, P.R., Aro, E.M., and Kallio, P. (2016) Pyridine nucleotide transhydrogenase PntAB is essential for optimal growth and photosynthetic integrity under low-light mixotrophic conditions in *Synechocystis* sp. PCC 6803. New Phytol 214(1): 194-204.
doi: 10.1111/nph.14353

Kaneko, T., Nakamura, Y., Wolk, C.P., Kuritz, T., Sasamoto, S., Watanabe, A., Iriguchi, M., *et al.* (2001) Complete genomic sequence of the filamentous nitrogen-fixing cyanobacterium *Anabaena* sp. strain PCC 7120. DNA Res 8(5): 205-213. doi: 10.1093/dnares/8.5.227

Karkehabadi, S., Taylor, T.C., and Andersson, I. (2003) Calcium supports loop closure but not catalysis in Rubisco. J Mol Biol 334(1): 65-73. doi: 10.1016/j.jmb.2003.09.025

Kerfeld, C.A., and Melnicki, M.R. (2016) Assembly, function and evolution of cyanobacterial carboxysomes. Curr Opin Plant Biol 31: 66-75. doi: 10.1016/j.pbi.2016.03.009

Khudyakov, I.Y., and Golden, J.W. (2001) Identification and inactivation of three group 2 sigma factor genes in *Anabaena* sp. strain PCC 7120. J Bacteriol 183(22): 6667-6675.
doi: 10.1128/JB.183.22.6667-6675.2001

Kirilovsky, D. (2015) Modulating energy arriving at photochemical reaction centers: orange carotenoid protein-related photoprotection and state transitions. Photosynth Res 126(1): 3-17.
doi: 10.1007/s11120-014-0031-7

Klimov, V.V., Klevanik, A.V., Shuvalov, V.A., and Kransnovsky, A.A. (1977) Reduction of pheophytin in the primary light reaction of photosystem II. FEBS Lett 82(2): 183-186.
doi: 10.1016/0014-5793(77)80580-2

Klipp, W., Masepohl, B., Gallon, J.R., and Newton, W.E. (2005) Genetics and regulation of nitrogen fixation in free-living bacteria. Springer Dordrecht. 10.1007/1-4020-2179-8

Koropatkin, N.M., Koppenaal, D.W., Pakrasi, H.B., and Smith, T.J. (2007) The structure of a cyanobacterial bicarbonate transport protein, CmpA. J Biol Chem 282(4): 2606-2614. doi: 10.1074/jbc.M610222200

Kosourov, S., Leino, H., Murukesan, G., Lynch, F., Sivonen, K., Tsygankov, A.A., Aro, E.M., *et al.* (2014) Hydrogen photoproduction by immobilized n2-fixing cyanobacteria: understanding the role of the uptake hydrogenase in the long-term process. Appl Environ Microbiol 80(18): 5807-5817. doi: 10.1128/AEM.01776-14

Kumar, K., Mella-Herrera, R.A., and Golden, J.W. (2010) Cyanobacterial heterocysts. Cold Spring Harb Perspect Biol 2(4): a000315.
doi: 10.1101/cshperspect.a000315

Kumari, S., and Chaurasia, A.K. (2015) *In silico* analysis and experimental validation of lipoprotein and novel Tat signal peptides processing in *Anabaena* sp. PCC7120. J Microbiol 53(12): 837-846. doi: 10.1007/s12275-015-5281-3

Kurisu, G., Zhang, H., Smith, J.L, and Cramer, W.A. (2003) Structure of the cytochrome b6f complex of oxygenic photosynthesis: tuning the cavity. Science 302(5647): 1009-1014.
doi: 10.1126/science.1090165

Ladig, R., Sommer, M.S., Hahn, A., Leisegang, M.S., Papasotiriou, D.G., Ibrahim, M., Elkehal, R., *et al.* (2011) A high-definition native polyacrylamide gel electrophoresis system for the analysis of membrane complexes. Plant J 67(1): 181-194.
doi: 10.1111/j.1365-313X.2011.04577.x

Lan, E.I., and Liao, J.C. (2011) Metabolic engineering of cyanobacteria for 1-butanol production from carbon dioxide. Metab Eng 13(4): 353-363. doi: 10.1016/j.ymben.2011.04.004

Lazaroff, N., and Vishniac, W. (1962) The participation of filament anastomosis in the developmental cycle of *Nostoc muscorum*, a blue-green alga. J Gen Microbiol 28: 203-10. doi: 10.1099/00221287-28-2-203

Lea-Smith, D.J., Bombelli, P., Vasudevan, R., and Howe, C.J. (2016) Photosynthetic, respiratory and extracellular electron transport pathways in cyanobacteria. Biochim Biophys Acta 1857(3): 247-255. doi: 10.1016/j.bbabio.2015.10.007

Lee, D.W., and Hwang, I. (2018) Evolution and design principles of the diverse chloroplast transit peptides. Mol Cells 41(3): 161-167.
doi: 10.14348/molcells.2018.0033

Leganés, F. (1994) Genetic evidence that *hepA* gene is involved in the normal deposition of the envelope of both heterocysts and akinetes in *Anabaena variabilis* ATCC 29413. FEMS Microbiol Lett 123(1-2): 63-67.
doi: 10.1111/j.1574-6968.1994.tb07202.x

Leganés, F., Fernández-Piñas, F., and Wolk, C.P. (1994) Two mutations that block heterocyst differentiation have different effects on akinete differentiation in *Nostoc ellipsosporum*. Mol Microbiol 12(4): 679-684.
doi: 10.1111/j.1365-2958.1994.tb01055.x

Leganés, F., Forchhammer, K., and Fernández-Piñas, F. (2009) Role of calcium in acclimation of the cyanobacterium *Synechococcus elongatus* PCC 7942 to nitrogen starvation. Microbiology 155(Pt 1): 25-34. doi: 10.1099/mic.0.022251-0

Leganés, F., Martínez-Granero, F., Muñoz-Martín, M.Á., Marco, E., Jorge, A., Carvajal, L., Vida, T., *et al.* (2014) Characterization and responses to environmental cues of a photosynthetic antenna-deficient mutant of the filamentous cyanobacterium *Anabaena* sp. PCC 7120. J Plant Physiol 171(11): 915-926. doi: 10.1016/j.jplph.2014.03.005

Li, H., Rao, A., and Hogan, P.G. (2011) Interaction of calcineurin with substrates and targeting proteins. Trends Cell Biol 21(2): 91-103.
doi: 10.1016/j.tcb.2010.09.011

Linhartová, I., Bumba, L., Mašín, J., Basler, M., Osička, R., Kamanová, J., Procházková, K., *et al.* (2010) RTX proteins: a highly diverse family secreted by a common mechanism. FEMS Microbiol Rev 34(6): 1076-1112.
doi: 10.1111/j.1574-6976.2010.00231.x

Liu, H., Zhang, H., Niedzwiedzki, D.M., Prado, M., He, G., Gross, M.L., and Blankenship, R.E. (2013) Phycobilisomes supply excitations to both photosystems in a megacomplex in cyanobacteria. Science 342(6162): 1104-1107.
doi: 10.1126/science.1242321

Liu, L.N., Chen, X.L., Zhang, Y.Z., and Zhou, B.C. (2005) Characterization, structure and function of linker polypeptides in phycobilisomes of

cyanobacteria and red algae: an overview. Biochim Biophys Acta 1708(2): 133-42.
doi: 10.1016/j.bbabio.2005.04.001

Long, B.M., Hee, W.Y., Sharwood, R.E., Rae, B.D., Kaines, S., Lim, Y.L., Nguyen, N.D., *et al.* (2018) Carboxysome encapsulation of the CO_2-fixing enzyme Rubisco in tobacco chloroplasts. Nat Commun 9(1): 3570.
doi: 10.1038/s41467-018-06044-0

López-Igual, R., Picossi, S., López-Garrido, J., Flores, E., and Herrero, A. (2012) N and C control of ABC-type bicarbonate transporter Cmp and its LysR-type transcriptional regulator CmpR in a heterocyst-forming cyanobacterium, *Anabaena* sp. Environ Microbiol 14(4): 1035-1048.
doi: 10.1111/j.1462-2920.2011.02683.x

López-Igual, R., Wilson, A., Leverenz, R.L., Melnicki, M.R., Bourcier de Carbon, C., Sutter, M., Turmo, A., *et al.* (2016) Different functions of the paralogs to the N-terminal domain of the orange carotenoid protein in the cyanobacterium *Anabaena* sp. PCC 7120. Plant Physiol 171(3): 1852-1866. doi: 10.1104/pp.16.00502

MacColl, R. (1998) Cyanobacterial phycobilisomes. J Struct Biol 124(2-3): 311-334.
doi: 10.1006/jsbi.1998.4062

Magnuson, A., and Cardona, T. (2016) Thylakoid membrane function in heterocysts. Biochim Biophys Acta 1857(3): 309-319.
doi: 10.1016/j.bbabio.2015. 10.016

Malavath, T., Caspy, I., Netzer-El, S.Y., Klaiman, D., and Nelson, N. (2018) Structure and function of wild-type and subunit-depleted photosystem I in *Synechocystis*. Biochim Biophys Acta Bioenerg 1859(9): 645-654.
doi: 10.1016/j.bbabio.2018.02.002

Maldener, I., Lockau, W., Cai, Y.P., and Wolk, C.P. (1991) Calcium-dependent protease of the cyanobacterium *Anabaena*: molecular cloning and expression of the gene in *Escherichia coli*, sequencing and site-directed mutagenesis. Mol Gen Genet 225(1): 113-120. doi: 10.1007/BF00282649

Markwell, M.A., Haas, S.M., Bieber, L.L., and Tolbert, N.E. (1978) A modification of the Lowry procedure to simplify protein determination in membrane and lipoprotein samples. Anal Biochem 87(1): 206-210.
doi: 10.1016/0003-2697(78)90586-9

McAinsh, M.R., and Pittman, J.K. (2009) Shaping the calcium signature. New Phytol 181(2): 275-294.
doi: 10.1111/j.1469-8137.2008.02682.x

Meeks, J.C., and Castenholz, R.W. (1971) Growth and photosynthesis in an extreme thermophile, *Synechococcus lividus* (Cyanophyta). Arch Mikrobiol 78(1): 25-41. doi: 10.1007/BF00409086

Meeks, J.C., and Elhai, J. (2002) Regulation of cellular differentiation in filamentous cyanobacteria in free-living and plant-associated symbiotic growth states. Microbiol Mol Biol Rev 66(1): 94-121. doi: 10.1128/MMBR.66.1.94-121.2002

Mella-Herrera, R.A., Neunuebel, M.R., Kumar, K., Saha, S.K., and Golden, J.W. (2011) The *sigE* gene is required for normal expression of heterocyst-specific genes in *Anabaena* sp. strain PCC 7120. J Bacteriol 193(8): 1823-1832.
doi: 10.1128/JB.01472-10

Merino-Puerto, V., Mariscal, V., Mullineaux, C.W., Herrero, A., and Flores, E. (2010) Fra proteins influencing filament integrity, diazotrophy and localization of septal protein SepJ in the heterocyst-forming cyanobacterium *Anabaena* sp. Mol Microbiol 75(5): 1159-1170.
doi: 10.1111/j.1365-2958.2009.07031.x

Merino-Puerto, V., Mariscal, V., Schwarz, H., Maldener, I., Mullineaux, C.W., Herrero, A., and Flores, E. (2011) FraH is required for reorganization of intracellular membranes during heterocyst differentiation in *Anabaena* sp. strain PCC 7120. J Bacteriol 193(24): 6815-6823.
doi: 10.1128/JB.05995-11

Mi, H., Endo, T., Ogawa, T., and Asada, K. (1995) Thylakoid membrane-bound, NADPH-specific pyridine nucleotide dehydrogenase complex mediates cyclic electron transport in the cyanobacterium *Synechocystis* sp. PCC 6803. Plant Cell Physiol 36(4): 661-668.
doi: 10.1093/oxfordjournals.pcp.a078807

Michiels, J., Xi, C., Verhaert, J., and Vanderleyden, J. (2002) The functions of Ca(2+) in bacteria: a role for EF-hand proteins? Trends Microbiol 10(2): 87-93. doi: 10.1016/S0966-842X(01)02284-3

Mitchell, P. (1975) The protonmotive Q cycle: a general formulation. FEBS Lett 59(2): 137-139. doi: 10.1016/0014-5793(75)80359-0

Mitchison, G.J., and Wilcox, M. (1972) Rule governing cell division in *Anabaena*. Nature 239: 110-111. doi: 10.1038/239110a0

Montoya, J.P., Holl, C.M., Zehr, J.P., Hansen, A., Villareal, T.A., and Capone, D.G. (2004) High rates of N_2 fixation by unicellular diazotrophs in the oligotrophic Pacific Ocean. Nature 430(7003): 1027-1032. doi: 10.1038/nature02824

Morone, J., Alfeus, A., Vasconcelos, V., and Martins, A. (2019) Revealing the potential of cyanobacteria in cosmetics and cosmeceuticals — A new bioactive approach. Algal Res 41: 101541. doi: 10.1016/j.algal.2019.101541

Mörschel, E., and Mühlethaler, K. (1983) On the linkage of exoplasmatic freeze-fracture particles to phycobilisomes. Planta 158(5): 451-457. doi: 10.1007/BF00397739

Müh, F., Renger, T., and Zouni, A. (2008) Crystal structure of cyanobacterial photosystem II at 3.0 A resolution: a closer look at the antenna system and the small membrane-intrinsic subunits. Plant Physiol Biochem 46(3): 238-264.
doi: 10.1016/j.plaphy.2008.01.003

Mullineaux, C.W. (2014) Co-existence of photosynthetic and respiratory activities in cyanobacterial thylakoid membranes. Biochim Biophys Acta 1837(4): 503-511.
doi: 10.1016/j.bbabio.2013.11.017

Muro-Pastor, M.I., Reyes, J.C., and Florencio, F.J. (2001) Cyanobacteria perceive nitrogen status by sensing intracellular 2-oxoglutarate levels. J Biol Chem 276(41): 38320-38328.
doi: 10.1074/jbc.M105297200

Murry, M.A., Olafsen, A.G., and Benemann, J.R. (1981) Oxidation of diaminobenzidine in the heterocysts of *Anabaena cylindrica*. Curr Microbiol 6(4): 201-206. doi: 10.1007/BF01566972

Nagarajan, A., and Pakrasi, H.B. (2016) Membrane-bound protein complexes for photosynthesis and respiration in cyanobacteria. In: eLS, John Wiley & Sons, Ltd (Ed.). doi: 10.1002/9780470015902.a0001670.pub2

Nayar, A.S., Yamaura, H., Rajagopalan, R., Risser, D.D., and Callahan, S.M. (2007) FraG is necessary for filament integrity and heterocyst maturation in the cyanobacterium *Anabaena* sp. strain PCC 7120. Microbiology 153(2): 601-607. doi: 10.1099/mic.0.2006/002535-0

Nelson, N., and Yocum, C.F. (2006) Structure and function of photosystems I and II. Annu Rev Plant Biol 57: 521-565.
doi: 10.1146/annurev.arplant.57.032905.105350

Nixon, P.J., Michoux, F., Yu, J., Boehm, M., and Komenda, J. (2010) Recent advances in understanding the assembly and repair of photosystem II. Ann Bot 106(1): 1-16. doi: 10.1093/aob/mcq059

Nogués, I., Hervás, M., Peregrina, J.R., Navarro, J.A., de la Rosa, M.A., Gómez-Moreno, C., and Medina, M. (2005) *Anabaena* flavodoxin as an electron carrier from photosystem I to ferredoxin-$NADP^+$ reductase. Role of flavodoxin residues in protein-protein interaction and electron transfer. Biochemistry 44(1): 97-104.
doi: 10.1021/bi048324d

Nomura, H., and Shiina, T. (2014) Calcium signaling in plant endosymbiotic organelles: mechanism and role in physiology. Mol Plant 7(7): 1094-1104. doi: 10.1093/mp/ssu020

Ochoa de Alda, J.A., Esteban, R., Diago, M.L., and Houmard, J. (2014) The plastid ancestor originated among one of the major cyanobacterial lineages. Nat Commun 5: 4937. doi: 10.1038/ncomms5937

Panjiar, N., Mishra, S., Yadav, A.N., and Verma, P. (2017). Functional foods from cyanobacteria. In: Microbial functional foods and nutraceuticals. V.K. Gupta, H. Treichel, V. Shapaval, *et al.* (eds). doi:10.1002/9781119048961.ch2

Pereira, S.B., Mota, R., Vieira, C.P., Vieira, J., and Tamagnini, P. (2015) Phylum-wide analysis of genes/proteins related to the last steps of assembly and export of extracellular polymeric substances (EPS) in cyanobacteria. Sci Rep 5: 14835. doi: 10.1038/srep14835

Pernil, R., Herrero, A., and Flores, E. (2010) Catabolic function of compartmentalized alanine dehydrogenase in the heterocyst-forming cyanobacterium *Anabaena* sp. strain PCC 7120. J Bacteriol 192(19): 5165-5172.
doi: 10.1128/JB.00603-10

Pfaffl, M.W. (2001) A new mathematical model for relative quantification in real-time RT–PCR. Nucleic Acids Res 29(9): e45. Retrieved from

https://www.ncbi.nlm.nih.gov/pmc/articles/PMC5 5695/?report=classic

Piccioni, R., and Mauzerall, D. (1978) Calcium and photosynthetic oxygen evolution in cyanobacteria. Biochim Biophys Acta 504(3): 384–397. doi: 10.1016/0005-2728(78)90061-0

Picossi, S., Flores, E., and Herrero, A. (2014) ChIP analysis unravels an exceptionally wide distribution of DNA binding sites for the NtcA transcription factor in a heterocyst-forming cyanobacterium. BMC Genomics 15: 22. doi: 10.1186/1471-2164-15-22

Picossi, S., Flores, E., and Herrero, A. (2015) The LysR-type transcription factor PacR is a global regulator of photosynthetic carbon assimilation in *Anabaena*. Environ Microbiol 17(9): 3341-3351. doi: 10.1111/1462-2920.12800

Piven, I., Ajlani, G., and Sokolenko, A. (2005) Phycobilisome linker proteins are phosphorylated in *Synechocystis* sp. PCC 6803. J Biol Chem 280(22): 21667-21672. doi: 10.1074/jbc.M412967200

Plegaria, J.S., and Kerfeld, C.A. (2018) Engineering nanoreactors using bacterial microcompartment architectures. Curr Opin Biotechnol 51: 1-7. doi: 10.1016/j.copbio.2017.09.005

Prasanna, R., Kumar, R., Sood, A., Prasanna, B.M., and Singh, P.K. (2006) Morphological, physiochemical and molecular characterization of *Anabaena* strains. Microbiol Res 161(3): 187-202. doi: 10.1016/j.micres.2005.08.001

Price, G.D., Sültemeyer, D., Klughammer, B., Ludwig, M., and Badger, M.R. (1998) The functioning of the CO_2 concentrating mechanism in several cyanobacterial strains: a review of general physiological characteristics, genes, proteins, and recent advances. Can J Bot 76(6): 973-1002. doi: 10.1139/b98-081

Price, G.D., Woodger, F.J., Badger, M.R., Howitt, S.M., and Tucker, L. (2004) Identification of a SulP-type bicarbonate transporter in marine cyanobacteria. Proc Natl Acad Sci U S A 101(52): 18228-18233. doi: 10.1073/pnas.0405211101

Price, G.D., Badger, M.R., Woodger, F.J., and Long, B.M. (2008) Advances in understanding the cyanobacterial CO_2-concentrating-mechanism (CCM): functional components, C_i transporters, diversity, genetic regulation and prospects for engineering into plants. J Exp Bot 59(7): 1441-1461. doi: 10.1093/jxb/erm112

Price, G.D. (2011) Inorganic carbon transporters of the cyanobacterial CO_2 concentrating mechanism. Photosynth Res 109(1-3): 47-57. doi: 10.1007/s11120-010-9608-y

Rae, B.D., Long, B.M., Förster, B., Nguyen, N.D., Velanis, C.N., Atkinson, N., and Hee, W.Y. (2017) Progress and challenges of engineering a biophysical CO_2-concentrating mechanism into higher plants. J Exp Bot 68(14): 3717-3737. doi: 10.1093/jxb/erx133

Raines, C.A. (2003) The Calvin cycle revisited. Photosynth Res 75(1): 1-10. doi: 10.1023/A:1022421515027

Raman, R., Rajanikanth, V., Palaniappan, R.U., Lin, Y.P., He, H., McDonough, S.P., Sharma, Y., and Chang, Y.F. (2010) Big domains are novel Ca^{2+}-binding modules: evidences from big domains of *Leptospira* immunoglobulin-like (Lig) proteins. PLoS One 5(12): e14377. doi: 10.1371/journal.pone.0014377

Rampelotto, P.H. (2013) Extremophiles and extreme environments. Life (Basel) 3(3): 482-485. doi: 10.3390/life3030482

Rippka, R., Deruelles, J., Waterbury, J.B., Herdman, M., and Stanier, R.Y. (1979) Generic assignments, strain histories and properties of pure cultures of cyanobacteria. J Gen Microbiol 111: 1-61. doi: 10.1099/00221287-111-1-1

Risser, D.D., and Callahan, S.M. (2007) Mutagenesis of *hetR* reveals amino acids necessary for HetR function in the heterocystous cyanobacterium *Anabaena* sp. strain PCC 7120. J Bacteriol 189(6): 2460-2467. doi: 10.1128/JB.01241-06

Rocha, A.G., and Vothknecht, U.C. (2012) The role of calcium in chloroplasts – an intriguing and unresolved puzzle. Protoplasma 249(4): 957-966. doi: 10.1007/s00709-011-0373-3

Rolland, V., Badger, M.R., and Price, G.D. (2016) Redirecting the cyanobacterial bicarbonate transporters BicA and SbtA to the chloroplast envelope: soluble and membrane cargos need different chloroplast targeting signals in plants. Front Plant Sci 7: 185. doi: 10.3389/fpls.2016.00185

Rusnak, F., and Mertz, P. (2000) Calcineurin: form and function. Physiol Rev 80(4): 1483-1521. doi: 10.1152/physrev.2000.80.4.1483

Saeki, K. (2004) Electron transport to nitrogenase: diverse routes for a common destination. In: Klipp, W., Masepohl, B., Gallon, J.R., Newton, W.E. (eds) Genetics and regulation of nitrogen fixation in free-living bacteria. Nitrogen fixation: origins, applications, and research progress, vol 2. Springer, Dordrecht. doi: 10.1007/1-4020-2179-8_11

Sai, J., and Johnson, C.H. (2002) Dark-stimulated calcium ion fluxes in the chloroplast stroma and cytosol. Plant Cell 14(6): 1279-1291.
doi: 10.1105/tpc.000653

Sánchez-Magraner, L., Viguera, A.R., García-Pacios, M., Garcillán, M.P., Arrondo, J.L., de la Cruz, F., Goñi, F.M., and Ostolaza, H. (2007) The calcium-binding C-terminal domain of *Escherichia coli* alpha-hemolysin is a major determinant in the surface-active properties of the protein. J Biol Chem 282(16): 11827-11835.
doi: 10.1074/jbc.M700547200

Schirrmeister, B.E., de Vos, J.M., Antonelli, A., and Bagheri, H.C. (2013) Evolution of multicellularity coincided with increased diversification of cyanobacteria and the Great Oxidation Event. Proc Natl Acad Sci U S A 110(5): 1791-1796. doi: 10.1073/pnas.1209927110

Schuurmans, R.M., Schuurmans, J.M., Bekker, M., Kromkamp, J.C., Matthijs, H.C., and Hellingwerf, K.J. (2014) The redox potential of the plastoquinone pool of the cyanobacterium *Synechocystis* species strain PCC 6803 is under strict homeostatic control. Plant Physiol 165(1): 463-475.
doi: 10.1104/pp.114.237313

Sedoud, A., López-Igual, R., Ur Rehman, A., Wilson, A., Perreau, F., Boulay, C., Vass, I., *et al.* (2014) The cyanobacterial photoactive orange carotenoid protein is an excellent singlet oxygen quencher. Plant Cell 26(4): 1781-1791. doi: 10.1105/tpc.114.123802

Sello, S., Moscatiello, R., Mehlmer, N., Leonardelli, M., Carraretto, L., Cortese, E., Zanella, F.G., *et al.* (2018) Chloroplast Ca^{2+} fluxes into and across thylakoids revealed by thylakoid-targeted aequorin probes. Plant Physiol 177(1): 38-51.
doi: 10.1104/pp.18.00027

Sengupta, A., Pakrasi, H.B., and Wangikar, P.P. (2018) Recent advances in synthetic biology of cyanobacteria. Appl Microbiol Biotechnol 102(13): 5457-5471. doi: 10.1007/s00253-018-9046-x

Shestakov, S.V., and Karbysheva, E.A. (2017) The origin and evolution of cyanobacteria. Biol Bull Rev 7(4): 259-272. doi: 10.1134/S2079086417040090

Shi, Y., Zhao, W., Zhang, W., Ye, Z., and Zhao, J. (2006) Regulation of intracellular free calcium concentration during heterocyst differentiation by HetR and NtcA in *Anabaena* sp. PCC 7120. Proc Natl Acad Sci U S A 103(30): 11334-11339.
doi: 10.1073/pnas.0602839103

Shi, Y. (2009) Serine/threonine phosphatases: mechanism through structure. Cell 139(3): 468-484. doi: 10.1016/j.cell.2009.10.006

Shibata, M., Katoh, H., Sonoda, M., Ohkawa, H., Shimoyama, M., Fukuzawa, H., Kaplan, A., and Ogawa, T. (2002) Genes essential to sodium-dependent bicarbonate transport in cyanobacteria: function and phylogenetic analysis. J Biol Chem 277(21): 18658-18664.
doi: 10.1074/jbc.M112468200

Shih, P.M., Wu, D., Latifi, A., Axen, S.D., Fewer, D.P., Talla, E., Calteau, A., *et al.* (2013) Improving the coverage of the cyanobacterial phylum using diversity-driven genome sequencing. Proc Natl Acad Sci U S A 110(3): 1053-1058.
doi: 10.1073/pnas.1217107110

Singh, S., and Mishra, A.K. (2014) Regulation of calcium ion and its effect on growth and developmental behavior in wild type and *ntcA* mutant of *Anabaena* sp. PCC 7120 under varied levels of $CaCl_2$. Microbiology 83(3): 235-246. doi: 10.1134/S002626171403014X

Singh, S., and Mishra, A.K. (2016) Unraveling of cross talk between Ca(2+) and ROS regulating enzymes in *Anabaena* 7120 and *ntcA* mutant. J Basic Microbiol 56(7): 762-778.
doi: 10.1002/jobm.201500326

Singh, S., Verma, E., Niveshika, Tiwari, B., and Mishra, A.K. (2016) Exopolysaccharide production in *Anabaena* sp. PCC 7120 under different $CaCl_2$ regimes. Physiol Mol Biol Plants 22(4): 557-566. doi: 10.1007/s12298-016-0380-0

Singh, S., Verma, E., Tiwari, B., Niveshika, and Mishra, A.K. (2017) Modulation of fatty acids and

hydrocarbons in *Anabaena* 7120 and its *ntcA* mutant under calcium. J Basic Microbiol 57(2): 171-183. doi: 10.1002/jobm.201600476

Singh, S.P., and Montgomery, B.L. (2011) Determining cell shape: adaptive regulation of cyanobacterial cellular differentiation and morphology. Trends Microbiol 19(6): 278-285. doi: 10.1016/j.tim.2011.03.001

Stadnichuk, I.N., Krasilnikov, P.M., and Zlenko, D.V. (2015) Cyanobacterial phycobilisomes and phycobiliproteins. Microbiology 84(2): 101-111. doi: 10.1134/S0026261715020150

Stael, S., Rocha, A.G., Robinson, A.J., Kmiecik, P., Vothknecht, U.C., and Teige, M. (2011) *Arabidopsis* calcium-binding mitochondrial carrier proteins as potential facilitators of mitochondrial ATP-import and plastid SAM-import. FEBS Lett 585(24): 3935-3940. doi: 10.1016/j.febslet.2011.10.039

Stael, S., Wurzinger, B., Mair, A., Mehlmer, N., Vothknecht, U.C., and Teige, M. (2012a) Plant organellar calcium signaling: an emerging field. J Exp Bot 63(4): 1525-1542. doi: 10.1093/jxb/err394

Sun, T., Li, S., Song, X., Diao, J., Chen, L., and Zhang, W. (2018) Toolboxes for cyanobacteria: Recent advances and future direction. Biotechnol Adv 36(4): 1293-1307.
doi: 10.1016/j.biotechadv.2018.04.007

Takahashi, Y., Yamaguchi, O., and Omata, T. (2004) Roles of CmpR, a LysR family transcriptional regulator, in acclimation of the cyanobacterium *Synechococcus* sp. strain PCC 7942 to low-CO(2) and high-light conditions. Mol Microbiol 52(3): 837-845. doi: 10.1111/j.1365-2958.2004.04021.x

Tamagnini, P., Leitão, E., Oliveira, P., Ferreira, D., Pinto, F., Harris, D.J., Heidorn, T., and Lindblad, P. (2007) Cyanobacterial hydrogenases: diversity, regulation and applications. FEMS Microbiol Rev 31(6): 692-720.
doi: 10.1111/j.1574-6976.2007.00085.x

Tang, K., Ding, W.L., Höppner, A., Zhao, C., Zhang, L., Hontani, Y., Kennis, J.T., *et al.* (2015) The terminal phycobilisome emitter, L_{CM}: A light-harvesting pigment with a phytochrome chromophore. Proc Natl Acad Sci U S A 112(52): 15880-15885. doi: 10.1073/pnas.1519177113

Thiel, T. (2004) Nitrogen fixation in heterocyst-forming cyanobacteria. In: Klipp, W., Masepohl, B., Gallon, J.R., Newton, W.E. (eds) Genetics and regulation of nitrogen fixation in free-living bacteria. Nitrogen fixation: origins, applications, and research progress, vol 2. Springer, Dordrecht.
doi: 10.1007/1-4020-2179-8_5

Thomas, J., Meeks, J.C., Wolk, C.P., Shaffer, P.W., and Austin, S.M. (1977) Formation of glutamine from [13n]ammonia, [13n]dinitrogen, and [14C]glutamate by heterocysts isolated from *Anabaena cylindrica*. J Bacteriol 129(3): 1545-1555. Retrieved from
https://jb.asm.org/content/129/3/1545

Tiwari, A., Singh, P., and Asthana, R.K. (2016) Role of calcium in the mitigation of heat stress in the cyanobacterium *Anabaena* PCC 7120. J Plant Physiol 199: 67-75. doi: 10.1016/j.jplph.2016.05.012

Torrecilla, I., Leganés, F., Bonilla, I., and Fernández-Piñas, F. (2000) Use of recombinant aequorin to study calcium homeostasis and monitor calcium transients in response to heat and cold shock in cyanobacteria. Plant Physiol 123(1): 161-176. doi: 10.1104/pp.123.1.161

Torrecilla, I., Leganés, F., Bonilla, I., and Fernández-Piñas, F. (2001) Calcium transients in response to salinity and osmotic stress in the nitrogen-fixing cyanobacterium *Anabaena* sp. PCC7120, expressing cytosolic apoaequorin. Plant Cell Environ 24(6): 641-648.
doi: 10.1046/j.0016-8025.2001.00708.x

Torrecilla, I., Leganés, F., Bonilla, I., and Fernández-Piñas, F. (2004a) Light-to-dark transitions trigger a transient increase in intracellular Ca^{2+} modulated by the redox state of the photosynthetic electron transport chain in the cyanobacterium *Anabaena* sp. PCC7120. Plant Cell Environ 27(7): 810-819.
doi: 10.1111/j.1365-3040.2004.01187.x

Torrecilla, I., Leganés, F., Bonilla, I., and Fernández-Piñas, F. (2004b) A calcium signal is involved in heterocyst differentiation in the cyanobacterium *Anabaena* sp. PCC7120. Microbiology 150(11): 3731-3739.
doi: 10.1099/mic.0.27403-0

Trotta, A., Suorsa, M., Rantala, M., Lundin, B., and Aro, E.M. (2016) Serine and threonine residues of plant STN7 kinase are differentially phosphorylated upon changing light conditions and specifically influence the activity and stability of the kinase. Plant J 87(5): 484-494. doi: 10.1111/tpj.13213

Tsujimoto, R., Kamiya, N., and Fujita, Y. (2014) Transcriptional regulators ChlR and CnfR are essential for diazotrophic growth in nonheterocystous cyanobacteria. Proc Natl Acad Sci U S A 111(18): 6762-6767. doi: 10.1073/pnas.1323570111

Umena, Y., Kawakami, K., Shen, J.R., and Kamiya, N. (2011) Crystal structure of oxygen-evolving photosystem II at a resolution of 1.9 Å. Nature 473(7345): 55-60. doi: 10.1038/nature09913

Valladares, A., Maldener, I., Muro-Pastor, A.M., Flores, E., and Herrero, A. (2007) Heterocyst development and diazotrophic metabolism in terminal respiratory oxidase mutants of the cyanobacterium *Anabaena* sp. strain PCC 7120. J Bacteriol 189(12): 4425-4430. doi: 10.1128/JB.00220-07

Valladares, A., Flores, E., and Herrero, A. (2008) Transcription activation by NtcA and 2-oxoglutarate of three genes involved in heterocyst differentiation in the cyanobacterium *Anabaena* sp. strain PCC 7120. J Bacteriol 190(18): 6126-6133. doi: 10.1128/JB.00787-08

Vega-Palas, M.A., Flores, E., and Herrero, A. (1992) NtcA, a global nitrogen regulator from the cyanobacterium *Synechococcus* that belongs to the Crp family of bacterial regulators. Mol Microbiol 6(13): 1853-1859. doi: 10.1111/j.1365-2958.1992.tb01357.x

Videau, P., Ni, S., Rivers, O.S., Ushijima, B., Feldmann, E.A., Cozy, L.M., Kennedy, M.A., and Callahan, S.M. (2014) Expanding the direct HetR regulon in *Anabaena* sp. strain PCC 7120. J Bacteriol 196(5): 1113-1121. doi: 10.1128/JB.01372-13

Videau, P., Rivers, O.S., Hurd, K., Ushijima, B., Oshiro, R.T., Ende, R.J., O'Hanlon, S.M., and Cozy, L.M. (2016) The heterocyst regulatory protein HetP and its homologs modulate heterocyst commitment in *Anabaena* sp. strain PCC 7120. Proc Natl Acad Sci U S A 113(45): E6984-E6992. doi: 10.1073/pnas.1610533113

Vygodina, T., Kirichenko, A., and Konstantinov, A.A. (2013) Direct regulation of cytochrome *c* oxidase by calcium ions. PLoS One 8(9): e74436. doi: 10.1371/journal.pone.0074436

Wang, H.L., Postier, B.L., and Burnap, R.L. (2004) Alterations in global patterns of gene expression in *Synechocystis* sp. PCC 6803 in response to inorganic carbon limitation and the inactivation of *ndhR*, a LysR family regulator. J Biol Chem 279(7): 5739-5751. doi: 10.1074/jbc.M311336200

Wang, Y., and Xu, X. (2005) Regulation by *hetC* of genes required for heterocyst differentiation and cell division in *Anabaena* sp. strain PCC 7120. J Bacteriol 187(24): 8489-8493. doi: 10.1128/JB.187.24.8489-8493.2005

Watanabe, M., Semchonok, D.A., Webber-Birungi, M.T., Ehira, S., Kondo, K., Narikawa, R., Ohmori, M., *et al.* (2014) Attachment of phycobilisomes in an antenna-photosystem I supercomplex of cyanobacteria. Proc Natl Acad Sci U S A 111(7): 2512-2517. doi: 10.1073/pnas.1320599111

White, P.J., and Broadley, M.R. (2003) Calcium in plants. Ann Bot 92(4): 487-511. doi: 10.1093/aob/mcg164

Whitney, S.M., Houtz, R.L., and Alonso, H. (2011) Advancing our understanding and capacity to engineer nature's CO_2-sequestering enzyme, Rubisco. Plant Physiol 155(1): 27-35. doi: 10.1104/pp.110.164814

Wilson, A., Ajlani, G., Verbavatz, J.M., Vass, I., Kerfeld, C.A., and Kirilovsky, D. (2006) A soluble carotenoid protein involved in phycobilisome-related energy dissipation in cyanobacteria. Plant Cell 18(4): 992-1007. doi: 10.1105/tpc.105.040121

Wiltbank, L.B., and Kehoe, D.M. (2018) Diverse light responses of cyanobacteria mediated by phytochrome superfamily photoreceptors. Nat Rev Microbiol 17(1): 37-50. doi: 10.1038/s41579-018-0110-4

Wolk, C.P. (1965) Control of sporulation in a blue-green alga. Dev Biol 12(1): 15-35. doi: 10.1016/0012-1606(65)90018-7

Wolk, C.P., Ernst, A., and Elhai, J. (1994) Heterocyst metabolism and development. In: The molecular biology of cyanobacteria. Bryant, D.E. (ed). Dordrecht, The Netherlands: Kluwer Academic: 769-823.

Wood, N.B., and Haselkorn, R. (1980) Control of phycobiliprotein proteolysis and heterocyst differentiation in *Anabaena*. J Bacteriol 141(3): 1375-1385. Retrieved from https://jb.asm.org/content/141/3/1375

Woodger, F.J., Bryant, D.A., and Price, G.D. (2007) Transcriptional regulation of the CO^2-concentrating mechanism in a euryhaline, coastal marine cyanobacterium, *Synechococcus* sp. strain PCC 7002: role of NdhR/CcmR. J Bacteriol 189(9): 3335-3347. doi: 10.1128/JB.01745-06

Yang, J., Yan, R., Roy, A., Xu, D., Poisson, J., and Zhang, Y. (2015) The I-TASSER Suite: protein structure and function prediction. Nat Methods 12(1): 7-8. doi: 10.1038/nmeth.3213

Yang, S.A., and Klee, C.B. (2000) Low affinity Ca^{2+}-binding sites of calcineurin B mediate conformational changes in calcineurin A. Biochemistry 39(51): 16147-16154. doi: 10.1021/bi001321q

Yoon, H.S., and Golden, J.W. (1998) Heterocyst pattern formation controlled by a diffusible peptide. Science 282(5390): 935-938. doi: 10.1126/science.282.5390.935

Yoon, H.S., and Golden, J.W. (2001) PatS and products of nitrogen fixation control heterocyst pattern. J Bacteriol 183(8): 2605-2613. doi: 10.1128/JB.183.8.2605-2613.2001

Zhang, C.C., Friry, A., and Peng, L. (1998) Molecular and genetic analysis of two closely linked genes that encode, respectively, a protein phosphatase 1/2A/2B homolog and a protein kinase homolog in the cyanobacterium *Anabaena* sp. strain PCC 7120. J Bacteriol 180(10): 2616-2622. Retrieved from https://jb.asm.org/content/180/10/2616

Zhang, C.C., Zhou, C.Z., Burnap, R.L., and Peng, L. (2018) Carbon/nitrogen metabolic balance: lessons from cyanobacteria. Trends Plant Sci 23(12): 1116-1130. doi: 10.1016/j.tplants.2018.09.008

Zhang, H., Wang, S., Wang, Y., and Xu, X. (2018) Functional overlap of HetP and HetZ in regulation of heterocyst differentiation in *Anabaena* sp. strain PCC 7120. J Bacteriol 200(9): e00707-e00717. doi: 10.1128/JB.00707-17

Zhang, P., Battchikova, N., Jansen, T., Appel, J., Ogawa, T., and Aro, E.M. (2004) Expression and functional roles of the two distinct NDH-1 complexes and the carbon acquisition complex NdhD3/NdhF3/CupA/Sll1735 in *Synechocystis* sp PCC 6803. Plant Cell 16(12): 3326-3340. doi: 10.1105/tpc.104.026526

Zhang, P., Allahverdiyeva, Y., Eisenhut, M., and Aro, E.M. (2009) Flavodiiron proteins in oxygenic photosynthetic organisms: photoprotection of photosystem II by Flv2 and Flv4 in *Synechocystis* sp. PCC 6803. PLoS One 4(4): e5331. doi: 10.1371/journal.pone.0005331

Zhang, P., Eisenhut, M., Brandt, A.M., Carmel, D., Silén, H.M., Vass, I., Allahverdiyeva, Y., *et al.* (2012) Operon *flv4-flv2* provides cyanobacterial photosystem II with flexibility of electron transfer. Plant Cell 24(5): 1952-1971. doi: 10.1105/tpc.111.094417

Zhao, Y., Shi, Y., Zhao, W., Huang, X., Wang, D., Brown, N., Brand, J., and Zhao, J. (2005) CcbP, a calcium-binding protein from *Anabaena* sp. PCC 7120, provides evidence that calcium ions regulate heterocyst differentiation. Proc Natl Acad Sci U S A 102(16): 5744-5748. doi: 10.1073/pnas.0501782102

Zhou, R., Wei, X., Jiang, N., Li, H., Dong, Y., Hsi, K.L., and Zhao, J. (1998) Evidence that HetR protein is an unusual serine-type protease. Proc Natl Acad Sci U S A 95(9): 4959-4963. doi: 10.1073/pnas.95.9.4959

Zhou, R., and Wolk, C.P. (2002) Identification of an akinete marker gene in *Anabaena variabilis*. J Bacteriol 184(9): 2529-2532. doi: 10.1128/JB.184.9.2529-2532.2002

Zhou, Y., Yang, W., Kirberger, M., Lee, H.W., Ayalasomayajula, G., and Yang, J.J. (2006) Prediction of EF-hand calcium-binding proteins and analysis of bacterial EF-hand proteins. Proteins 65(3): 643-655. doi: 10.1002/prot.21139

UNIVERSITY OF TURKU

Grano Oy - Turku, Finland 2019

ISBN 978-951-29-7740-6 (PRINT)
ISBN 978-951-29-7741-3 (PDF)
ISSN 0082-7002 (Print)
ISSN 2343-3175 (Online)